

INCREASED GROUNDWATER TEMPERATURES AND THEIR POTENTIAL FOR SHALLOW GEOTHERMAL USE IN URBAN AREAS

zum Erlangen des akademischen Grades einer

DOKTORIN DER NATURWISSENSCHAFTEN
(Dr. rer. nat.)

DISSERTATION

genehmigt

von der KIT-Fakultät für
Bauingenieur-, Geo- und Umweltwissenschaften
des Karlsruher Instituts für Technologie (KIT)

von
M. Sc. Carolin Tissen
aus Frankfurt am Main

Tag der mündlichen Prüfung:
15. Mai 2020

Referent: Prof. Dr. Philipp Blum
Korreferent: Prof. Dr. Stefan Hinz

Karlsruhe, 2020

*Dedicated to my beloved parents
who have always supported and encouraged me.*

Abstract

Climate change and heat input into the subsurface by anthropogenic activities affect and raise groundwater temperatures (GWT) worldwide. However, location, frequency of occurrence and drivers of GWT anomalies are poorly understood. Beside potential negative impacts of increased GWT on the chemical and physical state of groundwater and its fauna, they hold a huge energy potential for sustainable heat supply of city districts or whole cities, and if extracted efficiently they can help to save CO₂. One option to extract and exploit the full potential of this subsurface energy source is shallow geothermal energy. Yet, so far no detailed analysis of the spatial relationship between geothermal potential, heat input and heat demand was conducted.

In the first study, GWT data of 44,205 wells in ten central European countries are analysed to identify the most extreme, positive temperature anomalies. The anthropogenic heat intensity (AHI), which relates average rural background temperatures to local temperature measurements, is applied to detect GWT anomalies. Subsequently, these AHIs are categorised and separately studied for the three land cover classes: 'natural', 'agricultural' and 'artificial'. Since human impacts on groundwater are most relevant and localised in urban areas, special attention is paid to temperature anomalies related to artificial surfaces. Significant AHIs of 3 – 10 K in natural and agricultural areas result from anthropogenic sources such as landfills, wastewater treatment plants or mining activities. Beneath artificial surfaces, AHIs above 6 K are mostly related to heat inputs from underground car parks, heated basements and district heating pipes. These GWT anomalies even exceed the legal temperature thresholds that are applied to regulate open geothermal systems.

In the second study, the amount of thermal energy extractable by different shallow geothermal systems is compared to the energy demand for space heating and domestic hot water for an urban quarter in Karlsruhe, Germany. By investigating several scenarios with different legal regulations, varying space availability and hydro-/geological boundary conditions, the impact of certain constraining parameters, such as a local restriction in drilling depth is identified. The percentage to which the heat demand can be met, before and after a refurbishment of the building stock, is defined as heat supply rate. The heat supply before and after refurbishment achieves up to 59%, 152% and 25% for horizontal or vertical ground source heat pump or groundwater heat pump systems, respectively. After refurbishment, the heat supply rate of these three systems are 125%, 322% and 54%.

Based on the approach for the evaluation of the technical geothermal potential in the second study, the python-based tool GeoEnPy is developed in the final study. GeoEnPy computes, combines and spatially resolves the heat supply rate and theoretical sustainable potential, in order to identify key locations for shallow geothermal use in Vienna, Austria. For this purpose, the amount of thermal energy extractable by different shallow geothermal systems as well as the annual anthropogenic heat input into the subsurface is compared to the energy demand for Vienna's present space heating demand and for the case all buildings are refurbished.

Due to the smaller space demand, borehole heat exchanger (BHE) systems reach a higher supply rate than GWHP systems. On city-scale, the technical geothermal potential of BHEs can satisfy the heating demand of Vienna's unrefurbished buildings for 63% of the area. On district-scale, the eastern and southern districts of Vienna are the key locations for geothermal applications. Here, the average technical geothermal potential of BHE applications could easily meet the current heating demand. In addition, up to 58% of the demand could be sustainably supplied by the annual anthropogenic heat input.

Kurzfassung

Der globale Klimawandel und der Wärmeeintrag in den Untergrund durch anthropogene Aktivitäten beeinflussen und erhöhen Grundwassertemperaturen (GWT) weltweit. Lokation, Häufigkeit und Ursachen von GWT Anomalien sind jedoch nur unzureichend bekannt. Zwar haben erhöhte GWT negative Auswirkungen auf den chemischen und physikalischen Zustand des Grundwassers sowie die Grundwasser Fauna, jedoch bergen sie auch ein enormes Energiepotenzial für die nachhaltige Wärmeversorgung von Quartieren oder ganzen Städten. Wenn erhöhte GWT effizient genutzt werden kann zudem auch CO₂ eingespart werden. Eine Möglichkeit das volle Potenzial dieser unterirdischen Energiequelle zu gewinnen und auszuschöpfen ist die oberflächennahe Geothermie. Bisher wurde jedoch noch keine detaillierte Analyse des räumlichen Zusammenhangs von geothermischem Potenzial und Wärmeeintrag zum Wärmebedarf durchgeführt.

In der ersten Studie werden die GWT Daten von 44.205 Brunnen in zehn mitteleuropäischen Ländern analysiert, um die extremsten, positiven Temperaturanomalien zu identifizieren. Die anthropogene Wärmeintensität (AHI), die Differenz der durchschnittlichen, unbeeinflussten GWT und einer lokal gemessenen GWT wird verwendet, um GWT Anomalien aufzuspüren. Anschließend werden diese AHIs kategorisiert und separat für die drei Landbedeckungsklassen "natürlich", "landwirtschaftlich" und "künstlich" untersucht. Da menschliche Einflüsse auf das Grundwasser hauptsächlich in Städten relevant sind und auch hier am häufigsten lokalisiert wurden, liegt das Augenmerk der Studie auf der Analyse von Temperaturanomalien im Zusammenhang mit künstlichen Oberflächen. Signifikante AHIs von 3 - 10 K in natürlichen und landwirtschaftlichen Gebieten resultieren von anthropogenen Quellen wie Deponien, Kläranlagen oder Bergbauaktivitäten. Brunnen, die von künstlichen Oberflächen umgeben sind, weisen AHIs von über 6 K auf. Diese hohen AHIs sind meist auf Wärmeeinträge aus Tiefgaragen, beheizten Kellern und Fernwärmeleitungen zurückzuführen. Diese GWT Anomalien überschreiten sogar die gesetzlichen Temperaturgrenzwerte, die zur Regulierung offener geothermischer Systeme angewendet werden.

In der zweiten Studie wird die Menge an thermischer Energie, die von verschiedenen oberflächennahen geothermischen Systemen gewonnen werden kann, mit dem Energiebedarf für Raumheizung und Warmwasserbereitung eines Stadtviertels in Karlsruhe (Deutschland) verglichen. Die Verwendung mehrerer Szenarien mit unterschiedlichen gesetzlichen Regelungen, unterschiedlichem Raumangebot und hydro-/geologischen Randbedingungen, ermöglicht es den Einfluss einschränkender Parameter, wie z.B. einer lokalen Einschränkung der Bohrtiefe, zu bestimmen. Der Prozentsatz, zu dem der Wärmebedarf vor und nach einer Sanierung des Gebäudebestands gedeckt werden kann, wird als Wärmedeckungsgrad definiert. Der Wärmedeckungsgrad vor und nach der Sanierung erreicht jeweils bis zu 59%, 152% und 25% für horizontale oder vertikale Erdwärmepumpen- bzw. Grundwasser-Wärmepumpenanlagen. Nach der Sanierung beträgt der Wärmedeckungsgrad dieser drei Systeme 125%, 322% und 54%.

Basierend auf dem Ansatz für die Berechnung des technischen geothermischen Potenzials aus der zweiten Studie wird in der finalen Studie das auf Python Programm GeoEnPy entwickelt. GeoEnPy berechnet, kombiniert und löst die räumliche Verteilung des Wärmedeckungsgrads und des theoretischen, nachhaltigen Potenzials auf, um Standorte für die oberflächennahe geothermische Nutzung in Wien, Österreich, zu identifizieren. Zu diesem Zweck wird die Menge an thermischer Energie, die durch verschiedene oberflächennahe geothermische Systeme gewonnen werden kann, sowie der jährliche anthropogene Wärmeeintrag in den Untergrund mit dem Energiebedarf für den derzeitigen Raumwärmebedarf Wiens verglichen, und auch für den Fall, dass alle Gebäude saniert werden. Aufgrund des geringeren Raumbedarfs erreichen Erdwärmesondenanlagen (BHE) einen höheren Versorgungsgrad als GWHP-Anlagen. Auf Stadtebene kann das technische geothermische Potenzial von BHEs den Wärmebedarf der unsanierten Gebäude Wiens für 63% der Fläche decken. Auf Bezirksebene sind die östlichen und südlichen Bezirke Wiens die idealsten Standorte für geothermische Anwendungen. Hier könnte das durchschnittliche technische geothermische Potenzial der BHE-Anwendungen den aktuellen Wärmebedarf problemlos decken. Darüber hinaus könnten bis zu 58% des Bedarfs nachhaltig durch den jährlichen anthropogenen Wärmeeintrag gedeckt werden.

Contents

Abstract	v
Kurzfassung	vii
Contents	ix
List of Figures	xi
List of Tables	xiii
List of Abbreviations	xv
1 Introduction	1
1.1 Motivation	1
1.2 Groundwater Temperatures and Subsurface Urban Heat Island Effect	1
1.3 Shallow Geothermal Energy	3
1.3.1 Shallow Geothermal Systems	3
1.3.2 Geothermal Potential	3
1.4 Objective	5
1.5 Thesis Structure	6
2 Groundwater Temperature Anomalies in Central Europe	9
Abstract	9
2.1 Introduction	9
2.2 Materials and Methods	11
2.2.1 Groundwater Temperatures	11
2.2.2 Anthropogenic Heat Intensity	11
2.2.3 Land Cover Classification	13
2.2.4 Groundwater Temperature Anomalies	13
2.3 Results and Discussion	13
2.3.1 Statistics of Groundwater Temperature Anomalies (AHI_{max})	13
2.3.2 GWT Anomalies (AHI_{max}) Beneath Artificial Surfaces	15
2.3.3 Heat Sources of AHI_{max}	16
2.3.4 Regulations	18
2.4 Conclusion	19
Acknowledgements	19
3 Meeting the Demand: Geothermal Heat Supply Rates for an Urban Quarter in Germany	21
Abstract	21
3.1 Introduction	21
3.2 Materials and Methods	23
3.2.1 Study Site	23
3.2.2 Geological and Hydrogeological Data	24

3.2.3	Evaluation of the Heat Supply Rate	25
	Horizontal Ground Source Heat Pump (hGSHP) System	26
	Vertical Ground Source Heat Pump (vGSHP) System	27
	Groundwater Heat Pump (GWHP) System	28
3.3	Results and Discussion	30
3.3.1	Horizontal Ground Source Heat Pump (hGSHP) System	30
3.3.2	Vertical Ground Source Heat Pump (vGSHP) System	30
3.3.3	Groundwater Heat Pump (GWHP) System	33
3.3.4	Comparison	34
3.4	Conclusion	36
	Acknowledgements	36
4	Identifying Key Locations for Shallow Geothermal Use in Vienna	37
	Abstract	37
4.1	Introduction	37
4.2	Materials and Methods	39
4.2.1	Study Site	39
4.2.2	Input Data	40
4.2.3	Methods	42
	Calculation of the Anthropogenic Heat Flux and Flow	42
	Calculation of the Technical Geothermal Potential and Heat Supply Rate	44
4.3	Results and Discussion	45
4.3.1	Anthropogenic Heat Flux	45
4.3.2	Sustainable and Technical Geothermal Potential	46
4.3.3	Heat Supply Rate	48
4.3.4	Key Locations for Shallow Geothermal Use	50
4.4	Conclusion	50
	Acknowledgements	52
5	Synthesis	53
5.1	Conclusion	53
5.2	Perspective and Outlook	58
A	Appendix	61
	Appendix - Chapter 2	61
	Appendix - Chapter 3	69
	Appendix - Chapter 4	71
	References	83
	Acknowledgements	99
	Declaration of Authorship	101

List of Figures

2.1	Overview of the study site, GWT, AHI and AHI_{max}	12
2.2	Distribution of AHI and AHI_{max} wells for natural, agricultural and artificial land covers	14
2.3	Colour coded segmentation of the land utilisation classes	15
3.1	Overview of the study site "Rintheimer Feld"	24
3.2	Impressions of the study site "Rintheimer Feld"	25
3.3	Hydrogeological map of the "Rintheimer Feld"	26
3.4	Illustration of the three studied shallow geothermal systems	27
3.5	Results of the evaluation of the heat supply rate in the "Rintheimer Feld"	31
4.1	Location of Vienna, its 23 urban districts and measuring sites for GWT and GW level	41
4.2	Workflow of the calculation of the heat flux and the heat supply rate	43
4.3	Map of the total average anthropogenic heat flux and boxplot of the anthropogenic heat flow	46
4.4	Comparison of the heating demand, anthropogenic heat flow, the technical geothermal potentials of BHE and GWHP	47
4.5	Map and bar graph of the heat supply rate	49
4.6	Spatial distribution of the average heat supply rate per district without a district heating network	51
5.1	Overview of AHI_{max} and the seven heat sources	54
5.2	Main results of the case study "Rintheimer Feld"	56
5.3	Spatial distribution of the key locations for shallow geothermal energy and bar graphs for the average theoretical sustainable potential and heat supply rate of BHE and GWHP	57
A.1	Median rural background GWT	61
A.2	Corine Land Cover (CLC) data of Europe	62
A.3	AHI wells colour coded according to their CLC class	62
A.4	AHI versus measurement depth	63
A.5	GWT versus rural GWT	63
A.6	Histograms of GWT and rural GWT	64
A.7	Violin plot of AHI	64
A.8	Percentage of wells per main class and country for AHI and AHI_{max} wells	65
A.9	Violin plot of all AHI_{max}	65
A.10	Pictures of the six land utilisation classes (LUC)	66
A.11	GWT time series of a district heating pipe	66
A.12	Time series of air temperature and GWT of an underground carpark in Switzerland	67
A.13	GWT time series of the 19 identified heat sources	67

A.14 Hydrogeological zones of Vienna	71
A.15 Location of iButtons to measure the air temperature in basements and underground car parks.	72
A.16 Interpolation of mean GW level and GWT	72
A.17 Spacing of GWHP in Vienna	73
A.18 Boxplots of the spatial variability and uncertainty of the individual anthropogenic heat fluxes	73
A.19 Results of the spatial variability and uncertainty analysis of the an- thropogenic heat flux	74
A.20 Results of the spatial variability for BHE and GWHP systems	74

List of Tables

2.1	GWT and AHI of the seven heat source classes	17
3.1	Results of the geothermal potential and the inverse analysis of BHE . .	32
3.2	Results of the spatial analysis and the geothermal potential for the GWHP system	33
A.1	Countries of the survey area, number of wells, depth and data source information	68
A.2	Input parameters for the estimation of the heat supply rate of the "Rintheimer Feld"	70
A.3	List of input files and parameters for the anthropogenic heat flux and heat supply rate calculation	75
A.4	Land use categories and temperature values for the GST estimation . .	79
A.5	Spearman's rank correlation coefficient ρ and p-value for the spatial analysis and the uncertainty analysis of the heat flux	80
A.6	Spearman's rank correlation coefficient ρ and p-value for the spatial analysis of the heat supply rate	81

List of Abbreviations

AHF	anthropogenic heat flux
AHI	anthropogenic heat intensity
AMD	acid mine drainage
ATES	aquifer thermal energy storage
BHE	borehole heat exchanger
BTES	borehole thermal energy storage
COP	coefficient of performance
CLC	CORINE Land Cover
DEM	digital elevation model
DH	district heating
DHW	domestic hot water
GBA	Geological Survey of Austria
GIS	geographical information system
GSHP	ground source heat pump
GST	ground surface temperature
GW	groundwater flow
GWT	groundwater temperature
GWT _r	rural background groundwater temperature
HD	heating demand
hGSHP	horizontal ground source heat pump
LU	land use
LUC	land utilisation class
RF	Rintheimer Feld
RDD	restriction of the drilling depth
SUHI	subsurface urban heat island
URG	Upper Rhine Graben
T1, T2, T3	1 K, 2 K and 3 K temperature isotherms of thermal plumes
vGSHP	vertical ground source heat pump

Subscripts

a	after refurbishment
b	before refurbishment
LA	Lower Aquifer
UA	Upper Aquifer
UA+LA	combined Upper and Lower Aquifer

1 Introduction

1.1 Motivation

The report "EU pathways to a decarbonised building sector" by the company ECO-FYS reveals the vast and far-reaching impact of space heating demand on the European energy use and CO₂ budget:

"Heating and cooling today account for half of the EU energy consumption¹, [...]. The carbon dioxide emissions from residential heating account for a significant share of the average individual's carbon dioxide emissions, and 30% of the EU overall carbon dioxide emissions." Manteuffel et al. (2016)

To achieve the European goal to cut CO₂ emissions to at least 40% of the 1990 level by 2030, and to put a halt on global climate change, heat supply has to be shifted towards renewable energies. One option for a renewable and environmentally friendly heat supply are shallow geothermal systems. According to Yousefi, Abbaspour, and Seraj (2019), the energy production by direct use of geothermal systems will generate over 500 TWh by 2030 whereby more than 100 million tones CO₂ emissions could be globally saved, showcasing a great potential to reduce carbon dioxide emissions. Unlike other renewable energies, shallow geothermal energy is independent of time, season or weather conditions and, except for horizontal ground source heat pump systems, has a low space requirement above ground. Furthermore, geothermal energy is practically everywhere available and continuously regenerates itself through heat input above and below ground. In urban areas, where GWTs are increased and annual heat input by anthropogenic heat sources act as a natural replenishment, potential and sustainability of shallow geothermal use are augmented.

1.2 Groundwater Temperatures and Subsurface Urban Heat Island Effect

Defining and understanding the thermal regime of the shallow subsurface is crucial for the use of shallow geothermal energy. The shallow thermal regime, comprising the first few decameters below the surface (Stauffer et al., 2014), is continuously replenished from heat sources above and below. The heat sources from below are residual heat from planetary accretion and radioactive decay (Böttcher et al., 2016). This terrestrial heat input, known as geothermal heat flux, is on average 0.065 W/m². In contrast, the heat input from above by solar radiation on the Earth's surface in Central Europa is 1000 kWh/m² (Stober and Bucher, 2012). The seasonal signal by solar radiation at the ground surface can be traced up to a depth of 10–15 m (Taylor and Stefan, 2009). Below this point, seasonal temperature fluctuations are damped and groundwater temperatures (GWT) are relatively stable with temperatures equal to the mean annual air temperature (Dwyer and Evans, 2010). However, due to climate change not only air temperatures increased over the past decade but also

ground surface temperatures (GST) and GWT (Beltrami, Ferguson, and Harris, 2005; Beltrami et al., 2006; Menberg et al., 2014; Pollack, 1998). Beltrami (2002) mathematically inverted borehole log data and observed a global GST increase by 0.45 K over the past 200 years. Yet, elevated soil and groundwater temperatures, in particular in urban areas are not exclusively explainable by global climate change. Land use changes and an increase in subsurface structures due to urbanisation cause elevated GWT (Taylor and Stefan, 2009; Taniguchi, Uemura, and Jago-on, 2007). GWT beneath urban areas are up to 5 K higher than in comparison to undisturbed GWT in rural surroundings (Zhu et al., 2015; Menberg et al., 2013a; Taylor and Stefan, 2009; Ferguson and Woodbury, 2004). This warming of GWT in urban areas is known as the subsurface urban heat island (SUHI) effect and observed in cities worldwide (e.g. Bidarmaghz et al., 2019; Hemmerle et al., 2019; Ferguson and Woodbury, 2007; Taniguchi et al., 2009; Huang et al., 2009; Arola and Korkka-Niemi, 2014). The heat input into the subsurface by increased GST and urban subsurface structures, causing high GWT, can be described by thermal conduction (Baehr and Stephan, 2011; Carslaw and Jaeger, 1959; Smerdon et al., 2003).

The conductive heat transport is defined as a heat flux q due to a temperature difference ΔT in a media of thickness d with the thermal conductivity λ and is expressed by Fourier's Law:

$$|q| = \lambda \cdot \frac{\Delta T}{d} \quad (1.1)$$

The heat transfer from the ground surface through the unsaturated zone to a shallow aquifer is dominant in the vertical direction and can be described by one-dimensional conduction models (Taylor and Stefan, 2009). Based on Fourier's law (Equation 1.1) Menberg et al. (2013b) and Benz et al. (2015) developed a 1D analytical and statistical heat flux model to compute the anthropogenic heat flux (AHF) in the unsaturated zone. The AHF defines the heat input into the shallow subsurface caused by elevated GST and anthropogenic subsurface infrastructures, such as road tunnels, sewers, district heating pipes, buildings and basements. Moreover, Benz et al. (2015) used the term anthropogenic heat flow to refer to the sum of all generated heat fluxes over the entire city area. Both studies identified elevated GST and basements as the dominant heat source for the evolution of SUHIs. There are also plenty of other studies identifying basements and increased GST as main drivers for the evolution of SUHIs (e.g. Benz et al., 2018a; Dahlem, 2000; Epting, Händel, and Huggenberger, 2013; Nawalany and Sokołowski, 2019; Kupfersberger, Rock, and Draxler, 2017). Beside the diffuse and widespread warming of the urban subsurface, anthropogenic heat sources also induce local hotspots with GWT above 30 °C (Menberg et al., 2013a; Kerl et al., 2012; Ferguson and Woodbury, 2004). GWT anomalies could be ascribed to underground car parks, construction sites, wastewater treatment plants, mines, landfills or power stations (Benz, Bayer, and Blum, 2017a; Benz et al., 2018a; Bucci et al., 2017; Epting et al., 2017b). Benz, Bayer, and Blum (2017b) applied the anthropogenic heat intensity (AHI) to identify temperature anomalies in the air, surface and groundwater (GW). Concerning GWT anomalies, AHI is defined as the difference between the locally measured GWT and the average rural background GWT. They also identified local hot spots and emphasized the huge impact of human activity on GWT, not only in cities but also in agricultural areas. However, they did not further investigate the local heat sources of these GWT anomalies. Up to now, far too little attention has been paid to locations, frequencies and implications of small scale and local temperature anomalies and the associated heat sources.

1.3 Shallow Geothermal Energy

The heat stored in the subsurface, the shallow geothermal energy, can be harnessed by open- and closed-loop shallow geothermal systems. Shallow geothermal energy is characterised by drillings with a maximum depth of 400 m (Bauer et al., 2018). Since the temperature range in the shallow subsurface is too low for direct heating, the heat exchanger is coupled with a heat pump to raise the temperature to a level required by the space heating system.

1.3.1 Shallow Geothermal Systems

Open-looped geothermal systems, known as groundwater heat pump (GWHP), directly use groundwater as heat transfer medium. The groundwater is pumped to the surface through a production well. There, the heat of groundwater is extracted and returned to the aquifer via a reinjection well. The power of a GWHP depends on the extractable temperature difference ΔT , exploitable aquifer thickness and hydraulic conductivity. Site and performance of GWHP systems strongly depend on the site-specific GW conditions. Pore aquifers with a low water hardness as well as low sulphate, iron and manganese concentration are most suitable. Fractured and karst aquifers are less feasible for GWHP systems, due to their risk of not finding GW, or of a thermal short circuit during system operation (Baden-Württemberg, 2009a).

Closed-loop systems are heat exchangers which are also combined with a heat pump and referred to as ground source heat pump systems (GSHP). The heat exchangers are horizontally (hGSHP) or vertically (vGSHP) installed tubes in which a heat transfer fluid circulates. Horizontal GSHP, also called collectors, are horizontally aligned tubes, buried below the local frost line (Baden-Württemberg, 2008). The extractable energy per area [W/m^2] depends on the annual operation time and site-specific ground properties. Due to the shallow installation depth, collectors are perfectly suitable for areas with a drilling depth limitation. However, collectors have an extremely large space demand which is about the size of the heated building area.

Vertical GSHP (vGSHP) systems utilise vertically installed borehole heat exchanger (BHE) to extract heat from the subsurface and thus cool the area around the tube. The amount of extractable energy per meter, the heat extraction rate [W/m], and the new influx of energy from the BHE surroundings depend on the thermal conductivity. An additional advective heat input by GW flow increases thermal conductivity, thus higher heat extraction rates up to 114 W/m are achievable (Viesi et al., 2018; Erol, 2011). These high heat extraction rates, and the related immense energy gain, are one advantage of BHEs. Further benefits of BHE are their low space demand above ground and their suitability for almost all subsurface conditions. On the other hand, the drilling of the boreholes causes high costs (Blum, Campillo, and Kölbel, 2011).

1.3.2 Geothermal Potential

In general, the ability of a geothermal system to extract the available heat is defined as geothermal potential. Researchers have developed various approaches to evaluate the geothermal potential on different scales and introduced diverse specific definitions of this term. For instance, Zhang, Soga, and Choudhary (2014) and Zhu et al. (2010) defined the local heat content stored in the subsurface as theoretical geothermal potential. García-Gil et al. (2015) and Alcaraz et al. (2016) used analytical solutions of heat transport equations to calculate a low-temperature geothermal potential (LTGP) for open- and closed-loop systems. According to Götzl et al. (2010),

the shallow geothermal potential combines the energy supplied by the subsurface with the application potential on demand side. Viesi et al. (2018) and Galgaro et al. (2015) also included the heating demand in their calculation and definition of the geo-exchange potential. Nam and Ooka (2011) and Noorollahi, Gholami Arjenaki, and Ghasempour (2017) incorporated numerical simulations and Epting et al. (2018), Epting and Huggenberger (2013), and Fujii et al. (2007) the numerical ground-water flow and heat-transport model tool FEFLOW[®] to optimise the estimation of the geothermal potential. Other studies utilised a geographical information system (GIS) to combine spatial geodata, such as temperature, hydro- and geological data, and to map the final geothermal potential (e.g. Gemelli, Mancini, and Longhi, 2011; Ondreka et al., 2007; Casasso and Sethi, 2016; García-Gil et al., 2015; Bezelgues-Courtade et al., 2010). The various geothermal potentials were estimated on quarter- (Zhang, Soga, and Choudhary, 2014; Miglani, Orehounig, and Carmeliet, 2018), city- (Schiel et al., 2016; Luo et al., 2018; Böttcher et al., 2019; Epting et al., 2020a), regional-scale (Ondreka et al., 2007; Gemelli, Mancini, and Longhi, 2011) or country-scale (Götzl et al., 2010; Rudakov and Inkin, 2019). While a variety of definitions for the geothermal potential have been suggested, this dissertation will use the definitions suggested by Bayer et al. (2019). They defined the physically existing energy, for example the energy stored in an aquifer, as theoretical geothermal potential. The technical geothermal potential is the portion of the theoretical geothermal potential that can be actually extracted with a specific system. It takes account of hydro- and geological conditions as well as legal constraints.

Legal constraints refer to a drilling depth of boreholes, system spacings or temperature limitations of the reinjected water by GWHP. The studies by Hähnlein, Bayer, and Blum (2010), Hähnlein, Blum, and Bayer (2011), Tsagarakis et al. (2018), Jaudin et al. (2013), and Somogyi, Sebestyén, and Nagy (2017) provided a European and worldwide overview of the licensing practice for geothermal use. The different legislations vary from country to country, based on technical guidelines, national or regional water management and are established by ground-water protection authorities or different ministries. In some countries, such as Austria, Denmark and the Netherlands regulations are legally binding, in other countries like Germany, they are just recommendations. VDI 4640 part 2 (2015) recommends a minimum spacing between a geothermal system and a building of 2 m, between a system and a subsurface supply line of 1 m and between BHEs of 6 m. However, on a federal level, different guidelines can exist. In the state of Baden-Wuerttemberg, a BHE spacing of 10 m is recommended to avoid thermal interference (Baden-Württemberg, 2005). Since special licensing according to the German federal mining law (BBergG, 2017) is required for boreholes deeper than 100 m, the typical BHE length in Germany is 100 m. The guidelines also have a significant influence on the technical geothermal potential of GWHPs. The tolerable temperature difference between the extracted and reinjected water is $\Delta T = 6$ K, while the minimum and maximum reinjection temperature have to stick to 5 °C and 20 °C, respectively. Especially in cities, where GWTs are already increased, this upper-temperature boundary limits the possible temperature difference which is required to efficiently run a cooling system (Epting, Händel, and Huggenberger, 2013; Ferguson and Woodbury, 2004).

Long-term system efficiency of geothermal systems requires sophisticated planning and management adapted to the local hydro-, geological and thermal conditions of the subsurface. For example, an insufficient spacing between two systems leads to thermal interference (Meng et al., 2019; Vienken et al., 2015; Kurevija, Vulin, and Krapec, 2012; Zhang et al., 2018). When geothermal systems are over-sized, e.g.

more heat is extracted than the subsurface can provide or can replenish from surroundings, the ground temperatures decrease and systems become inefficient (e.g. Patton et al., 2020; Ferguson and Woodbury, 2006; Bonsor et al., 2017). One way to maintain system efficiency is a coupling of GSHP with solar panels (Abu-Rumman, Hamdan, and Ayadi, 2020; Georgiev, Popov, and Toshkov, 2020). Few studies also proposed to benefit from annual anthropogenic heat input by recycling this waste heat to enhance the geothermal potential (Mueller, Huggenberger, and Epting, 2018; Epting et al., 2020b; Rivera, Blum, and Bayer, 2015a).

Most studies on geothermal potential only focused on either one (e.g. Arola et al., 2014; Ondreka et al., 2007; Casasso and Sethi, 2016; Noorollahi, Gholami Arjenaki, and Ghasempour, 2017) or maximum two (García-Gil et al., 2015; Götzl et al., 2010; Casasso and Sethi, 2017) different shallow geothermal systems. Furthermore, the studies are restricted on rough or standardised approximations of the present heating demand of the building stock (e.g. Gemelli, Mancini, and Longhi, 2011; Schiel et al., 2016; Zhang, Soga, and Choudhary, 2014) or rather assumed low-energy buildings (e.g. Perego, Pera, and Galgaro, 2019; Noorollahi, Gholami Arjenaki, and Ghasempour, 2017). No previous study compared the potentials and feasibility of two or three different geothermal systems and their likelihood to meet the present and future heating demand, when all buildings are thermally refurbished. In addition, the majority of present studies either centre upon shallow geothermal potentials on district- (Tissen et al., 2019; Zhang, Soga, and Choudhary, 2014; Miglani, Orehounig, and Carmeliet, 2018) or city-scale (Schiel et al., 2016; Luo et al., 2018; Böttcher et al., 2019), or upon the anthropogenic heat input into the subsurface (Kupfersberger, Rock, and Draxler, 2017; Menberg et al., 2013a). Few studies interrelate the anthropogenic heat input with the heating demand of a city (e.g. Benz et al., 2015; Benz et al., 2018a; Zhu et al., 2010). Yet, these studies only focused on the general budget of inflow and demand but not spatially resolved the local potential of sustainability on city-scale.

1.4 Objective

The following research questions can be derived from the above literature review and discussion:

- What causes positive groundwater temperature anomalies and where can we find them?

The diffuse and widespread anthropogenic heat input into the subsurface of cities causing SUHIs have been largely studied. Yet, quantity, spatial variability and influencing factors of local and small-scale GWT anomalies are poorly understood. The objective of the study in Chapter 2 is to localise, identify and classify GWT anomalies and their main drivers in central Europe.

- Where and how big is the geothermal potential in urban areas?

Over the past decades, a considerable amount of literature has been published on shallow geothermal systems and their potential to meet the heat demand of a quarter, city or region. Nevertheless, these studies rather draw their attention on either one or two different kinds of shallow geothermal systems and steady heat demand. Therefore, the second and third study aims to point out and spatially resolve the impact of hydro-, geological and legislative constraints on the shallow geothermal potentials of two to three different systems on quarter-

and city-scale. A further goal is to locally determine whether and for which geothermal system a shift in heat demand, specifically a heat demand before and after a thermal refurbishment of the building stock, can be met.

- What and where are the benefits of increased groundwater temperatures in urban areas?

Research to date solely connected annual heat demand and heat input theoretically, on large-scale or only for few anthropogenic heat sources. By doing so, they disregard the spatial and small-scale variation in heat demand and heat input. To overcome this knowledge gap, the third study investigates the spatial conditions and relation between heat demand and anthropogenic heat input, causing SUHI and GWT anomalies. Moreover, heat input is linked to the technical geothermal potential of open- and closed geothermal systems to identify the most suitable areas for geothermal use regarding heating supply and sustainability.

1.5 Thesis Structure

This cumulative dissertation consist of three independent studies presented in Chapter 2 - 4. All three studies were submitted to peer-reviewed, international journals, whereby the first two studies are already published.

The first study in Chapter 2 identifies the most extreme, positive temperature anomalies in central Europe. For this purpose, a huge GWT data set of 44,205 wells from ten European countries is statistically analysed. The anthropogenic heat intensity (AHI), which relates the median rural background GWT to local, multi-annual mean GWT, is applied to quantify and detect GWT anomalies. AHI within the top three percentiles, defined as AHI_{max} , are categorised and separately studied for the three land cover classes 'natural', 'agricultural' and 'artificial'. Since human impacts on groundwater are most relevant and localised in urban areas, I paid particular attention to temperature anomalies related to artificial surfaces. According to their type of land cover, AHI_{max} of wells within artificial surfaces are summarised and classified in six land utilisation (LU) classes. Furthermore, the heat sources of these hot spots are identified and combined in seven heat source classes. Finally, the significance and implications of GWT anomalies and their heat sources are discussed in context to regulations for shallow geothermal systems.

The second study in Chapter 3 compares the amount of thermal energy extractable by different shallow geothermal systems to the energy demand for space heating and domestic hot water for an urban quarter in Karlsruhe, Germany. For the first time, the technical geothermal potentials of hGSHP, vGSHP and GWHP are related to a measured heat demand before and after energy-saving refurbishment. The theoretical geothermal potential of GWHPs is also taken into consideration. The impact of legal regulations, varying space availability and hydro-/geological conditions on the geothermal potentials are analysed in nine different scenarios. A final inverse analysis of BHE spacing determines the minimum spacing, or rather the maximum amount of BHE, required to meet the heat demand before and after refurbishment

The third study, presented in Chapter 4, is a further development of the heat flux and heat flow calculations by Benz et al. (2015) and the evaluation of the technical geothermal potential described in Chapter 3. The approach by Benz et al. (2015) is transformed into a python-based code and, together with potential analysis, integrated into the tool GeoEnPy. This tool reads, process and combines (geo-)data and

is applied to Vienna, Austria. GeoEnpy computes the anthropogenic heat flux and heat flow into the subsurface, the technical geothermal potentials of BHE and GWHP systems, theoretical sustainable potential and heat supply rate. The anthropogenic heat flow acts as a continuous heat source, which thermally recharges the ground, and is therefore referred to as the theoretical sustainable potential. The term heat supply rate expresses the percentage of space heat demand before and after a thermal refurbishment of Vienna's building stock that can be satisfied by either BHE or GWHP systems. Both, the anthropogenic heat flow and technical geothermal potential are spatially resolved and related to Vienna's annual heating demand to identify key locations for geothermal use.

The final Chapter 5 summarises and connects the major results of the studies in Chapter 2 - 4. A final paragraph addresses implications and perspectives of increased GWT, and gives an outlook for future studies.

2 Groundwater Temperature Anomalies in Central Europe

Reproduced from: Tissen, C., Benz, S. A., Menberg, K., Bayer, P. and Blum, P.: Groundwater temperature anomalies in central Europe, *Environ. Res. Lett.*, 14(10), 104012, doi:10.1088/1748-9326/ab4240, 2019.

Abstract

As groundwater is competitively used for drinking, irrigation, industrial and geothermal applications, the focus on elevated groundwater temperature affecting the sustainable use of this resource increases. Hence, in this study groundwater temperature (GWT) anomalies and their heat sources are identified. The anthropogenic heat intensity (AHI), defined as the difference between GWT at the well location and the median of surrounding rural background GWTs, is evaluated in over 10,000 wells in ten European countries. Wells within the upper three percentiles of the AHI are investigated for each of the three major land cover classes (natural, agricultural and artificial). Extreme groundwater temperatures ranging between 25 - 47 °C are attributed to natural hot springs. In contrast, AHIs from 3 - 10 K for both natural and agricultural surfaces are due to anthropogenic sources such as landfills, wastewater treatment plants or mining. Two-thirds of all anomalies beneath artificial surfaces have an AHI > 6 K and are related to underground car parks, heated basements and district heating systems. In some wells, the GWT exceeds current threshold values for open geothermal systems. Consequently, a holistic management of groundwater, addressing a multitude of different heat sources, is required to balance the conflict between groundwater quality for drinking and groundwater as an energy source or storage media for geothermal systems.

2.1 Introduction

Groundwater is an important resource for society and industry. Within the European Union, it is the main source of drinking water, supplying about 50% of the total demand (Commission, 2016). However, it is equally important for agriculture. Depending on the country and type of agricultural production, up to 90% of the water for irrigation originate from groundwater (eurostat, 2019). In the industrial, commercial and residential sectors the use of groundwater as a resource for heating and cooling purposes is increasing worldwide (Lund and Boyd, 2016). Additionally, the surrounding ecosystem strongly depends on the groundwater quality and temperature (Arning et al., 2006; Bonte et al., 2011a; Bonte et al., 2011b; Brielmann et al., 2009; Brielmann et al., 2011; Brons et al., 1991; Griffioen and Appelo, 1993; Possemiers, Huysmans, and Batelaan, 2014). Multiple uses of groundwater lead to high competition between different interest groups. Consequently, a holistic groundwater

management in terms of quantitative, qualitative and thermal issues, as well as sensible regulations of this highly demanded source are essential (Datta, 2005; Flörke, Schneider, and McDonald, 2018).

The European Union (EU) Water Framework Directive (WFD) (WFD, 2000) defines the status of groundwater in terms of quantity and chemical quality. Groundwater quality and dependent ecosystems strongly rely on physical and chemical properties, which are in turn influenced by the groundwater temperatures (Riedel, 2019; Sharma et al., 2012). The temperature determines natural bacterial and fauna community composition as well as biogeochemical processes (Briellmann et al., 2009; Hall, Neuhauser, and Cotner, 2008). An increase in groundwater temperatures (GWTs) enhances the propagation of pathogen microorganisms, which in turn endanger the hygienic state of groundwater and therefore its use as a drinking water resource (Briellmann et al., 2011). Thus, the WFD classifies heat input into the aquifer as pollution. However, a study by Hähnlein et al. (2010) on the legal status of shallow geothermal energy use reveals great differences between European countries. In the countries, regulations are based on national or regional water management and/or ground-water protection authorities, different ministries or technical guidelines with the main purpose of the protection of groundwater as drinking water resource (Tsagarakis et al., 2018). Furthermore, these regulations mostly concentrate on the temperature of reinjected water from industrial cooling processes and/or open geothermal systems. Until now, little attention has been paid to other anthropogenic heat sources, which may have an even larger and more widespread impact on groundwater temperatures (Epting, 2017; Epting and Huggenberger, 2013; Menberg et al., 2013b; Menberg et al., 2013a).

Shallow GWTs are subject to seasonal variations down to a depth of 10 - 15 m (Taylor and Stefan, 2009). Comparable to air temperatures, GWTs also depend on altitude and latitude (Benz, Bayer, and Blum, 2017a). For instance, mean GWT fluctuates between 2 °C to 20 °C between northern and southern Europe (Bonsor et al., 2017). However, the natural state of GWT is altered by human activities. While groundwater is globally affected by increasing temperatures due to climate change (Beltrami, Ferguson, and Harris, 2005; Benz et al., 2018b; Green et al., 2011; Gunawardhana and Kazama, 2012; Kurylyk, Bourque, and MacQuarrie, 2013; Menberg et al., 2014; Singh and Kumar, 2010), there are regional, anthropogenic impacts elevating GWT above its average and natural state. Changes in land use and advancing urbanisation in particular, directly influence groundwater recharge, level and temperature (Colombani, Giambastiani, and Mastrocicco, 2016; Sharp, 2010). Increased surface temperatures due to artificial, sealed surfaces and underground structures, raise the groundwater temperature beneath cities leading to so-called subsurface urban heat islands (SUHI) (Benz et al., 2018a; Ferguson and Woodbury, 2007; Taniguchi, Uemura, and Jago-on, 2007; Zhu et al., 2015). These SUHIs are often quantified by measuring the urban heat island intensity, which is defined as the difference between GWT in the urban area and in the rural background. In Germany, Menberg et al. (2013a) determined average SUHI intensities of about 3 to 7 K, but also detected local hot spots with GWT up to 20 K warmer than the rural background temperature.

Further GWT anomalies induced by underground car parks, construction sites, wastewater treatment plants, mine, landfills or power stations are also observed (Benz, Bayer, and Blum, 2017a; Benz et al., 2018a; Bucci et al., 2017; Epting et al.,

2017b). In their study on GWTs in Germany, Benz, Bayer, and Blum (2017b) introduced the anthropogenic heat intensity (AHI), which relates average rural background temperatures to local temperature measurements. They found GWTs to be much more impacted by human activity than by atmospheric and surface temperatures. However, they did not comprehensively discuss the encountered GWT anomalies. Hence, there is still a lack of understanding of these temperature extremes, and many questions remain unanswered in regard to the locations, frequencies, implications and associated point sources of such small scale and local temperature anomalies.

This study therefore aims to map, track and discuss the occurrence of temperature anomalies in shallow aquifers in central Europe. Based on (multi-)annual mean GWT data from ten European countries (table S1), we determine the corresponding anthropogenic heat intensities (AHIs) to identify extreme, positive groundwater temperature anomalies. The AHI_{\max} , defined as the upper 3% percentile of all AHIs, are selected for each of the three major land cover classes (natural, agricultural and artificial) and linked to the detailed CORINE land cover types. We chose the upper 3% to assure significant AHIs, which are significantly above the measurement accuracy. Wells located under artificial surfaces, often in vulnerable aquifers, are examined in more detail in order to identify potential heat sources. Finally, we briefly discuss these GWT anomalies in the context of national regulations and assess the current and potential impact on our society.

2.2 Materials and Methods

2.2.1 Groundwater Temperatures

Shallow GWT data from 44,205 wells in ten countries in central Europe are the basis for this study. GWT data originate from monitoring networks and are provided by local authorities, environmental agencies or hydrogeological services (table S1). While 11% of the wells are equipped with GWT data loggers, most wells were monitored manually as part of chemical analyses. The highest well densities can be found in France, south-west Germany and Belgium, whereas only few sampled wells are located in Denmark and Slovakia (Figure 2.1a). To standardise the data set and to eliminate seasonal GWT variations, data from all wells are averaged over the time span from 2003 to 2017 following the procedure given in Benz et al. (2017a). In their approach, each temperature measurement is represented by a vector of a unit length of 1 and directed towards the month of measurement for a clocklike segmentation of the months. The output is the mean of all measurement vectors for one location, known as seasonal radius r , which is equal to zero for uniformly distributed measured data, and equal to one if they were collected in the same month. Following the recommendation by Benz et al. (2017a), all wells with a depth ≤ 60 m and $r \leq 0.25$, which indicates a bias-free annual mean, are considered for the further analysis (Figure A.1).

2.2.2 Anthropogenic Heat Intensity

For each well the anthropogenic heat intensity (AHI) is defined as the difference between GWT at the well location and the median of surrounding rural background groundwater temperatures (GWT_r) (Benz, Bayer, and Blum, 2017b) (equation 2.1). Based on the AHI definition by Benz, Bayer, and Blum (2017b), AHI is a measure of

the anthropogenic influence on GWTs. Yet, in this study AHI also detects thermal disturbances caused by natural sources, as we apply it to wells in urban as well as rural areas.

$$AHI = GWT - median(GWT_r) \quad (2.1)$$

The input parameters to determine the rural background temperature are the bias-free GWT, geographical elevation and nighttime light intensity. Elevation data are extracted from the Global 30 Arc-Second Elevation (GTOPO30) model and downloaded with Google Earth Engine (2015). Nighttime lights from Version 4 of the DMSP-OLS Nighttime Lights Time Series, processed by NOAA, were also extracted with Google Earth Engine. Since the night light data are only available up to January 2014, a 10 year average (01/2004 to 12/2013) was chosen. Nighttime light intensity is expressed as a digital number (DN) running from 0 to 63 indicating an increasing urban activity (Li, Zhao, and Li, 2016). All wells with a nighttime light of $DN < 15$, an elevation ± 90 m and within a distance of 47 km to the analysed location are considered for the calculation of rural background temperature (Benz, Bayer, and Blum, 2017b). To ensure meaningful statistics and to avoid an impact by outliers AHI is only determined, if at least five wells fulfil these criteria.

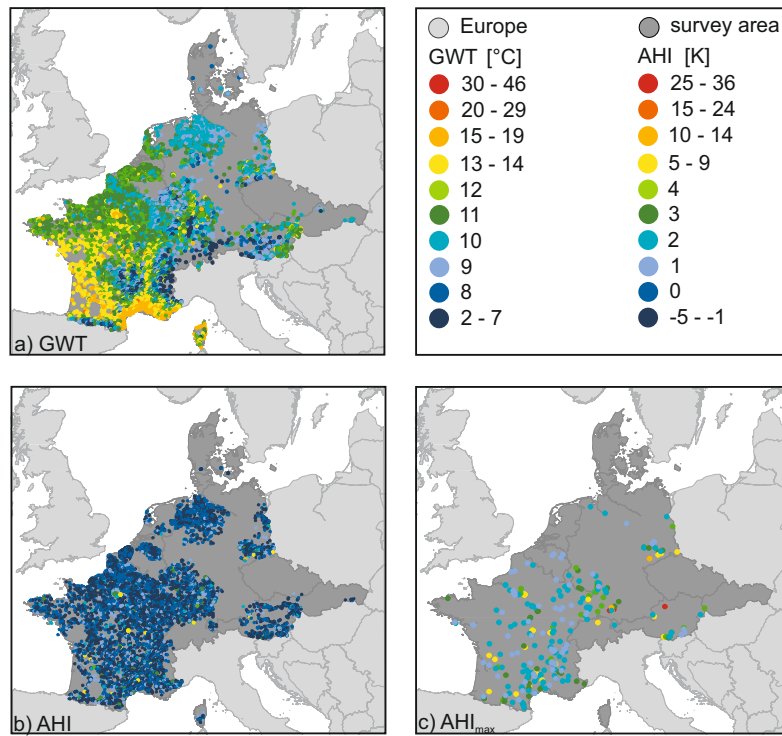


Figure 2.1: a) Overview of the survey area and distribution of all 12,151 wells with bias-free annual mean groundwater temperatures (GWTs), b) all 10,656 wells for which an anthropogenic heat intensity (AHI) could be determined, and c) the upper 3% percentiles of the three land cover classes natural, agricultural and artificial resulting in 318 hot spots (AHI_{max}).

2.2.3 Land Cover Classification

The CORINE Land Cover (CLC) (CORINE, 2016) classification scheme consists of three hierarchical levels with 44 land cover classes at the third and most detailed level (Figure S2). Based on Level 1, we define three main land cover classes: (1) natural, (2) agricultural and (3) artificial. The natural class is a combination of CLC's classes "forest and semi natural areas" and "wetlands". The agricultural class contains CLC's "agricultural areas" and the artificial class includes all "artificial surfaces". The calculated AHIs are categorised into and separately analysed for these three main classes (Figure S3).

2.2.4 Groundwater Temperature Anomalies

The wells within the upper 3% percentile of each class are specified as temperature anomalies AHI_{max} . All AHI_{max} wells within the artificial land cover class are closely inspected via satellite images (Google Earth). Based on observed common characteristics, such as land use, economic activity and settlement structures, we defined specific land utilisation classes with detailed subclasses and identified possible heat sources of these hot spots.

2.3 Results and Discussion

2.3.1 Statistics of Groundwater Temperature Anomalies (AHI_{max})

Based on the bias-free annual mean GWT (12,151 wells) an AHI could be evaluated for 10,656 wells (Figure 2.1b). AHI is uniformly distributed over all known measurement depths, proving its independence of depth (Figure S4). Its distribution is given in Figure S5 - S7. Figure 2.1c displays the wells within the top three percentiles, which represent 318 GWT anomalies (AHI_{max}) in total. 97% of these hot spots are located in Austria, France and Germany, which have the highest AHI well density overall. In Belgium, hot spots exist only in agricultural areas. Slovakia, Switzerland and Luxembourg have only one hot spot in the class artificial and natural, respectively. Czech Republic, Denmark and Netherlands do not show any (Figure S8). The hot springs in Austria and Southwest Germany, as well as accumulations of hot spots in the Upper Rhine Graben URG and Eastern Germany clearly stand out (Figure 2.1c). The URG is a densely urbanised region with multiple industrial areas, while East Germany is widely known for its former coal and ore mining. The minimum values of AHI_{max} of the classes natural, agriculture and artificial are 2.3 K, 1.7 K and 3.9 K respectively (Figure S9).

To illustrate the link between land cover and temperature anomalies, the Level 3 CLC classes for wells with an AHI are compared with the CLC classes of the AHI_{max} wells (Figure 2.2). A shift in the percentages of wells in each land cover class between these two sets is evident. Hence, it becomes apparent for which land cover temperature anomalies appear more frequently. For wells located on natural land cover, the percentage of wells in coniferous and mixed forests decreases from AHI to AHI_{max} , whereas the percentage of wells associated with transitional woodland-shrub and natural grasslands triples. The latter are therefore more likely to contain GWT anomalies. One explanation is that soil temperatures and/or GWT beneath

grass or farming land are typically higher than those beneath a forest, due to differences in incident solar radiation and evapotranspiration (Beltrami and Kellman, 2003; Kupfersberger, Rock, and Draxler, 2017).

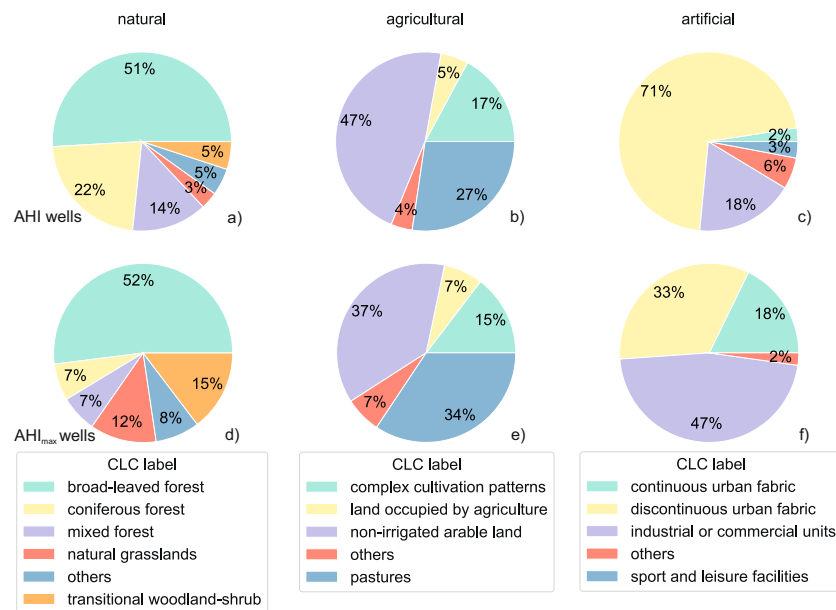


Figure 2.2: Percentage of wells falling into specific CORINE land cover (CLC) Level 3 classes for natural, agricultural and artificial classes, respectively. Upper row: All 10,656 wells having an anthropogenic heat intensity (AHI) (a-c), bottom row: 318 AHI_{max} wells representing the upper 3% percentile of all AHI wells (d-f).

In contrast, the shift from non-irrigated arable land to pastures in the agricultural class cannot be exclusively explained by physical effects due to vegetation or shielding foliage. According to Herb et al. (2008), ground surface temperatures (GSTs) beneath grass and land with different plant canopies are similar. A possible explanation for the anomalies is deforestation, which is known to cause subsurface temperature anomalies (Brink et al., 2007; Foley, 2005; Lewis and Wang, 1998; Taniguchi et al., 1999), that are detectable at depths of 20 to 100 m (Ferguson and Beltrami, 2006). Regarding the temporal and horizontal extent of such temperature anomalies, a lateral spread of several hundred meters over 100 years can occur (Bense and Beltrami, 2007). Nevertheless, one has to notice that AHIs > 3 K under both natural and agricultural surfaces result from hot springs or local anthropogenic sources, such as contamination caused by landfills, mining or waste water treatment plants.

In the artificial class, the share of discontinuous urban fabric shifts towards industrial areas and continuous urban fabric. Multiple previous studies on SUHIs indicated local hot spots within dense urban areas and industrial sites, which is also evident in our current findings here. Epting et al. (2017b), Menberg et al. (2013a) and Ferguson and Woodbury (2004) noticed a strong correlation between the highest underground temperatures and the density of buildings, in particular buildings with heated basements. For the city centre of Cologne and Winnipeg, Zhu et al. (2010) found an increase in GWT of up to 5 K, which compares closely with the median of the AHI_{max} of artificial surfaces in this study (Figure S9). Epting et al. (2017a) observed an increase of GWT up to 6 and 8 K in dense industrial and commercial

areas of Basel. Single point heat sources in industrial areas were also mentioned by Ferguson and Woodbury (2005), Bucci et al. (2017) and Menberg et al. (2013a).

2.3.2 GWT Anomalies (AHI_{max}) Beneath Artificial Surfaces

The outcome of the detailed visual inspection and examination of the surroundings of the 45 artificial AHI_{max} wells are six land utilisation classes (LUC) with 20 detailed subclasses (Figure 2.3 and S10). With a mean AHI of 7 K, the LUC "factory" has by far the largest impact on GWT, whereas the mean AHI of "industry parks" is the smallest with on average 5 K. With regard to the share of each utilisation class, most of the hot spots are within "city" (33%), followed by "factory" and "industry park" with 27% and 24%, respectively. In the following, possible heat sources within specific land utilisation classes are discussed.

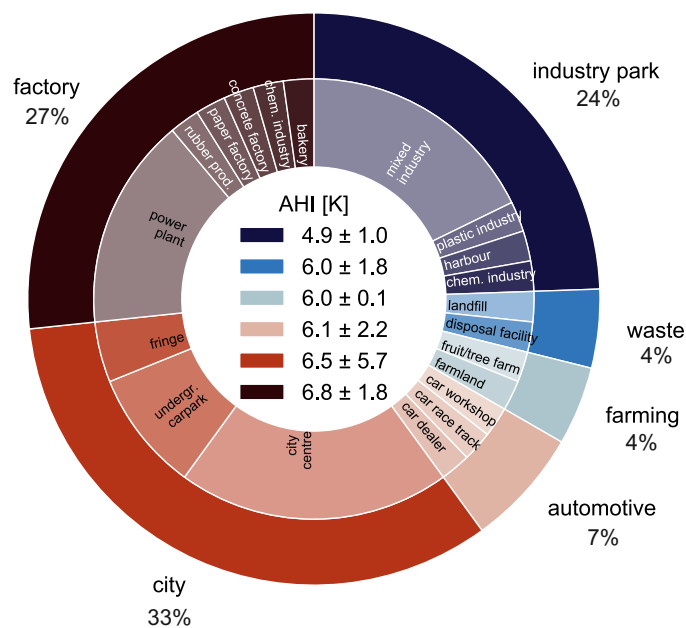


Figure 2.3: Segmentation of land utilisation classes (LUC, outer circle), colour coded according to their mean anthropogenic heat intensity (AHI) and standard deviation (\pm), and more detailed subclasses (inner circle) of the 45 AHI_{max} of artificial surfaces.

In the LUC "industry park", different industrial branches such as plastic, paper, electronic, chemical or machinery construction companies are mixed with office buildings and supermarkets. Here, high GWTs can originate from multiple heat sources such as basements with heating installations, sealed surfaces or injection of cooling water. These interfere with each other and can add up so that the distinct heat source of the groundwater anomaly is difficult to identify. Bucci et al. (2017) also referred to heat fluxes from buildings into the ground originating from industrial exothermic processes inside the buildings as cause for high GWT above 17 °C in an industrial district close to Turin city.

In the LUC "waste", one well is close to a landfill with an enclosed waste recycling plant, while the other one is on the premises of a waste disposal facility with detention basins and compensating reservoir. Benz et al. (2018a) also identified a wastewater treatment plant in Osaka, Japan, as a local heat source for increased GWT.

Despite a high thematic accuracy of over 85%, wrong classifications of CLC classes can also occur (EEA, 2006). Here, two wells in the artificial class are located on farmland and a fruit plantation, and thus actually fall into the agricultural class and the LUC "farming".

The LUC "automotive" refers to wells located at a car workshop, a car race track and car dealer. The common characteristic of the automotive class are sealed surfaces and possible contamination with petroleum hydrocarbons (Akankpo and Igboekwe, 2011).

The high mean AHI and standard deviation of the LUC "city" stand out and reflect the significant, yet variable impact of the different subclasses and of the corresponding heat sources. High GWT in city centres are due to the interference and superposition of heat input by sealed surfaces and underground structures, as already described in several SUHI studies (Benz et al., 2015; Benz et al., 2016; Benz et al., 2018a; Bucci et al., 2017; Epting et al., 2017b; Menberg et al., 2013a; Oke, 1973; Taniguchi et al., 1999; Taniguchi, Uemura, and Jago-on, 2007; Zhu et al., 2010). A conspicuous cluster of wells showing increased GWT were observed close to underground car parks and therefore, classified as separate subclasses. The fringe subclass contains less dense urban areas. A hot spring in Austria, having the highest AHI (27.0 K) of all artificial wells, falls within this subclass and causes the overall high AHI and standard deviation of LUC "city". Disregarding this natural temperature anomaly leads to a mean "city" AHI of 5.0 ± 1.7 K.

The LUC "factory" comprises wells situated on the property of a detached, single factory that is not part of an industrial park. All seven wells in the subclass power plant are at the same location in France, whereas the remaining subclasses are only represented by one well location each. GWT anomalies with temperatures over 30 °C in the vicinity of power plants were also reported by Menberg et al. (2013a).

2.3.3 Heat Sources of AHI_{max}

For 16 out of the 45 hot spots of the class artificial, we were able to identify potential heat sources summarised into seven classes (table 1). It is important to note that other underground heat sources such as industrial cooling, geothermal applications or sewage pipes are likely (Benz et al., 2015; Menberg et al., 2013b; Zhu et al., 2015; Bucci et al., 2017), but could not be detected with the here proposed method relying on satellite imagery and local knowledge. The highest temperature anomaly is associated with a hot spring in Austria. All remaining temperature anomalies and heat source classes refer to anthropogenic activities. Based on their spatial extent and impact magnitude they can be divided into two groups. The first group consists of heat sources that are scarce, but have a large extent, such as contaminations and mining operations. Basements, district heating networks, swimming pools and underground car parks are the second group. They are rather local sources, but are more frequent in urban environments and therefore also have an extensive impact on GWTs.

The first group, containing the heat sources contamination and mining, exhibits the highest GWT and AHI of all identified anthropogenic heat sources with temperatures of up to 8 K warmer than the rural surrounding. The three wells in the class contamination refer to two wells in LUC "waste", and one well is at a car race track (LUC "automotive"). Exothermic chemical and biological degradation processes in landfills or contaminated sites can result in higher groundwater temperatures (Bucci et al., 2017; Menberg et al., 2013a). Krümpelbeck (2000) reported temperatures up to 60 °C in a landfill. Similar to landfills, exothermic biogeochemical weathering

Table 2.1: Individual values, means and standard deviations (std) of the groundwater temperature (GWT) and anthropogenic heat intensity (AHI) for the 16 identified heat sources and seven heat source classes of the hot spots (AHI_{max}) within artificial areas.

Heat source	Nr. of locations	Parameter	Values					Mean	std	
Hot spring	1	GWT [°C]	37.9					37.9	0.0	
		AHI [K]	27.0					27.0	0.0	
Contamination	3	GWT [°C]	23.3	18.2	17.6				19.7	2.5
		AHI [K]	9.2	7.7	4.2				7.0	2.1
Mining	2	GWT [°C]	20.9	16.7				18.8	2.1	
		AHI [K]	10.6	6.2				8.4	2.2	
Basement	1	GWT [°C]	15.9					15.9	0.0	
		AHI [K]	4.0					4.0	0.0	
District heating	3	GWT [°C]	15.6	15.4	14.3				15.1	0.6
		AHI [K]	4.4	4.2	4.0				4.2	0.1
Swimming pool	1	GWT [°C]	16.0					16.0	0.0	
		AHI [K]	4.1					4.1	0.0	
Undergr. car park	5	GWT [°C]	17.1	17.3	14.3	15.0	15.3	15.8	1.2	
		AHI [K]	6.8	5.3	4.5	4.3	4.0	5.0	1.0	

processes, called acid mine drainage (AMD), cause high temperatures in mines and their remote surroundings (Willscher et al., 2010). Reports by Felix et al. (2009) and LfULG (2010) confirm AMD as heat source of one particular well in the LUC subclass fringe, situated in a hard coal mining district in eastern Germany. Furthermore, they described increased GWT in remote observation wells due to coal seam fires reaching temperatures up to 90 °C within the pithead stocks. The high GWT and AHI of the well in the subclass "farmland", located in an area in eastern Germany famous for ore mining, could also be associated with AMD.

The second group includes the small scale and local heat sources basements, district heating (DH) networks, swimming pool and underground car parks. The well linked to warming from basements, is 2 m away from a shopping mall in Karlsruhe, Germany. While the AHI of this well is lower than the ones associated with contamination and mining, almost every building in a city has a basement, which typically also hosts the heating installation of the building. Epting and Huggenberger (2013), Benz et al. (2015) and Epting, Händel, and Huggenberger (2013) also emphasised the large impact of basements on GWT and due to their high heat flux and dominant area, named them as the dominant drivers of SUHIs.

Correlating local district heating (DH) network plans with well positions, we could classify the heat source of three wells of the subclass city centre as DH. In district heating networks, water with temperatures up to 160 °C circulates under high pressure through pipes under many urban areas (Wien Energie, 2013). Depending on season and type of insulation, heat losses up to 20% occur (Recknagel, Sprenger, and Schramek, 2007). Benz et al. (2015) pointed out that DH pipes are a prominent source of anthropogenic heat fluxes. The time series in Figure S11 also clearly demonstrate the impact of DH heat fluxes on a groundwater observation well 3.5 m away from the pipe. Regarding the mean GWT at 6 m depth, representing the middle of the aquifer, AHI is as high as 8 K. Consequently, the heat input by DH pipes, especially in case of a local leakage is not negligible and should be considered more carefully. Water with lower temperatures than in DH pipes is also released into aquifers by

leaking swimming pools. Cracks in the pool or loose tiles can cause leakage rates of $70 \text{ m}^3/\text{day}$ (Water, 2011). Another case study about a municipal swimming pool in Montreal reports a leakage rate of 350 to 700 m^3 per day into the underlying aquifer (Chapuis, 2010). Even if the swimming pool is watertight, the basin releases heat to the subsurface. One of the wells in LUC "city" is located 4 m away from a municipal swimming pool in Germany and the GWT of $16 \text{ }^\circ\text{C}$ is likely to be influenced by the heat release of the pool. Menberg et al. (2013a) even noticed a GWT of $20 \text{ }^\circ\text{C}$ for an observation well next to a swimming pool in Frankfurt, Germany. At another municipal swimming pool in Germany $25 \text{ }^\circ\text{C}$ beneath the swimming pool and increased GWT of 1 K to 3 K in the downgradient were measured (Blum et al., 2018).

In previous SUHI studies, underground car parks were intensively discussed as sources for GWT anomalies (Epting and Huggenberger, 2013; Menberg et al., 2013b; Zhu et al., 2010). This is in accordance with our findings that reveal underground car parks as the most frequent heat source of temperature anomalies in the class artificial (table 1). Warm, exhausted fumes and a poor ventilation lead to heat accumulation, so air temperature strongly increases in underground car parks. Iskander, Aboumoussa, and Gouvin (2001) recorded temperatures above $25 \text{ }^\circ\text{C}$ in summer at the lowest level of an underground car park. We also recorded air temperatures of up to $30 \text{ }^\circ\text{C}$ in an underground car park and correspondingly high GWT of almost $20 \text{ }^\circ\text{C}$ in an observation well within this car park (Figure S12). The correlation between these two temperatures is obvious and therefore the heat input of underground car parks into the aquifer is evident.

2.3.4 Regulations

Despite the multitude of underground heat sources, only open geothermal systems are currently regulated by legally binding temperature thresholds in Austria ($20 \text{ }^\circ\text{C}$), Denmark ($25 \text{ }^\circ\text{C}$) and the Netherlands ($25 \text{ }^\circ\text{C}$) (Hähnlein, Bayer, and Blum, 2010; Hähnlein, Blum, and Bayer, 2011). Four wells out of all 318 hotspots exceed the $25 \text{ }^\circ\text{C}$ threshold value, though they are natural hot springs in Germany and Austria. A maximum temperature (T_{max}) of modified groundwater of $20 \text{ }^\circ\text{C}$ and a relative change (ΔT) in GWT of $\pm 6 \text{ K}$ is given in the geothermal installation guidelines in Austria (legally binding) and Germany (recommended) (Hähnlein, Bayer, and Blum, 2010; Hähnlein, Blum, and Bayer, 2011). For all hot spots, we detected 13 wells that exceed T_{max} and 38 with an AHI exceeding ΔT of 6 K . While four of these temperature anomalies are associated with natural hot springs, the remaining nine temperature infringements, or rather 34 for AHI exceeding ΔT , are associated with anthropogenic heat sources. The majority of wells with a higher AHI than the 6 K temperature difference (ΔT) are in the artificial land cover class and located in Austria, France, Germany and Switzerland. When comparing our results with the accepted ΔT and T_{max} , we found that the mean AHI of the LUCs "automotive", "city" and "factory" are slightly above the ΔT limit, while the mean AHI linked to the heat source classes "contamination" and "mining" are 1 K or even more than 2 K above the criteria respectively. Since GWT is averaged, the information of seasonal positive or negative extreme values of the time series is not accounted for in this analysis. Individual GWT measurements might exceed the maximum groundwater temperature T_{max} more frequently. From the GWT time series in Figures S11 to S13, it becomes apparent that GWT peaks caused by basements, contamination, mining and district heating surpass the T_{max} -limit several times while annual mean values remain below the threshold. In case of aquifer thermal energy storage (ATES) systems, seasonal variation of GWTs also cannot be detected by AHI since the mean GWT is equal or

close to the GWT_r . Accordingly, the number of wells momentarily exceeding 20 °C is expected to be significantly higher than those found based on annual mean GWTs.

2.4 Conclusion

This study detects GWT anomalies in central Europe and identifies large- and small-scale anthropogenic heat sources such as mining and underground car parks. These extreme and until now unregulated heat sources seriously impact our groundwater. When GWTs continue to increase, groundwater cooling systems are no longer efficient (Epting, Händel, and Huggenberger, 2013; Ferguson and Woodbury, 2004). Furthermore, high GWT might also affect groundwater quality and ecology (e.g. (Bonte et al., 2011a; Bonte et al., 2011b; Danielopol et al., 2004; Hahn, Schweer, and Griebler, 2018; Hähnlein et al., 2013)). In some urban areas, where aquifers are already contaminated with heavy metals and organic compounds, an increase of GWT by only 5 K might also entail a decrease of dissolved oxygen and may lead to a mobilisation of other contaminants such as arsenic (Bonte et al., 2013; Bonte, Breukelen, and Stuyfzand, 2013; Bonte, Stuyfzand, and Breukelen, 2014; Griebler et al., 2014). Nevertheless, elevated GWTs provide the opportunity to harness more energy from the aquifer using shallow geothermal systems or make the operation of such systems more efficient (Arola and Korkka-Niemi, 2014; Bayer et al., 2019; Menberg et al., 2015; Rivera, Blum, and Bayer, 2017; Zhu et al., 2010). Overall, increased GWTs have multiple, long-term consequences and therefore, the complex interaction between heat sources and heat sinks in consideration of the aquifer characteristics should be further studied and also regulated. All these influencing factors have to be incorporated into future urban subsurface planning. Regulations should be more flexible, so that depending on the specific aims of the policy of cities and communities, the focus of groundwater management can be on groundwater as a resource for drinking water and/or as an energy resource. The use of numerical heat transport models could maximise the positive effects of increased GWT in order to meet the needs of various interest groups and to preserve the natural state of our groundwater ecosystems.

Acknowledgements

C. Tissen is grateful to the funding received through GRACE, the Graduate School for PhD students of the KIT-Center Climate and Environment at the Karlsruhe Institute of Technology (KIT). The work was also supported by the German Research Foundation (project no. B2850/3-1). The authors thank Alistair Fronhoffs (Vlaamse Milieumaatschappij), Arlette Liétar (Bruxelles Environnement), Martin Hansen (Geological Survey of Denmark and Greenland), Jürgen Gruber (Bayerisches Landesamt für Umwelt), Christian Gläser (Landesamt für Umwelt Brandenburg), Roland Funck (Der Senator für Umwelt, Bau und Verkehr), Mario Hergesell (Hessisches Landesamt für Naturschutz, Umwelt und Geologie), Lisa Beilharz (Tiefbauamt Karlsruhe), Gunter Wriedt (Niedersächsische Landesbetrieb für Wasserwirtschaft, Küsten- und Naturschutz), Peter Neumann (Landesamt für Natur, Umwelt und Verbraucherschutz), Wolfgang Plaul (Landesamt für Umwelt Rheinland-Pfalz), Sarah Melchior (Landesamt für Umwelt und Arbeitsschutz), Ulf Nilius (Landesbetrieb für Hochwasserschutz und Wasserwirtschaft Sachsen-Anhalt), Andreas Riese (Thüringer Landesamt für Umwelt und Geologie), Tom Michel (Administration de la Gestion de

l'Eau), Janco van Gelderen (Informatiehuis Water), Eugen Kullman (Slovak Hydrometeorological Institute) and Jessica Stapleton (Bundesamt für Umwelt) for the provision of data and additional information. Special recognition is also given to Nicolas Weidenthaler for the field work and collection of groundwater temperature data in Mannheim, Germany. We also thank the two reviewers for their comments.

3 Meeting the Demand: Geothermal Heat Supply Rates for an Urban Quarter in Germany

Reproduced from: Tissen, C., Menberg, K., Bayer, P. and Blum, P.: Meeting the demand: geothermal heat supply rates for an urban quarter in Germany, *Geothermal Energy*, 7(1), doi:10.1186/s40517-019-0125-8, 2019.

Abstract

Thermal energy for space heating and for domestic hot water use represents about a third of the overall energy demand in Germany. An alternative to non-renewable energy-based heat supply is the implementation of closed and open shallow geothermal systems, such as horizontal ground source heat pump systems, vertical ground source heat pump (vGSHP) systems and groundwater heat pump systems. Based on existing regulations and local hydro-/geological conditions, the optimal site-specific system for heat supply has to be identified. In the presented technical feasibility study, various analytical solutions are tested for an urban quarter before and after building refurbishment. Geothermal heat supply rates are evaluated by providing information on the optimal system and the specific shortcomings. Our results show that standard vGSHP systems are even applicable in older and non-refurbished residential areas with a high heat demand by using a borehole heat exchanger with a length of 100 m or in conjunction with multiple boreholes. After refurbishment, all studied shallow geothermal systems are able to cover the lowered heat demand. The presented analysis also demonstrates that ideally, various technological variants of geothermal systems should be evaluated for finding the optimal solution for existing, refurbished and newly developed residential areas.

3.1 Introduction

In 2016, the annual energy consumption for space heating and domestic hot water (DHW) in Germany was 2,987 PJ, which corresponded to approximately a third of Germany's total energy consumption. The main energy sources are still coal, oil and gas, which emit large amounts of CO₂ and contribute to global climate warming. For space heating and DHW, only 15% of the energy consumption was provided by renewable energies (BMWi, 2018). Among this 15% portion, shallow geothermal energy systems are particularly appealing, since they are continuously available. Lund and Boyd (2016) showed that 149.1 million tonnes of CO₂ could be annually saved by the direct utilisation of geothermal energy. Bayer et al. (2012) estimated that the potential heat supply by ground source heat pump (GSHP) systems for nineteen European countries is 100,000 TJ, corresponding to CO₂ savings of 3.7 million tonnes. Therefore, there is a great potential for geothermal energy systems to lower current

greenhouse gas emissions.

Shallow geothermal systems, which can be classified into closed and open systems, enable the direct use of geothermal energy. In closed systems, a synthetic heat carrier fluid is circulated in tubes that are installed in the ground for heat exchange. Open systems utilize wells to access groundwater as a heat carrier. In both variants, heat pumps are often employed for extracting heat and supplying heating applications. Closed-loop systems include horizontal (hGSHP) and vertical ground source heat pump (vGSHP) systems. In general, the ability of these systems to provide heating and/or cooling is described as the geothermal potential, for which multiple definitions and concepts exist. For example, Zhu et al. (2010) and Zhang, Soga, and Choudhary (2014) computed the theoretical geothermal potential as the heat content stored in a given volume of the subsurface for a given temperature reduction. According to Götzl et al. (2010), the potential of shallow geothermal energy is a combination of the technical potential, i.e. the energetic supply, and the applicability on part of energy consumers. A similar definition was given by Zhang, Soga, and Choudhary (2014) and Galgaro et al. (2015), who defined a ratio of the maximum amount of energy exchanged between the ground and vGSHP system to the heat or cooling demand. In our study, we follow the same concept and for a simplification, use the term “heat supply rate”.

Depending on the type of system, the geothermal potential can be evaluated in different ways. To estimate the very shallow geothermal energy potential of hGSHP systems, Bertermann et al. (2014) included legal constraints, climatic parameters and soil textures. García-Gil et al. (2015) proposed a low temperature geothermal potential (LTGP) for open- and closed-loop systems. They estimated the LTGP of the saturated zone using a steady-state analytical solution for conductive and advective heat transfer in porous media and applying a line source model for the unsaturated zone. Bezelgues-Courtade et al. (2010) created a geothermal potential map by combining several criteria such as transmissivity, temperature and hydrochemistry in a geographical information system (GIS).

Previous studies typically focused on the potential of one type of geothermal system. Mostly, vGSHP systems were examined by, for example, Casasso and Sethi (2016), Noorollahi, Gholami Arjenaki, and Ghasempour (2017) and Ondreka et al. (2007). Until now, evaluations of the potential of hGSHP and GWHP systems have attracted less attention (Bertermann, Klug, and Morper-Busch, 2015; Bezelgues-Courtade et al., 2010). Epting, Händel, and Huggenberger (2013) and (2018) focus on the potential of the groundwater body in the city of Basel. For the city of Barcelona, García-Gil et al. (2015) contrasted the results for vGSHP and GWHP systems. Götzl et al. (2010) conducted a comparative analysis of hGSHP and vGSHP systems for Austria. So far, however, no study has examined all three types of systems on a common ground, and a detailed comparison of the systems’ abilities to meet the heat demand of an urban quarter is still lacking. As the different technologies have different requirements, they are not equally suited. As a consequence, their geothermal potential will be different.

Many concepts of the geothermal potential refer to the actual heat (or cooling) demand of the study area, which is typically not exactly known. Though such data is often collected by the energy supplier, it is rarely publicly available. For this reason,

the heat demand is often estimated based on various assumptions and limited available data, such as building footprint and year of construction. Various studies use settlement types to categorize buildings and link them to the height and floor area of typical buildings (Gemelli, Mancini, and Longhi, 2011; Rivera, Blum, and Bayer, 2017; Schiel et al., 2016; Zhang, Soga, and Choudhary, 2014). The estimation of Götzl et al. (2010) also included the year of construction and climatic conditions. Schiel et al. (2016) pointed out that the imprecise estimation of the heat demand causes a large error in the determination of the borehole heat exchanger length required to supply urban demand by means of geothermal systems. Thus, a more accurate assessment of the feasible geothermal supply rate requires more precise, i.e. measured, energy consumption data.

The actual heat demand of an urban quarter is largely determined by the age of the buildings, or more precisely the energy standard. Eicker et al. (2011) considered only modern buildings with a typical low energy consumption. Noorollahi, Gholami Arjenaki, and Ghasempour (2017) worked with the heating and cooling demand of a new building and extrapolated it to the whole of Iran. Schiel et al. (2016) obtained a wider range of values for their calculations of the heat demand of the city Ludwigsburg in Germany, as their study distinguished old and new buildings with different energy standards. Eicker et al. (2011) and Blum, Campillo, and Kölbel (2011) noted that GSHP systems in Germany are typically installed in new, single-family buildings with a low heat demand, which are usually supplied with heat by two borehole heat exchangers (BHE). However, as stated by De Carli et al. (2014) and Solomon (2017), it is more reasonable to plan geothermal systems for an entire quarter or city instead of focusing only on individual houses.

This technical feasibility study explores and compares the potential of the three major shallow geothermal technologies (hGSHP, vGSHP and GWHP) by a spatial analysis using ArcGIS and analytical solutions for estimating the heat supply rate. For this, existing regulations and local hydro-/geological conditions are considered. In particular, we address the question whether the heat demand for space heating and domestic hot water (DHW) before and after the refurbishment of an urban quarter can be satisfied by one of these geothermal systems. For this purpose, we compute the heat supply rate that compares the geothermal potential of the three systems to the measured heat demand in an urban quarter of Karlsruhe, Germany.

3.2 Materials and Methods

3.2.1 Study Site

The study site is called "Rintheimer Feld" (RF), an urban quarter of 0.13 km² in the eastern part of Karlsruhe, which is located in the south-west of Germany and in the northern part of the Upper Rhine Graben (Figure 3.1). This study focuses on 31 multi-family houses providing living space for approximately 2,500 inhabitants (Jank, 2013). The area is characterized by wide green spaces with shrubbery and trees used for playgrounds and recreational purposes (Figure 3.2). The houses are owned by the municipal real estate company called "Volkswohnung GmbH" and

were built between the 1950s and 1970s (Figure 3.2). Housing complexes of the post-war era dominate the northern part of the quarter, whereas the southern part contains high-rise buildings of the 1960s and 1970s. With the aim to reduce CO₂ emissions and costs for heat supply, all buildings were refurbished in multiple stages between 1998 and 2014. The total costs of refurbishment amount to around 70 Mio. €. In this study, recently constructed buildings in the southern part are not considered, since the space for system installation and the heating area would change before and after refurbishment, and a direct comparison of the heat supply rate for these two cases is not feasible. For the purpose of an optimized refurbishment, the real estate company collected heat energy data before the refurbishment based on the gas consumption from 2005 to 2007. Since the refurbishment, all buildings are supplied by the municipal district heating network, and installed data loggers record the heat energy consumption on a monthly basis.

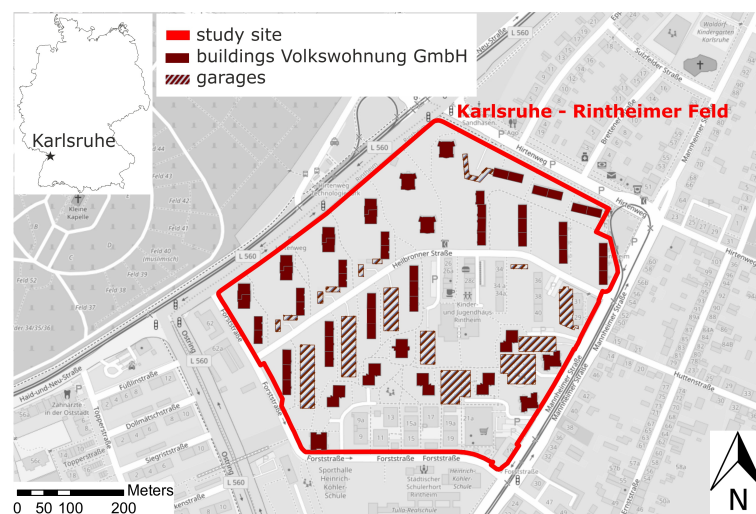


Figure 3.1: Overview of the study site “Rintheimer Feld”, an urban quarter in the eastern part of Karlsruhe, showing the location of the 31 multi-family houses and of garages.

3.2.2 Geological and Hydrogeological Data

The subsurface of Karlsruhe is characterized by the geology of the Upper Rhine Graben (URG), a Cenozoic continental rift valley mainly filled with Tertiary and Quaternary sands and gravels. The study site is located on a separate structural block close to the main Graben fault and confined by faults to the east and west (Figure 3.3).

The hydrogeological map in Figure 3.3 and the cross-sections in Figure 3.4 show the varying structure of the aquifers in the northern and southern part of the study area. In the north, the groundwater body is subdivided into an Upper and Lower Aquifer (Wirsing and Luz, 2005). The Lower Aquifer (LA) has a thickness of 18 m and is composed of Pliocene fluvial and limnic sediments, such as sands and silts. The Upper Aquifer (UA) consists of gravels and sands with a thickness of 13 m and represents the only aquifer in the south. Thus, the total aquifer thickness is higher in the north (31 m) than in the south (13 m). To protect the Lower Aquifer as a drinking water resource, restrictions for the maximum allowed drilling depth exist in some areas of the URG. According to the online information system for shallow



Figure 3.2: Impressions of the study site: Housing complexes of the 1950s (b) and high-rise buildings of the 1960s and 70s (a) separated by green spaces with trees and shrubbery and playgrounds. Photo c) shows an example of an underground car park.

geothermal energy of the state of Baden-Württemberg, called ISONG (LGRB, 2017), this restriction of the drilling depth (RDD) is set to 17 m below ground level in the entire study site, which is equivalent to the transition depth between the Upper and Lower Aquifer (Figure 3.4) in the northern study area. The delineation of the RDD is outlined in Figure 3.3 and follows local streets. Underlying both aquifers are Tertiary sedimentary rocks, composed of argillite, marlstone and marly sandstones. All hydro-/geological properties, such as hydraulic conductivity and porosity, are listed in Table A.2.

3.2.3 Evaluation of the Heat Supply Rate

The geothermal heat supply rate represents the percentage to which the required thermal energy for heating and DHW can be supplied by a specific geothermal system. Our method for evaluating the heat supply rate for each system is done in three steps. The first step is a spatial analysis using the geographical information system ArcGIS to evaluate the specific space available for each system type. The results of the spatial analysis represent the input parameters for the estimation of the geothermal potential in the second step. The geothermal potential E represents the maximum extractable thermal energy, which can be harnessed annually by each system. To account for the additional energy supplied by a heat pump, a coefficient of performance (COP) of 4 is assumed (Equation 3.2, 3.3, 3.4). The impacts of constraints imposed by existing regulations and hydro-/geological characteristics are investigated in nine scenarios, which are described in the following subsections. In the third and last step, we obtain the percental heat supply rate, S , by comparing the geothermal potential E for each system, E_{hGSHP} , E_{vGSHP} , E_{GWHP} , derived in each scenario with the measured heat consumption before or after refurbishment, H :

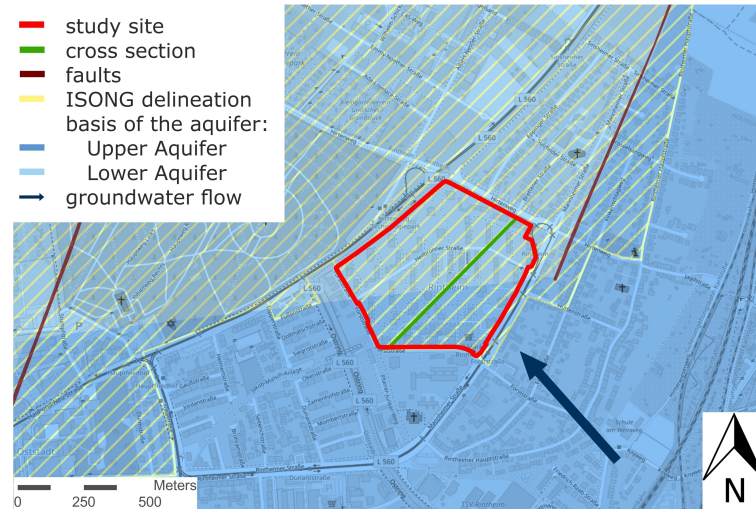


Figure 3.3: The hydrogeological map shows the basic hydro-/geological characteristics of the study site (red). The aquifer in the northern part of the study area contains the Upper and Lower Aquifer, the one in the south consists only of the Upper Aquifer. The area with a restriction on the allowed drilling depth defined by the online information system for shallow geothermal energy for the state of Baden-Württemberg, called ISONG (LGRB, 2017) is marked yellow, and the cross-section used for the energy flow approach is indicated by the green line. The groundwater flow direction is north-westwards.

$$S = \frac{E}{H} \cdot 100 \quad (3.1)$$

Horizontal Ground Source Heat Pump (hGSHP) System

For the hGSHP system, collectors consisting of a horizontal alignment of tubes, which are connected in series or parallel formation, are buried in very shallow depths of a few meters (Baden-Württemberg, 2008). The advantages of such hGSHP systems are low investment costs and their suitability for areas with drilling restrictions. However, the collector installation requires a ground surface that is free of shrubbery or trees, sealed surfaces and underground infrastructure, and the required areas are equal to or higher than the heated area of a building.

In the spatial analysis, the available, free area A_{hGSHP} to install the horizontal system within the study site is derived in ArcGIS based on available land use data. For this, the area covered by playgrounds, streets, buildings and garages, as well as a buffer zone of 1 m for hGSHP around buildings and garages (VDI 4640 part 1, 2010) is subtracted from the total area of the study site. This resulting area multiplied by the operational time t_h , the heat extraction rate q_{hGSHP} and the coefficient of performance (COP) yields the geothermal potential E_{hGSHP} (Equation 3.2):

$$E_{hGSHP} = q_{hGSHP} \cdot t_h \cdot A_{hGSHP} / (1 - 1/COP) \quad (3.2)$$

In accordance with Ramming (2007), who considers a spacing of the collector tubes of 0.26 m, the same soil type and local climate zone as at our study site, a maximum heat extraction rate $q_{hGSHP} = 33 \text{ W/m}^2$ is applied.

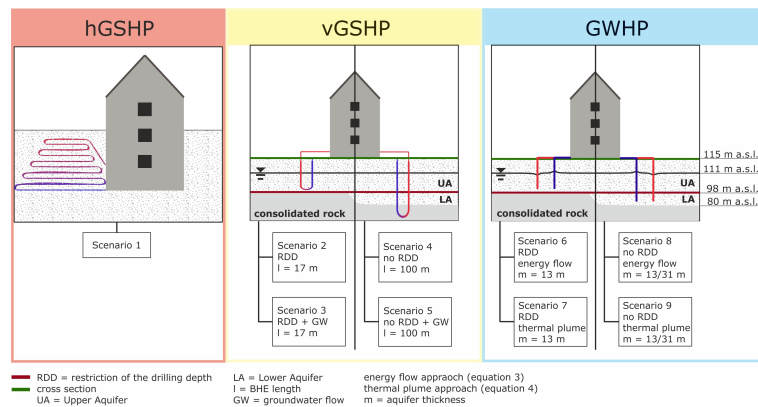


Figure 3.4: Illustration of the three studied shallow geothermal systems: horizontal ground source heat pump (hGSHP), vertical ground source heat pump (vGSHP) systems and groundwater heat pump (GWHP) systems. The nine studied scenarios consider variable heat extraction rates q (depending on groundwater flow GW , aquifer thickness m , a restriction of the drilling depth (RDD, no RDD), different BHE lengths l , and a fixed borehole heat exchanger (BHE) spacing $d = 10$ m). The cross-section along the green profile line (Fig. 3.3) shows the variation in aquifer thicknesses within the study site (UA = Upper Aquifer and LA = Lower Aquifer), the ground level and the depth of the water table.

Vertical Ground Source Heat Pump (vGSHP) System

Vertical GSHP systems use vertically installed plastic tubes, called borehole heat exchangers (BHE), to harness geothermal and solar energy (Rivera, Blum, and Bayer, 2015b). The standard length for a BHE varies for each country. For example, in the UK, the typical length is 150 m (Zhang, Soga, and Choudhary, 2014) or in Austria 110 m (Götzl et al., 2010). In Germany, BHE typically have a length of up to 100 m since deeper BHE require special licensing according to the German federal mining law (BBergG, 2017). A detailed overview of the corresponding legislation for the use of shallow geothermal energy is provided by Hähnlein, Bayer, and Blum (2010). The advantage of vGSHP systems is high heat extraction rates of up to 114 W/m in cases with favourable groundwater conditions (Erol, 2011). However, the drilling costs for the boreholes are higher than for a hGSHP system and therefore are also a disadvantage of this variant (Blum, Campillo, and Kölbl, 2011).

The spatial analysis of the vGSHP system is conducted in ArcGIS within two steps. First, the area available for boreholes is determined. Second, the maximum number of boreholes for a given BHE spacing d is determined. As recommended by the German technical guideline VDI 4640 part 2 (2015), a minimum distance between BHE and the buildings is ensured by setting a buffer zone of 2 m. In contrast, the studies by Zhang, Soga, and Choudhary (2014) and Miglani, Orehounig, and Carmeliet (2018) apply a distance of 3 m between borehole and building. According to Zhang, Soga, and Choudhary (2014), we assume that BHE can be installed beneath pavements and parking areas. Consequently, in the first step of the spatial analysis, only the area of buildings and garages and a buffer zone of 2 m around buildings is subtracted from the total area of the RF to obtain the available space for BHE installations. In the second step of the spatial analysis, the ArcGIS tool called "Create Fishnet" is utilized to receive a Cartesian grid with an edge length equal to

the BHE spacing d . This grid is clipped to the available space for BHE installations. The centre of each cell represents the location of a BHE, hence a number n of equally distributed BHE within the available space is obtained.

After the spatial analysis, the input parameters listed in Figure 3.4 and Table A.2 are used and Equation 3.3 is applied to each scenario to calculate the geothermal potential of the vGSHP system:

$$E_{vGSHP} = \sum_i^n q_{vGSHP,i} \cdot t_h \cdot l_{vGSHP,i} / (1 - 1/COP) \quad (3.3)$$

To account for varying legal and hydro-/geological conditions, we have defined four different scenarios for the vGSHP system (Scenarios 2 - 5, Figure 3.4). For all of the four vGSHP scenarios, a conservative BHE spacing of $d = 10 \text{ m}$ is applied (Baden-Württemberg, 2005). Scenarios 2 and 3 consider the drilling limitation of 17 m as defined by ISONG ($l_{vGSHP} = 17 \text{ m}$). However, to investigate the effect of the given drilling limitation on the geothermal potential and the heat supply rate, a typical BHE length of $l_{vGSHP} = 100 \text{ m}$ is employed for Scenarios 4 and 5. The heat extraction rate $q_{vGSHP} = 60 \text{ W/m}$ for Scenarios 2 and 4 is based on the site-specific heat extraction rate suggested by ISONG. In Scenarios 3 and 5, groundwater flow velocities of $0.76 - 1 \text{ m/d}$ are considered, suggesting a higher heat extraction rate of 100 W/m for the part of the BHE within the aquifer (VDI 4640 part 2, 2015). Hence, the BHE length related to the enhanced heat extraction rate is adjusted to the corresponding aquifer thickness in the north (31 m) and south (13 m).

The feasibility of higher heat extraction rates for BHE located in an aquifer with substantial groundwater has proved to be applicable by a local drilling company in Karlsruhe. By application of an innovative hollow stem auger drilling technique, no backfilling material for the BHE is required, and so the thermal connection between the ground and the BHE is improved (Krämer, 2010). In a BHE field experiment, Wang et al. (2009) presented a heat transfer rate improvement by approximately 13% for an aquifer containing coarse sands and gravels. Also, higher ground and groundwater temperatures positively affect the heat extraction rate. The studies by Benz et al. (2015), Zhu et al. (2015) and Menberg et al. (2013a) show that groundwater temperatures beneath cities are up to 7 K higher compared to rural areas. Due to this so-called subsurface heat island effect, the exploitation rate can be raised from 13 - 33% (Rivera, Blum, and Bayer, 2017).

In order to optimise the system, by minimising the number of BHE required to fully meet the heat demand of the study site before and after refurbishment, an additional, inverse analysis is conducted. For this purpose, the values for t_h , q_{vGSHP} and l_{vGSHP} are adopted from Scenarios 2 to 5. Furthermore, we assume that q_{vGSHP} is constant and independent of the BHE spacing (Rivera, Blum, and Bayer, 2017). The BHE spacing d is adjusted by changing the edge length of the fishnet grid in 0.5 m steps during the spatial analysis. This adjustment is repeated for each scenario and both, before and after refurbishment until a heat supply of at least 100% is achieved.

Groundwater Heat Pump (GWHP) System

A GWHP system is an open-loop geothermal system, which directly uses groundwater for heating and cooling. The heat is extracted from the pumped groundwater, which is reinjected into the aquifer afterwards at a cooler temperature. Since the wells of a GWHP system are typically shallower than the boreholes for BHE, the total drilling costs are usually lower (Self, Reddy, and Rosen, 2013). A disadvantage is the systems' dependency of groundwater availability and its chemical composition.

For the evaluation of the geothermal potential of GWHP systems, two different approaches are studied: (1) energy flux approach and (2) thermal plume approach. Since the annual average groundwater temperature within the study site is 13.6 °C (Tiefbauamt, City of Karlsruhe), a maximum tolerable temperature reduction of $\Delta T = 6 \text{ K}$ is feasible without falling below the allowed temperature minimum for reinjected water of 5 °C (Baden-Württemberg, 2009b). The results for both approaches are presented with (Scenarios 6, 7) and without (Scenarios 8, 9) consideration of a limited drilling depth.

The energy flux approach enables the estimation of the energy input into the study site due to groundwater flow (Epting and Huggenberger, 2013; Mueller, Huggenberger, and Epting, 2018). For the spatial analysis of the energy flux approach, the length of the profile sections perpendicular to the groundwater flow direction is determined, which corresponds to the Upper Aquifer as well as the combined Upper and Lower Aquifer (Figure 3.3, green line). Multiplying the section lengths with the corresponding thickness m of the aquifers results in two flow areas A_{UA} and A_{UA+LA} . The geothermal potential E_{GWHP} of the heat flux approach is equal to the thermal energy, which is released, when the volume of groundwater flowing through the cross-section of the aquifers beneath the study site per year, Q , is cooled by 6 K (Equation 3.4b). This volume of groundwater is calculated by Darcy's law (Equation 3.4a). In this step, the specific length of the profile obtained by the spatial analysis and the input parameters listed in Table A.2 are used to obtain the theoretical geothermal potential E_{GWHP} (Equation 3.4b).

$$Q = v_{fUA} \cdot A_{UA} + v_{fUA+LA} \cdot A_{UA+LA} \quad (3.4a)$$

$$E_{GWHP} = Q \cdot t_y \cdot \Delta T \cdot c_{pw} / (1 - 1/COP) \quad (3.4b)$$

In the case of the thermal plume approach, the thermal plume caused by the cold reinjected water is analytically simulated to find the maximum number of wells without an interference of the 1 K isotherm. Similar to the spatial analysis for the vGSHP system, the ArcGIS tool "Create Fishnet" is used to design a rectangular grid with the edge length equal to the maximum thermal plume dimension of the 1 K isotherm. Since the thermal plumes have to be oriented in groundwater flow direction and the created fishnet is north-south directed, the fishnet is rotated in the same direction (NW). The centre of each grid cell defines a possible well location. The following Equation 3.5 by Kinzelbach (1992) is currently used in the guideline for the use of small GWHP systems (< 45,000 kWh per year) by the Federal State of Baden-Württemberg (Baden-Württemberg, 2009a). It represents an analytical solution to estimate the thermal plume length and width due to advection and conduction.

$$\Delta T(x, y, t) = \frac{Q \cdot \Delta T}{4 \cdot p \cdot m \cdot v_a \cdot \sqrt{\pi \cdot \alpha_T}} \cdot \exp\left(\frac{x-r}{2 \cdot \alpha_L}\right) \cdot \frac{1}{\sqrt{r}} \cdot \operatorname{erfc}\left(\frac{r - v_a \cdot t/R}{2 \cdot \sqrt{v_a \cdot \alpha_L \cdot t/R}}\right)$$

$$r = \sqrt{x^2 + y^2 \frac{\alpha_L}{\alpha_T}} \quad (3.5)$$

Considering the different properties of the Upper Aquifer and combined Upper and Lower Aquifer, the thermal plumes for 1 K, 2 K and 3 K isotherms are simulated at every well location and plotted in ArcMap (Figure 3.5c). For this purpose, Equation 3.5 is implemented in Python, which has an interface with ArcGIS. The well

coordinates x and y are the results from the spatial analysis, while the remaining input parameters are listed in Table A.2. Since Equation 3.5 is only valid for small systems with $< 45,000$ kWh per year, which corresponds to Q values between 0.1 l/s and 0.3 l/s, the pumping rate Q is set to 0.2 l/s per well (Baden-Württemberg, 2009a; Pophillat et al., 2018). The technical geothermal potential for the thermal plume approach is computed by multiplying the energy supplied per GWHP system (Equation 3.4b) with the total number of wells n .

3.3 Results and Discussion

This section is structured as follows: First, the results of the spatial analysis, the geothermal potential and the heat supply rate of the heat demand before and after refurbishment for each system and scenario are presented. Second, we investigate how the BHE spacing of the vGSHP system has to be adapted in order to achieve a heat supply rate of at least 100% before and after refurbishment. Third, the results for all systems are compared and discussed with those from related studies.

3.3.1 Horizontal Ground Source Heat Pump (hGSHP) System

The spatial analysis for the hGSHP system shows that 60% (i.e. 80,032 m²) of the original surface area can be used to install collectors, as illustrated in red in Figure 3.5a. The corresponding geothermal potential results in a heat supply rate of 59% before refurbishment, and 125% afterwards. However, the heat supply rate would be lower, if the open space and subsurface occupied by vegetation and subsurface infrastructure, such as sewers and underground cables, were incorporated. The effects of the bending number of the collector tubes, burial depth or a different pipe spacing on the thermal performance of the hGSHP system also have to be considered (Pu et al., 2018). In addition, the heat extraction rate in the shadow of trees and buildings might be lower than the assumed 33 W/m². Since the heat supply rate after refurbishment exceeds the required percentage by 25%, a satisfying result should be still ensured even if a further reduction in surface area due the above issues was considered.

3.3.2 Vertical Ground Source Heat Pump (vGSHP) System

The spatial analysis yields the maximum number of BHE positions and available area for the system installation. Based on the assumption that BHE can be installed beneath bituminized areas, the available space for the vertical system installation is 10% larger than the area for the horizontal system. In the case of a standard 10 m BHE spacing for Scenarios 2 - 5, 974 BHE can be installed.

Table 3.1 provides the geothermal potential and heat supply rate for a COP = 4 of the four scenarios with a standard 10 m BHE spacing. Regarding Scenarios 2 and 3 in comparison to Scenarios 4 and 5, the impact of the RDD is obvious. The geothermal potential rises by a factor of 5.9 and 4.5, respectively, if a BHE length of 100 m is employed. The geothermal potential of Scenario 3 is 1.5 times higher than of Scenario 2, which demonstrates the significant impact of the groundwater flow and the corresponding increase in the heat extraction rate on the geothermal potential. The improvement from Scenario 4 to 5 is by a factor of 1.2. So, with an increasing BHE length, the influence of the groundwater flow diminishes. This implies that

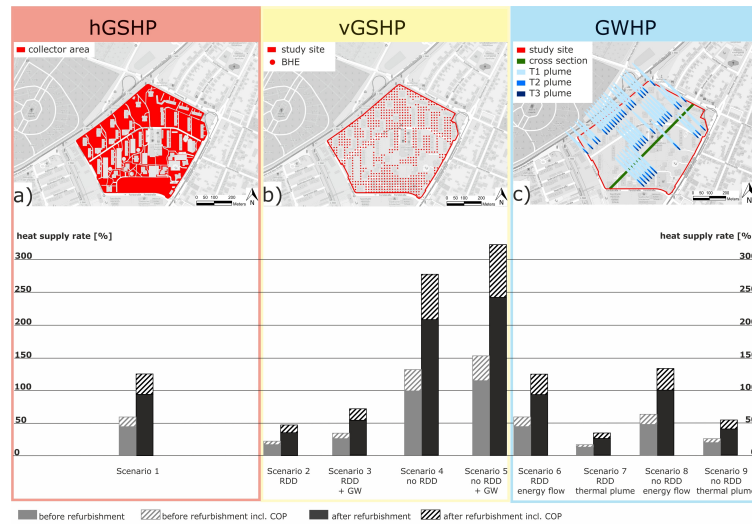


Figure 3.5: Results of the evaluation of the heat supply rate with and without the coefficient of performance ($COP = 4$) for three different shallow geothermal systems: horizontal ground source heat pump (hGSHP), vertical ground source heat pump (vGSHP) and groundwater heat pump (GWHP); a) presents the area for collector installation; b) shows the maximum number n of BHE ($n = 974$) with a 10 m BHE spacing; c) displays the temperature plumes for the 1 K, 2 K and 3 K isotherms (T1, T2, T3 plume) and the cross-section used for the energy flow approach. The bar diagram shows the heat supply rate before and after refurbishment for the nine scenarios (Figure 3.4). The latter considers a restriction of the drilling depth (RDD, no RDD), optional groundwater flow (GW) and the two different approaches for the GWHP system: energy flow and thermal plume approach.

the length of a BHE has a large influence on the geothermal potential. This is in accordance with the results by Casasso and Sethi (2014) and Schiel et al. (2016), who concluded that the BHE length has the largest impact on the heat supply rate.

Due to the RDD, Scenarios 2 and 3 attain only a heat supply rate of maximum 71% before and after refurbishment. Assuming a standard heat extraction rate of 60 W/m and no restriction of the drilling depth, the heat demand before refurbishment can be entirely satisfied by a vGSHP system. Due to higher heat extraction rates for Scenario 5, the heat supply rate before refurbishment is even higher. After refurbishment, the heat demand can be satisfied more than twice for both Scenarios 4 and 5.

In order to optimise the BHE spacing and determine the minimum number of BHE required to achieve a heat supply rate of at least 100% before ($E_{vGSHP} \approx 10 \text{ GWh}$) and after ($E_{vGSHP} \approx 5 \text{ GWh}$) refurbishment for Scenarios 2 - 5, the BHE spacing is adjusted accordingly and inversely obtained. Table 3.1 illustrates the huge variation in BHE spacing between 4.5 m and 17.5 m depending on the particular combination of calculation input parameters. In view of the official regulation of the VDI 4640 part 2 (2001) a BHE spacing of 4.5 m, however, would not be acceptable. So, for Scenario 2 the energy demand can only be satisfied after refurbishment and a BHE spacing of 6.5 m which is consistent with the official regulatory framework. Attention should be paid to the large number of BHE for Scenarios 2 and 3. The space

Table 3.1: Results of the estimation of the geothermal potential for the vGSHP system with a COP = 4 for Scenarios 2 to 5 and the heat supply rate S before and after refurbishment with a fixed BHE spacing. Results of the inverse analysis: The minimum BHE spacing and number of BHE for which a heat supply rate of at least 100% before or after refurbishment can be achieved. The four scenarios consider variable heat extraction rates q depending on groundwater flow (GW) and two different BHE lengths (17 m and 100 m) corresponding to the restriction of the drilling depth (RDD, no RDD).

Scenario	Fixed BHE spacing $d=10$ m			Inverse Analysis			
	E [GWh]	S [%]		BHE spacing [m]		Number of BHE	
		Before	After	Before	After	Before	After
2: RDD	2.3	22	47	4.5	6.5	4675	2242
3: RDD + GW	3.4	34	71	5.5	8	3121	1473
4: no RDD	13.3	131	277	11	16	783	377
5: no RDD + GW	15.4	152	322	12	17.5	657	302

for the system installation is sufficient but the required number of BHE is unrealistically high and approaches the limit of practicability and cost efficiency. Moreover, our approach does not incorporate potential thermal interaction between individual BHEs or any dynamic effects over the lifetime of a BHE field. If the spacing is too small and/or the actual heat extraction too large, the subsurface could cool down due to a lack of thermal regeneration, and the system might become inefficient. The heat extraction rate of a BHE field investigated by Fujii et al. (2005) with 75 BHE with 50 m length and a spacing of 7.6 m, situated in Quaternary silts and fine sands, fell by 55% after a simulation period of 50 years. In contrast, the study by Kurevija, Vulin, and Krapec (2012) showed that for a 9 m spacing thermal interference could be neglected. Based on the heating and cooling conditions of a new building in Zagreb, Croatia, they studied the effects of BHE geometry and spacing on the performance of the system and thermal interference of the BHE. The optimal spacing for 42 BHE, regarding economic and efficiency aspects, was 6 m. Also, the study by De Carli et al. (2014) obtained a range in BHE spacing comparable to the one of our case study. In their case, the spacing depended on the energy demand of the housing district and the shape of the BHE field. For different BHE field configurations, the spacing varied between 6 m and 15 m. Alcaraz, Vives, and Vázquez-Suñé (2017) developed a method called T-I-GER which aims to optimise the position of BHE and maximise the extraction potential whilst at the same time minimises the thermal impact on neighbouring plots. Furthermore, a reduction in BHE spacing or increase in total BHE length without a strong decline of the ground temperature or a degradation of the longterm performance is feasible if a thermal regeneration of the ground during summer is incorporated in the optimisation. Long-term studies by Pahud (2015) showed a decrease of the system performance of BHE fields (3 - 62 BHE having a spacing of 5 - 9 m) after several years. He proposed two potential strategies to overcome this challenge: A reduction of the peak performance or thermal regeneration of the field. Kübert et al. (2010) included an annual regeneration of the BHE field due to the heat supply by a cogeneration unit. So they could reduce the total BHE length by 25% and determined 10 m as an optimal spacing for a field of 50 BHE à 115 m length. Bayer, Paly, and Beck (2014) demonstrated the regeneration of a BHE field by seasonal geothermal heating and cooling operation. These studies and other guidelines in Germany (Hähnlein, Blum, and Bayer, 2011), where

the required minimum distances are 5 m and 6 m, respectively, clearly indicate that the recommended spacing of 10 m by the guideline of Baden-Württemberg (2005) is a very conservative assumption. Thus, regardless of the case-specific properties or respective approach, an optimisation of the BHE spacing and adaption to local hydro-/geological conditions should always be carried out in order to maximise the systems' performance.

3.3.3 Groundwater Heat Pump (GWHP) System

According to the spatial analysis for the energy flux approach, the profile line of the cross-section in Figure 3.3 has a length of 448 m, with 203 m corresponding to the Upper Aquifer and 245 m to the Upper and Lower Aquifer. Consequently, the flow area is 2,639 m² and 7,595 m², respectively. For Scenario 6, Equation 3.4a yields a volumetric flow Q of 20.4 l/s per year and a corresponding geothermal potential of 5.94 GWh. In relation to the heat demand, this returns a heat supply rate of 59% before, and 124% after refurbishment. For Scenario 8 without the RDD, the volumetric flow Q is 6.7% higher and the geothermal potential amounts to 6.37 GWh.

For the thermal plume approach (Scenario 7 and 9), the dimension of the 1 K isotherm was used as input data for the spatial analysis. In total, the geothermal potential is 1.63 GWh for Scenario 7 and 2.57 GWh for Scenario 9 (Table 3.2).

Table 3.2: Results of the spatial analysis and estimation of the geothermal potential for the GWHP system: Maximal extension of the 1 K isotherm in x and y -direction, the number of wells, geothermal potential.

UA = Upper Aquifer, LA = Lower Aquifer

Scenario	Area	Max x [m]	Max y [m]	Number of Wells	E [GWh]	S [%]	
						Before	After
7	UA	162	13	28	1.6	16	34
9	UA	162	13	7	0.4	25	54
	UA and LA	127	12	37	2.2		

The thermal plumes are shorter and narrower in the northern part (Figure 3.5c and Table 3.2), as the same amount of thermal energy (i.e. 45,000 kWh) is exchanged with a larger volume of water due to larger aquifer thickness than in the Southern part. As a result of this and due to the different proportion of the available area, thirty additional reinjection wells can be set up in the north without an interference of the 1 K isotherm in Scenario 9. Due to the RDD in Scenario 7, only the Upper Aquifer is used as an energy source. As a result of the larger plume dimensions for the Upper Aquifer, only 28 instead of 44 wells could be installed without an interference of the 1 K isotherm.

Comparing these results with other studies highlights the variability in plume dimension in dependence on the aquifer thickness and design of the GWHP system. Keim and Lang (2008) employed a pumping rate $Q = 0.3$ l/s, a temperature reduction of 4 K, a groundwater velocity of 1.2 m/day and also a heat extraction of 45,000 kWh per year and well. Their study considered two cases, the first case with an aquifer thickness of 10 m and the second case with 30 m. For the first case, they received a maximum plume dimension of the 1 K isotherm of $x = 461$ m and $y = 28$ m, for the second case is $x = 175$ m and $y = 10$ m. The plume width of the second case is about the size of the one in Scenario 9 ($m = 31$ m). Contrasting the results of their

first case with Scenario 7, we obtained a plume length that is only a third. This discrepancy is caused by the differences in the above-listed input parameter especially in the aquifer thickness and pumping rate. Consequently, a smaller aquifer thickness, for example, due to a RDD, leads to longer and wider plumes, so fewer well locations are feasible and the overall heat supply rate is lower. If the thermal plumes are too long and cross the property line, the neighbouring parcel might be thermally affected. This could lead to a decrease in the system efficiency of the neighbouring geothermal system or, depending on the local legislation, the GWHP system would need to be shut down. For this reason, a detailed 3D geological model and a numerical groundwater flow model on the city level is desirable in order to properly plan a GWHP and avoid interactions of neighbouring systems.

When contrasting the results of the energy flow with the thermal plume approach, it is essential to notice that the energy flow approach represents the maximum available thermal energy and neither regards any technical conditions nor pays attention to overlapping isotherms or well positions. In contrast, the thermal plume approach is a more thorough method with several input parameters taking into account well configurations. As mentioned in section 3.2.3, the pumping rate Q for the thermal plume approach is limited to 0.2 l/s per well, and accordingly, the total Q for scenario 7 is 5.6 l/s and 8.8 l/s for Scenario 9. In contrast, the flow rate obtained with the energy flow approach in Scenarios 6 and 8 is 27% and 34% higher. The constraints of the thermal plume approach, such as a lower pumping rate and a limited number of wells, thus explain the smaller geothermal potential and heat supply rate in comparison to the one of the energy flux approach.

3.3.4 Comparison

The results of the spatial analysis and the evaluation of the heat supply rate of all nine scenarios before and after refurbishment with and without the portion of a heat pump are summarised in Figure 3.5. Standing out is the high heat supply rate of the vGSHP system in Scenarios 4 and 5 (without RDD) before and after refurbishment. Thus, the vGSHP is the optimal geothermal system to satisfy the heat demand of this study site. The results of the GWHP system demonstrate that theoretically, the energy available in the aquifer is sufficient to satisfy the heat demand after refurbishment. Yet, in practice, this geothermal potential cannot be fully extracted, if an overlapping of thermal plumes has to be avoided. Hence, the smallest heat supply rates are obtained in Scenarios 7 and 9. The larger aquifer thickness in the northern part enables deeper wells for a GWHP system or a higher heat extraction rate for BHE. Thus, the northern part is more suitable and economically attractive for vGSHP and GWHP systems. Interestingly, the hGSHP system achieves a full heat supply rate after refurbishment. The advantage of this system is its independence of drilling limitations and so it is the best alternative to the vGSHP system if we regard the RDD by ISONG.

A detailed inspection of Figure 3.3 reveals the deviation between the outline of the drilling limitation defined by ISONG and the boundary between the two bases of the aquifers. The delineation runs sharply and angularly along streets instead of following the hydrogeological and/or tectonic boundaries. Within the study site, the drilling depth is limited to 17 m, yet on the other side of the local street, the "Forststraße" in the south, there is no RDD. In addition, the hydrogeological map in Figure 3.3 and the cross-sections in Figure 3.4 imply that there is no separating

layer, such as an aquitard, between the two aquifers, which could protect the Lower Aquifer from contamination.

Consequently, detailed and permanently updated geological and hydrogeological data are necessary for a technical feasibility study and to improve the knowledge of underground risks in order to avoid negative effects. Epting, Händel, and Huggenberger (2013) also criticise the lack of information and recommend a sustainable thermal management of the subsurface that includes 3-D numerical groundwater flow and heat transport models as well as monitoring systems. Aside from this, possible conflicts of interest with subsurface infrastructure such as sewage systems and tunnels have to be detected and considered in a sustainable thermal management of the subsurface. Thus, in practice, geothermal systems might not be considered, due to the lack of true and reliable information.

Besides regulations and local hydro-/geological conditions, the ratio from available space for a system installation to heat demand is a decisive factor for a satisfying heat supply rate. In our study, 60% to 70% of the area is utilisable for hGSHP, vGSHP and GWHP system installations. In denser urban areas this space is likely to be smaller and due to higher buildings with a larger heat demand per m^2 building, we expect the heat supply rate to be smaller in such areas unless the amount of overall drilling meter increases significantly. The latter was demonstrated in the case study by De Carli et al. (2014), who proposed to identify the most suitable BHE solution for an urban area with two different building density types. They defined a low-density housing district with 2-floor buildings, and a medium-density housing district composed of buildings with six floors. The available space for the system installation is equal for both districts, yet the heat demand is more than two times higher for the district with higher buildings, which raised the required total BHE length from 13,860 m to 40,000 m. Relating this result to Scenario 4 and an optimal spacing, the total BHE length increases from 37,700 m to 78,300 m, comparing the heat supply rate after refurbishment to the one before. So, the two cases before and after refurbishment with their different heat demands can also be transferred and correlated to cases with a high and low building density or high- and low-rise buildings.

The study by Schiel et al. (2016) also confirmed that the possibility to meet the heat demand in Germany, in particular with a low number of BHE, is more likely in a residential, less dense urban quarter with low-rise buildings. In their study, the heat demand of only 40% of the parcels in an urban area with 87,000 inhabitants could be satisfied by vGSHP systems. In a case study investigating the district of Westminster in London, Zhang, Soga, and Choudhary (2014) reported that the heat demand of 69% of the buildings could be completely supplied by vGSHP systems. They also stated that only buildings with five floors or less and a maximum heat demand of 40 W/m^2 fall within this range. This low heat demand refers to the refurbished buildings in our case study (Table A.2). Since the number of BHE or the total BHE length is not mentioned by Schiel et al. (2016) or Zhang, Soga, and Choudhary (2014), a direct comparison to our results is not feasible. Nevertheless, these studies and our case study illustrate that a full heating energy supply by vGSHP systems is a challenging, yet achievable task in dense urban areas. A heat supply rate of 100% is feasible if sufficient space for system installation is available or in the case of an area with low-rise buildings or buildings with a low energy demand.

3.4 Conclusion

Based on a case study in a German urban quarter, we conducted a technical feasibility study under consideration of influencing and restrictive factors for the application of shallow geothermal systems. We considered three different shallow geothermal systems, namely horizontal (hGSHP) and vertical ground source heat pump (vGSHP) as well as groundwater heat pump (GWHP) systems. The results of this study highlight the capability of each system to satisfy the heat demand for space heating and domestic hot water before and after the refurbishment of an urban quarter in Karlsruhe.

The results demonstrate that the heat demand of an old non-refurbished urban quarter in Germany can be satisfied by a vGSHP system installed at a standard depth of 100 m. In the case of the GWHP system, the energy available in the aquifer suffices to meet the heat demand after refurbishment. Yet, when we apply an analytical model in order to avoid an interaction between thermal plumes, the heat supply rate declines to less than 54%. After refurbishment, the hGSHP system could also cover the heat demand with a heat supply rate of 125%. Thus, it is a decent alternative to the vGSHP system in the case of a restriction of the drilling depth.

We identify four major influencing and restrictive factors for the efficiency of shallow geothermal systems and the achievement of a full heat supply rate. First, the restriction of the drilling depth by authorities. Second, guidelines for critical design parameters provide conservative recommendations for heat extraction rates (60 W/m) and BHE spacing (10 m). For an optimal system planning, better knowledge of crucial physical parameters is mandatory and can be obtained by, for example, a thermal response test (TRT). Third, favourable hydro-/geological conditions, such as a moderate to high groundwater flow velocity, a sufficient aquifer thickness or thermal conductivity, are fundamental. Fourth, an optimal ratio of available space for system installation to heat demand is decisive for achieving a satisfactory heat supply rate.

We anticipate that our straightforward evaluation of the geothermal heat supply rate combined with a profound geological knowledge will reveal the ability of geothermal systems to satisfy the heat demand of any urban area. This way, it will help to realise future urban energy plans. Moreover, as climate change air temperatures in summertime and the demand for building cooling will increase. Cooling can also be supplied by geothermal systems while enhancing the thermal regeneration of the subsurface. Other subsurface structures, such as tunnels and sewer systems, should be incorporated in a further development of the spatial analysis. A single coefficient of performance (COP) for all three systems facilitates comparisons of the results, yet in the future, the COP has to be adapted to the individual systems.

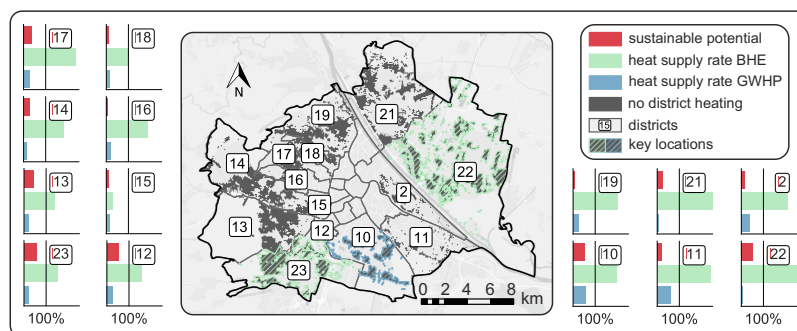
Acknowledgements

The authors thank Marcus Albert from the local authority real estate office in Karlsruhe for providing the real estate data of the “Rintheimer Feld”.

4 Identifying Key Locations for Shallow Geothermal Use in Vienna

Reproduced from: Tissen, C., Menberg, K., Benz, S. A., Bayer, P., Steiner, C., Götzl, G. and Blum, P.: Identifying key locations for shallow geothermal use in Vienna, *Renewable Energy*, (submitted manuscript).

Abstract



Decarbonising the heating sector is crucial for reducing CO₂ emissions. This is in particular true for Central European cities such as Vienna, where 28% of the total CO₂ emissions are caused by the energy supply for buildings. One promising option for environmental friendly heat supply is the use of shallow geothermal energy. To determine whether shallow geothermal systems are a feasible option to meet the urban heating demand, the Python tool GeoEnPy is developed and applied to the case study of Vienna. It allows the evaluation of the anthropogenic heat input into the subsurface, the theoretical sustainable potential, the technical geothermal potential, and the heat supply rate. The overall heat flow in Vienna is 17.6 PJ/a, which represent 38% of the current heating demand or indeed 99% once all buildings are thermally refurbished. The technical geothermal potential can satisfy the current heating demand for 63% (BHE system) or rather 8% (GWHP system) of the city area. GeoEnPy reveals that BHE systems are most feasible in the eastern and southern districts of Vienna. Our findings can guide integration of shallow geothermal use in spatial energy management focused on key locations to supply buildings with decentralised and sustainable heat from the subsurface.

4.1 Introduction

Ambitious goals and concepts to encourage application of renewable energy technologies and to reduce CO₂ emissions, especially in the heating sector, exist on EU- (European Union (EU), 2018), country- (Erneuerbare Energie Österreich, 2019) and city-level (Stadt Wien, 2016; Stadt Wien, 2017). From 1995 to 2016, Vienna's heating

sector moved away from fossil fuels (oil -44%, coal -99%, gas -8%) towards more renewable energy resources (+34%). Despite this progress, the building energy supply still causes 28% of CO₂ emissions (Stadt Wien, 2019). Shallow geothermal systems are one of the key technologies to replace fossil fuels, reduce CO₂ emissions and achieve low carbon cities (Blum et al., 2010; McMahon, Santos, and Mourão, 2018; Lund and Boyd, 2016; Bayer et al., 2012). They are a particularly good option for areas or districts with a low heat demand density, for which a connection to a district heating (DH) network is not economically and/or environmentally efficient (Jakob et al., 2014; Lund et al., 2010). Currently, 1070 closed- and 762 open-loop geothermal systems are already installed in Vienna, and an increased contribution from geothermal sources is anticipated, especially in city parts without a DH system and where new buildings are planned (GBA).

Closed- or open-loop geothermal systems extract the energy stored in the shallow subsurface. Closed-loop systems use borehole heat exchangers (BHE) to harness heat from the ground. Open-loop systems, known as groundwater heat pumps (GWHP), extract water from the aquifer, gain the thermal energy with a heat transfer system and re-inject the cooled water back into the aquifer (Stauffer et al., 2014). Thorough planning is crucial for the development of economically feasible systems that are optimised according to their hydro- and geological conditions. Numerous studies explored and estimated the feasibility of geothermal use in urban areas with various approaches (Böttcher et al., 2019; Luo et al., 2018; Sbrana et al., 2018; Noorollahi, Gholami Arjenaki, and Ghasempour, 2017; Casasso and Sethi, 2016). The basic concept of linking the energy available in the ground with the heat that can be used is a definition of a geothermal potential.

Bayer et al. (2019) defines the maximum amount of energy stored in the ground as theoretical potential and the amount of energy that can be extracted by a specific geothermal system as technical potential. Estimations of the geothermal potential of both, open and closed-loop systems, were done in various ways, using energy balance calculations, analytical or numerical models, and geographic information systems (GIS). GIS offers a comfortable way to process, analyse and combine spatial hydro-/geological data, and to display the final results as easily accessible geothermal potential maps (e.g. Gemelli, Mancini, and Longhi, 2011; Noorollahi, Gholami Arjenaki, and Ghasempour, 2017; Casasso and Sethi, 2016; García-Gil et al., 2015; Ondreka et al., 2007).

Much attention was so far given to the sustainability and long-term effects of geothermal energy. Intensive use or a high system density can lead to interference (Meng et al., 2019; Vienken et al., 2015; Kurevija, Vulin, and Krapec, 2012; Zhang et al., 2018). Furthermore, decreasing ground temperatures can lead to a decrease in efficiency over time, which in turn can cause conflicts amongst different geothermal users (e.g. Patton et al., 2020; Ferguson and Woodbury, 2006; Bonsor et al., 2017). To maintain system efficiency and to avoid overly cooling of the subsurface, some recent studies propose coupling of solar panels and ground source heat pump (GSHP) systems (Abu-Rumman, Hamdan, and Ayadi, 2020; Georgiev, Popov, and Toshkov, 2020). Another factor that enhances sustainable use is the natural replenishment of thermally-used ground, which is substantially augmented by passive anthropogenic heat input into the urban subsurface (Benz et al., 2018a; Mueller, Huggenberger, and Epting, 2018; Epting et al., 2020b; Rivera, Blum, and Bayer, 2015a). The heat input from buildings, increased ground surface temperature (GST) and subsurface infrastructures, such as district heating (DH) pipes and sewers, was studied in several

cities (e.g. Balke, 1977; Ferguson and Woodbury, 2004; Epting et al., 2017b; Krcmar et al., 2020). These heat sources also lead to increased groundwater temperatures (GWT) in urban aquifers. This phenomenon of urban ground and groundwater warming, which is observed globally on city-scale, is called subsurface urban heat island (SUHI) effect (e.g. Bidarmaghz et al., 2019; Hemmerle et al., 2019; Ferguson and Woodbury, 2007; Taniguchi et al., 2009; Taylor and Stefan, 2009). Menberg et al. (2013a) and Benz et al. (2015) developed a 1D analytical and statistical heat flux model to estimate the mean annual heat flux and flow from anthropogenic heat sources.

Although several studies relate the anthropogenic heat input to the heating demand (Benz et al., 2018a; Rivera, Blum, and Bayer, 2017; Mueller, Huggenberger, and Epting, 2018; Epting et al., 2020b; Zhu et al., 2010), the majority of studies focus either on geothermal potential on district- (Tissen et al., 2019; Zhang, Soga, and Choudhary, 2014; Miglani, Orehounig, and Carmeliet, 2018) or city-scale (Schiel et al., 2016; Luo et al., 2018; Böttcher et al., 2019), or on quantifying the anthropogenic heat input into the subsurface (Kupfersberger, Rock, and Draxler, 2017; Menberg et al., 2013a). Thus, so far there is little known about the role of enhanced heat fluxes into the urban ground for the technical performance and the sustainable operation of geothermal systems on city-scale.

The objective of this study is to compute, spatially resolve and combine the technical geothermal potential of open- and closed-loop systems with the annual anthropogenic heat input. By relating the technical geothermal potential to the heating demand, we identify key locations for shallow geothermal use in Vienna. The quantity used to assess the technical potential is the technically feasible heat supply rate, which considers the available space for system installation, as well as site-specific hydro-/geological conditions. Furthermore, the subsurface heat fluxes from seven different anthropogenic heat sources are calculated and contrasted to the local heat demand to estimate the sustainable potential. For this procedure, the Python based tool GeoEnPy is developed and applied.

4.2 Materials and Methods

4.2.1 Study Site

Vienna, the capital of Austria, consists of 23 districts with a total size of 415 km² (Figure 4.1) and is located at the easternmost extension of the Alps and at the western margin of the Vienna Basin. Hydrogeological areas with their distinct groundwater conditions are oriented parallel to the river Danube, which splits the city into an eastern and western part. From the Danube floodplains in the east to the Wienerwald in the west, so from the younger to the older strata, the following four hydrogeological zones can be distinguished: Holocene and Pleistocene gravel units, Miocene unconsolidated sediments of the Vienna Basin, and Alpine bedrock (Figure A.14). The Holocene gravel units of the Danube plain form a continuous, porous aquifer with a high permeability and an average thickness of 7 to 14 m (Pfleiderer and Hofmann, 2004). The gravel units at the bed valleys of Wienerwald consist of platy and loamy sandstone gravels and therefore are less permeable and less productive. Here, the groundwater flow direction is parallel to the local streams. The Pleistocene terraces only have moderate to low abundance of groundwater and the groundwater flow direction is from west to east. The Miocene sediments of the Vienna Basin are composed of silts, clays and fine sands and form only local, unconfined aquifers with a moderate yield. The Alpine bedrock in the western part comprises the fractured

aquifer of the Flysch zone and the karst aquifer of the calcareous Alps (Pfleiderer, 2019; Pfleiderer and Hofmann, 2007).

4.2.2 Input Data

The data used for anthropogenic heat flux, heat flow and heat supply rate computations includes point, line, areal, as well as raster data. The maps of the district heating (DH) network, air temperature, subway temperature and the heating demand are confidential and the Geological Survey of Austria (GBA) only shared them as Web Feature Service (WFS) for this study. All further data bases are freely accessible via the online open data portal of Vienna (Stadt Wien, Table A.3).

Temperature data from basements, underground carparks and subway tunnels as well as groundwater temperature (GWT) and groundwater (GW) level data are available as point features from 66 or rather 315 wells inside and outside of Vienna (Figure 4.1). Monthly mean GWT and GW level data are freely available (eHYD). Most monitoring wells are equipped with data loggers and record GWT and GW level data four times an hour (eHYD, 2015). Air temperature data in basements (57 locations) and underground carparks (12 locations) were recorded for one annual cycle using iButtons (Figure A.15). Air temperatures within subway tunnels were recorded for 38 locations by Wiener Linien.

Line data includes sewers, subway tunnels, and DH pipes. Most of the sewage network is operated as a mixed system; that is grey water and rainwater are discharged together (Wien Kanal). The total length is about 2,500 km and the available spatial data also includes information about the vertical dimensions of the sewers. Consequently, the exact diameter and vertical position of each sewer segment is known. The total length of the subway system running below ground is around 46 km. The district heating network is split into a primary and secondary network with different pressures and temperatures. This network has a total length of approx. 1230 km and supplies over 30% of Vienna's households with energy for heating and domestic hot water. (Wiener Stadtwerke, 2018; MA 20, 2019).

Areal data comprises WFSs, shapefiles and raster datasets. The heating demand (HD) was provided as a WFS in form of hexagonal polygons of 8657 m² each. The assessment of the HD involves the present and future heating demand, both expressed in MWh per year and hexagon. The heating demand of the present building stock was determined based on the construction period, building height, building use, gross floor area and heating degree days. The future heating demand refers to the OIB-RL6 standards and assumes that all buildings are thermally refurbished (Österreichisches Institut für Bautechnik, 2015). A detailed description of the heating demand assessment is given by Hartmann, 2016. Daily air temperature measurements were collected and interpolated by the Central Institute for Meteorology and Geodynamics (ZAMG). The interpolation explicitly takes into account the topographical characterization of the measurement location. The GBA supplied average air temperatures from 2006 – 2016 as WFS with a spatial resolution of 1 km by 1 km. By combining air temperature with an offset depending on the surface material, the ground surface temperature (GST) is estimated (Benz et al., 2015). The different offsets for grass, asphalt, bare soil and sand were determined by Dědeček, Šafanda, and Rajver (2012) and adapted to the land use categories described in the Urban Atlas (GMES). Continuous and discontinuous urban fabric make up 27% of Vienna's land use, whereas 22% are covered by green urban areas and forest. The distribution of Vienna's land use categories and the matching temperature offsets according to Dědeček, Šafanda, and Rajver (2012) are summarised in Table A.4.

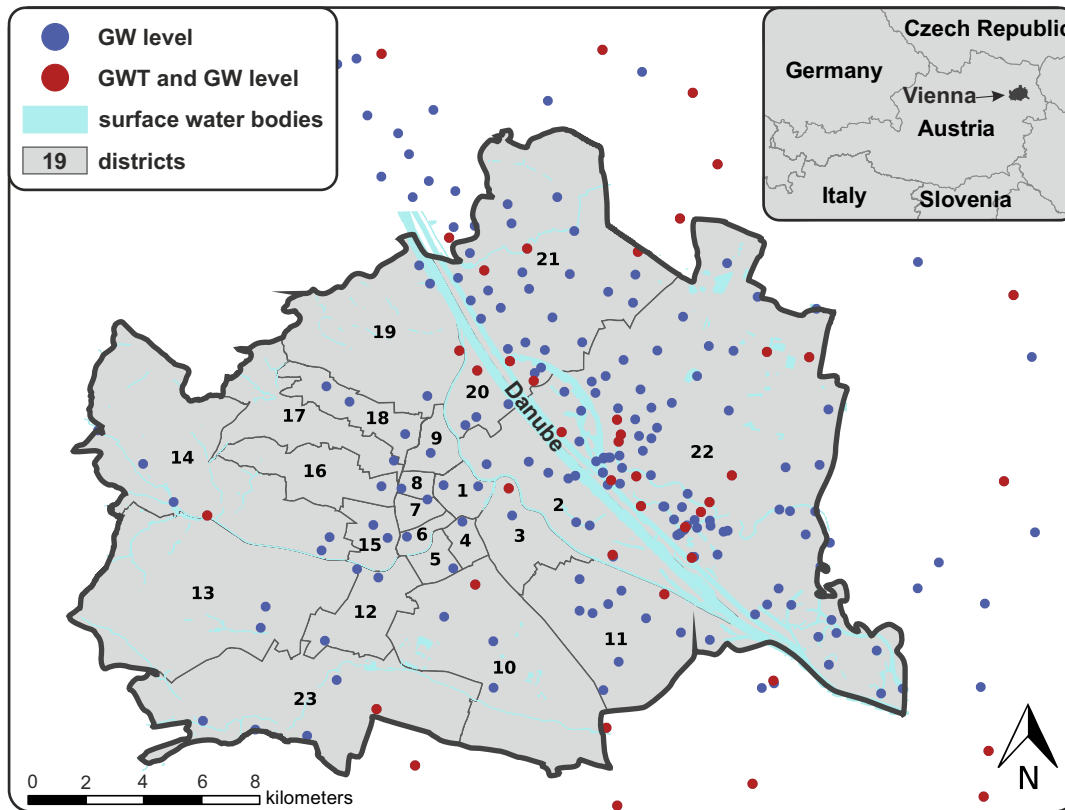


Figure 4.1: Location of Vienna, its 23 urban districts and measuring sites for groundwater temperature (GWT) and groundwater level (GW level).

Further areal data in the form of shapefiles are building and tunnel footprints, surface water, hydro- and geological data, as well as geothermal potential maps. The geothermal potential maps of borehole heat exchangers (BHE) and groundwater heat pumps (GWHP) give an overview on attractive locations by pointing out whether and for which type of use a location is suitable. A detailed description of the assessment for both geothermal potential maps can be found in Götzl et al. (2014). About 30% of the city area of Vienna are ideally suited for the use of shallow geothermal energy. Especially east of the Danube River, for example in the rapidly growing districts 21 and 22, one can expect high yields from thermal groundwater use. The potential maps for BHEs do not show an actual power potential in form of an amount of energy per area and time unit, but rather express the potential as thermal conductivity (in W/m/K) for different depth layers. The potential map of the geothermal use of groundwater displays the maximum thermal power of a single well system. Within each of the 14 hydrologically homogeneous areas, the thermal potential primarily reflects the hydraulically effective thickness of the aquifers. The estimated well performance to assess the thermal power is based on the assumption of a maximum cooling or warming of the extracted groundwater by 5 K and considers only the top groundwater body.

The digital elevation model (DEM) is available as a raster data file with a resolution of 1 m x 1 m. Additional data, such as sewage water temperature or heat loss rate of the DH system, as well as all input layers with their type, value, unit and source are listed in Table A.3.

4.2.3 Methods

Calculation of the Anthropogenic Heat Flux and Flow

The simulation of the vertical anthropogenic heat fluxes into the unsaturated zone is based on the method described by Benz et al. (2015). The heat flux q and heat flow Q calculation is accomplished on a regular grid with a 25 m by 25 m grid cell size, and comprises five steps (Figure 4.2). The spatial analysis of all five steps is implemented in the Python tool GeoEnPy, which uses the geoprocessing toolbox in ArcGIS. The first two steps prepare the input data, and steps three to five calculate the heat flux and flow.

In the first step, the GWT and GW level data from 2007 to 2016 are averaged and interpolated in ArcGIS using ordinary kriging. The resulting raster has a resolution of 25 m x 25 m (Figure A.16), which is consistent with the size of the grid layer. In the second step, all input layers are linked to one another and combined in different compositions according to the seven individual heat sources. These combined layers are the basis for the anthropogenic heat flux q and heat flow Q calculation in the third step. The anthropogenic heat flux q represents the conductive heat transport from the heat source to the groundwater surface and is described by Fourier's Law: $|q| = \lambda \cdot \Delta T / \Delta d$, where λ is the thermal conductivity, ΔT is the difference in temperature and Δd the distance between two points. As shown in Equation 4.1, Fourier's Law is adapted to each heat source except for the DH system. Advective heat transport is not considered in this study, since there are no data available for leakage rates of the sewage or district heating network.

$$q_s^g = (\lambda^s + \delta\lambda) \cdot \frac{T_s - (T_{GW}^g + \delta T_{GW})}{(d_{GW}^g + \delta d_{GW}) - d_s^g} \quad (4.1)$$

The resulting q_s^g represents the average heat flux as energy per square meter per grid cell g and heat source s . T_s is the respective temperature of the heat source s , T_{GW}^g is the GWT, λ^s is the thermal conductivity and d_{GW}^g as well as d_s^g the depth of the groundwater table and the heat source in the specific grid cell g . In order to account for spatial variability, Equation 4.1 is evaluated for the respective heat source s and within each grid cell g . In order to account for uncertainty in terms of measurement accuracy and parameter uncertainty, a Monte Carlo simulation is carried out. For this, Equation 4.1 is evaluated over 1000 iterations, where $\delta\lambda$, δT_{GW} and δd_{GW} reflect the uncertainties of the thermal conductivity, GWT and GW level. The anthropogenic heat flux from the DH network considers the percentage of downward directed heat flux P and the heat loss rate L for the primary and secondary DH pipes with a diameter D_{DH} :

$$q_{DH}^g = \frac{L \cdot P}{D_{DH}} \quad (4.2)$$

Equation 4.2 is applied for each grid cell g having an intersection with a DH pipe.

In the fourth step, the individual heat fluxes from each heat source are added up to obtain the total heat flux $q_{tot} = \sum q_s^g \cdot \frac{A_s}{A_g}$ per grid cell. Here, A_s and A_g are the areas of the heat source and grid cell, respectively.

In the last step, the heat flow Q of the entire city area of Vienna is calculated. For this, the heat flux q_s^g equations 4.1 and 4.2 are multiplied with the source area. The sum of these products gives the total vertical ground heat flow of Vienna for the anthropogenic heat sources considered and expressed in PJ/a.

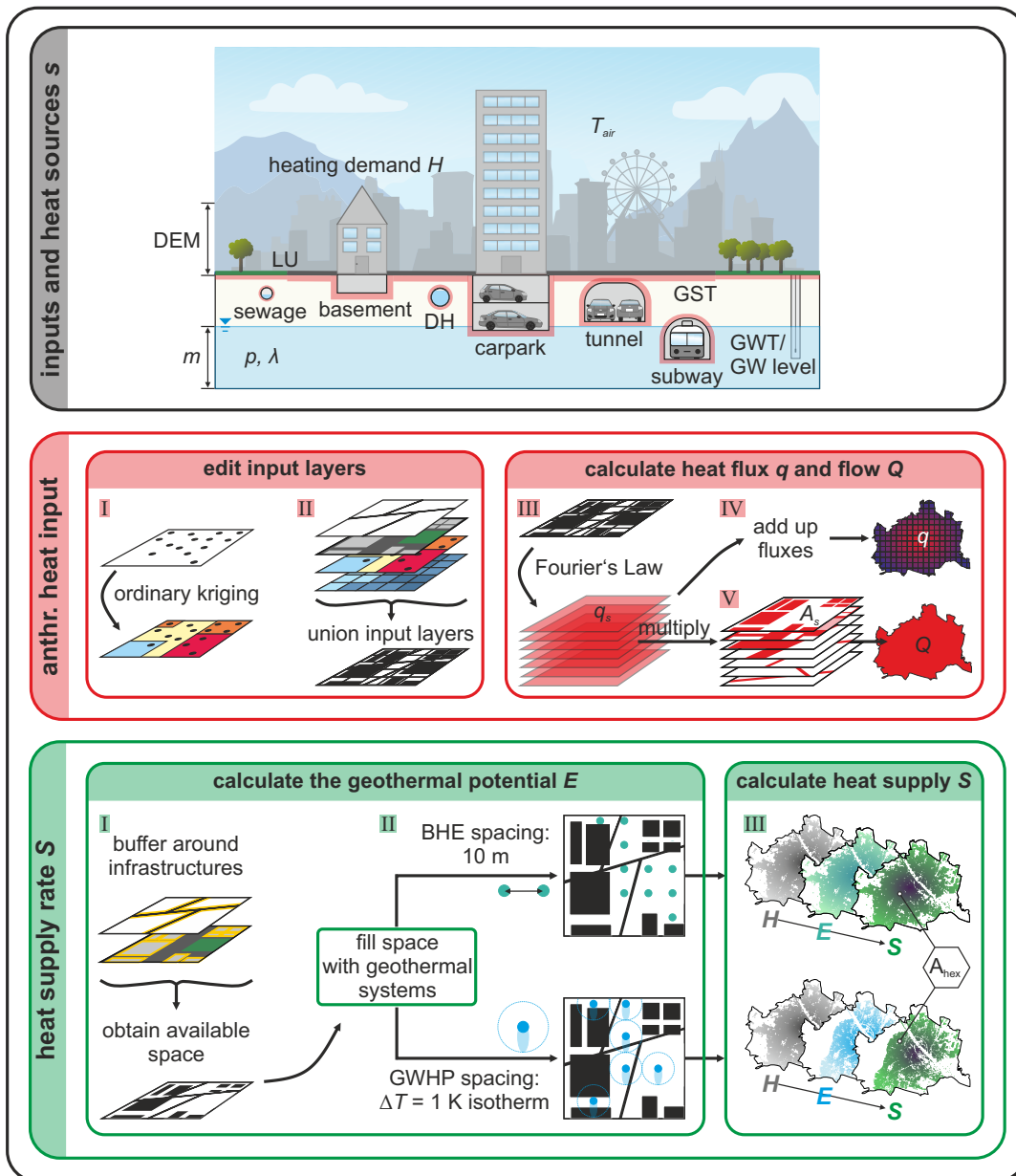


Figure 4.2: Workflow of the calculation of the heat flux and the heat supply rate including the anthropogenic heat flux model with its input data and anthropogenic heat sources. List of used abbreviations: hexagon area ($A_{hex} = 8657 \text{ m}^2$), area of the anthropogenic heat source (A_s), digital elevation model (DEM), district heating (DH), temperature difference (ΔT), technical geothermal potential (E), ground surface temperature (GST), groundwater (GW), groundwater temperature (GWT), heating demand (H), thermal conductivity (λ), land use (LU), aquifer thickness (m), porosity (p), total heat flux (q), heat flux per heat source (q_s), heat flow (Q), heat supply rate (S) and air temperature (T_{air}).

Calculation of the Technical Geothermal Potential and Heat Supply Rate

The following procedure for estimating the technical geothermal potential and the heat supply rate is in line with the evaluation steps described by Tissen et al. (2019). However, for the present study of Vienna, no data for domestic hot water demand is available, so the heat supply rate S is defined as ratio of the technical geothermal potential E to space heating demand H . The technical geothermal potential is evaluated in several steps, before the heat supply rates for borehole heat exchanger (S_{BHE} , S_{BHE_h}) and groundwater heat pump (S_{GWHP}) systems are calculated in an additional step.

To calculate heat supply rates for BHE systems (S_{BHE} , S_{BHE_h}), the geothermal potential, expressed as thermal conductivity (Stadt Wien), first has to be transformed into a specific standard q_{BHE} and raised q_{BHE_h} heat extraction rate. The transformation is conducted in two different ways. On the one hand, the Swiss Norm SIA 384/6 (2009) is employed to deduce the standard heat extraction rate q_{BHE} for a thermal conductivity value. On the other hand, higher heat extraction rates q_{BHE_h} due to groundwater flow are considered and the specific heat extraction rates by VDI 4640 part 2 (2001) are applied for the individual rock types of the aquifers.

The first step of the evaluation is a spatial analysis that yields the available space for the installation of BHE and GWHP systems. Here, a buffer of 2 m is placed around each building, tunnel and underground carpark, as well as a smaller buffer of 1 m around each subsurface supply pipe (VDI 4640 part 2, 2015). The buffer zones are merged and subtracted from the total city area to obtain the available space for geothermal system installation.

In a second step, this available space is filled with BHE and GWHP systems considering technology-specific spacings. In case of BHEs, the spacing is 10 m (best practice by GBA). In case of GWHP systems, the well space is defined as maximum extension of the thermal plume for a temperature reduction ΔT by 1 K. A detailed description of the plume evaluation is given by Tissen et al. (2019). Based on the input data listed in Table A.3, an $\Delta T = 1K$ isotherm for each hydrogeological unit is evaluated (Figure A.17). For simplicity, and because the heating demand is given per hexagon, the number of possible BHEs and GWHPs per grid cell g are summed up to obtain the maximum feasible number of system installations per hexagon h .

The product of the number of BHE n_{BHE}^h , a BHE length l of 150 m (best practice by GBA) and the average heat extraction rate q_{BHE}^h or $q_{BHE_h}^h$ yields the technical geothermal potential E_{BHE} or E_{BHE_h} . In contrast, E_{GWHP} is the product of the number of well pairs n_{GWHP}^h and the average GWHP potential q_{GWHP}^h per hexagon h .

In a third step, the heat supply rates S_{BHE} , S_{BHE_h} and S_{GWHP} are calculated for each hexagon h :

$$S_{BHE}^h = \frac{q_{BHE}^h \cdot l \cdot n_{BHE}^h \cdot t \cdot COP}{(COP - 1) \cdot H^h} \cdot 100 \quad (4.3a)$$

$$S_{GWHP}^h = \frac{q_{GWHP}^h \cdot n_{GWHP}^h \cdot t \cdot COP}{(COP - 1) \cdot H^h} \cdot 100 \quad (4.3b)$$

The heat supply rates [%] consider an operation time t of 1800 h/a and coefficient of performance (COP) of 4. The heat supply rates are evaluated for a heating demand H referring to the current building stock in the hexagon and for a future scenario in which all building have been thermally refurbished according to the OIB-RL6 standards of Austria (Österreichisches Institut für Bautechnik, 2015).

Furthermore, we define the ratio between total annual heat flow Q and heating demand H as theoretical sustainable potential.

4.3 Results and Discussion

4.3.1 Anthropogenic Heat Flux

The computed anthropogenic heat flux (AHF) q of all seven individual heat sources and the total heat flux show a significant spatial variability (Figure A.18). The highest mean heat flux originates from underground car parks ($15.38 \pm 5.20 \text{ W/m}^2$) and DH systems ($13.67 \pm 1.91 \text{ W/m}^2$). Whereas the smallest positive median heat flux rate is caused by elevated GST ($0.11 \pm 0.01 \text{ W/m}^2$) and buildings ($2.58 \pm 2.15 \text{ W/m}^2$). Tunnels have a negative mean heat flux ($-1.13 \pm 0.09 \text{ W/m}^2$). However, these results are based on two tunnels with a length of just 2.1 km and 0.21 km, respectively, and efficient ventilation systems. Hence, we assumed that the mean annual air temperature inside and outside of the tunnels are equal, and therefore cooler than the mean GWTs. Thus, tunnels act as heat sinks and cool the urban underground when multi-annual mean temperatures are used for assessment. Seasonal patterns might differ.

Benz et al. (2015) and Benz et al. (2018a) also calculated the anthropogenic heat flux by applying Fourier's Law in the two German cities, Karlsruhe and Cologne, as well as in Osaka, Japan. In the German cities the DH system causes the highest AHF, with the mean heat flux by the DH system in Karlsruhe being four times larger than in Vienna. One reason for this difference is the generally low heat loss of Vienna's DH network, which is reported to be below the average heat loss rate of European DH networks (Wiener Stadtwerke, 2015). The mean heat flux by buildings in Vienna is in good accordance with the results for Karlsruhe ($3.61 \pm 3.37 \text{ W/m}^2$), yet higher than in Cologne ($0.57 \pm 0.25 \text{ W/m}^2$) and Osaka ($0.32 \pm 0.18 \text{ W/m}^2$). In contrast, relatively high heat fluxes of 5.9 to 8.0 W/m^2 are reported for buildings in Basel, Switzerland (Mueller, Huggenberger, and Epting, 2018). This wide range of heat flux values from buildings in different cities is mainly due to differences in ground thermal conductivity, groundwater flow velocity, insulation and temperatures in buildings, and whether basements are within the un- or saturated zone (Mueller, Huggenberger, and Epting, 2018; Epting, Händel, and Huggenberger, 2013; Benz et al., 2018a; Dahlem, 2000).

The sum of all seven AHFs per grid cell, the total heat flux, is displayed in Figure 4.3a. In general, areas with shallower groundwater (GW) have a higher AHF. The shallowest depth to water table is along the Danube River and the old Danubian channel, as well as close to small streams in the north-western parts (Figure 4.1). Here the total heat flux is above 3 W/m^2 . Moreover, GST also significantly influences the total heat flux (Figure A.19). In green urban areas and forests (Wiener Wald) the total heat flux is negative, with GWT being higher than GST, and thus the groundwater releases heat towards the ground surface. In contrast, regions with sealed surfaces and a high building density in continuous and discontinuous urban fabrics represent areas of high total (downward) heat flux.

The mean total heat flux per pixel is $5.22 \pm 0.82 \text{ W/m}^2$. The mean heat flux per pixel without underground car parks, tunnels and subway system is $1.07 \pm 0.32 \text{ W/m}^2$, which is in good accordance with the mean heat flux per pixel in Karlsruhe with $1.10 \pm 0.73 \text{ W/m}^2$ (Benz et al., 2015). A main reason for this is that the average groundwater depth below the surface in Vienna (6.2 m) is similar to the one given

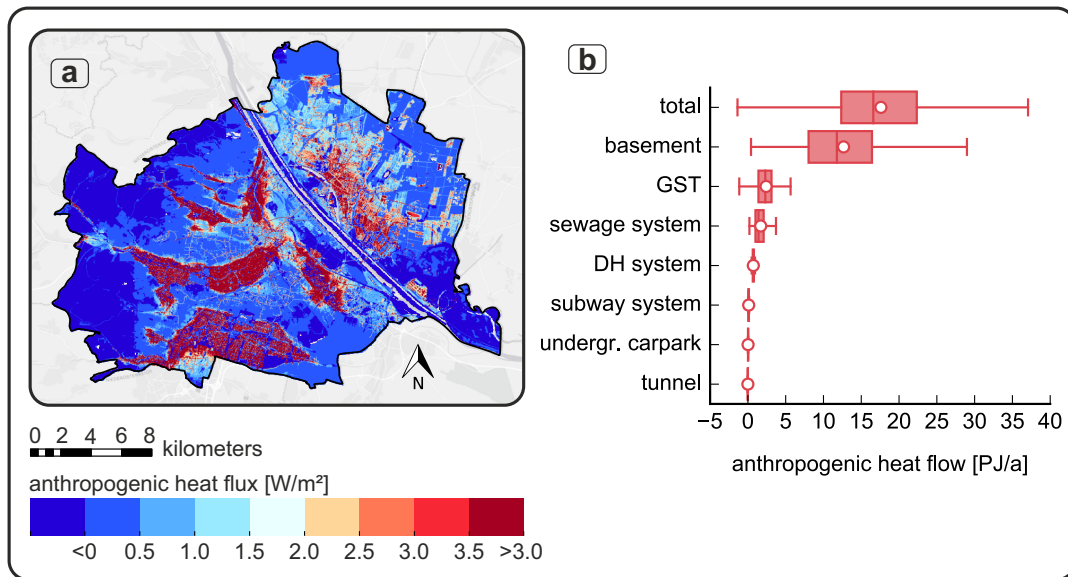


Figure 4.3: Map of the total average anthropogenic heat flux q per grid (25 m by 25 m resolution) (a) and boxplots of the total and individual anthropogenic heat flow Q (b). Mean values are indicated by a white dot.

for Karlsruhe (5.4 m). In contrast, for the city of Cologne, where the mean water table is around 10 m below surface, the total heat flux is only $0.39 \pm 0.12 \text{ W/m}^2$.

Locally, underground car parks and subway tunnels have the largest anthropogenic heat impact, yet on city scale the bulk contribution of these features is smallest. The highest heat flow over the entire city area arises from buildings ($12.65 \pm 6.45 \text{ PJ/a}$) and increased GST ($2.41 \pm 1.21 \text{ PJ/a}$), whereas the lowest heat flow originates from underground car parks ($0.02 \pm 0.01 \text{ PJ/a}$) and tunnels ($-4.48 \pm 0.36 \text{ TJ/a}$) (Figure 4.3b). The high standard deviations of the total heat flow values here reflect the interplay of parameter uncertainty in the calculation of the heat flows and the spatial variability over the study area (Figure A.18, A.19). Buildings and sealed ground cover 14% and 82% of the area of Vienna, whereas the twelve underground car parks and the two tunnels only account for 0.01% and 0.03% of Vienna's area, respectively. Consequently, the diffuse heat input in cities not only depends on the heat flux and its governing factors (such as basement depth and temperature), but on the large scale mainly on the size of the heat source. Menberg et al. (2013b) and Benz et al. (2015) and Benz et al. (2018a) also identified buildings and increased GST as main contributors to the annual ground heat flow and heat anomalies beneath Karlsruhe, Cologne and Osaka.

4.3.2 Sustainable and Technical Geothermal Potential

The calculated anthropogenic heat flow indicates a continuous heat input into the subsurface throughout the year. In principle, this means that an annual amount of $17.6 \pm 6.99 \text{ PJ/a}$ can be used by geothermal technologies to sustainably satisfy Vienna's heating demand. Considering a steady-state system and neglecting the impact of increasing heat flow in case of decreasing GWT, on average 37.7% of the current heating demand, and actually 99.5% of the future heating demand (in case

of thermally refurbished buildings) could be supplied sustainably (Figure 4.4). Differing values for the sustainable potentials, expressed as the ratio between available energy from heat flow Q to heating demand H , were reported by Benz et al. (2015) and Benz et al. (2018a) for Karlsruhe (32%) and Cologne (9%) in Germany, and smaller rates between 3% and 5% in Osaka, Japan. The sustainable potential as it is computed here gives an indication of how much heat is annually recharged from the surface and could be utilized theoretically. However, it does not include the presently stored heat, nor the additional geothermal heat flux from below, which are both part of the sustainably extractable energy. The computed values here can therefore be considered as a lower boundary of the full sustainable potential. Moreover, they are also conservative estimates, as ground heat extraction enhances the heat flux towards cooled ground regions. Finally, sustainable heat extraction rates could be also increased by recharging the ground in the summer season using heat release from geothermal cooling systems or waste heat.

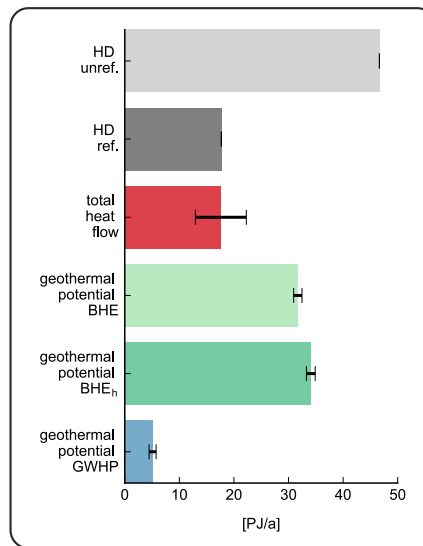


Figure 4.4: Comparison of the current (unref.) and future (ref.) heating demand (HD) with the total mean anthropogenic heat flow and the mean technical geothermal potentials of borehole heat exchanger with standard (BHE) and higher (BHE_h) heat extraction rate, and groundwater heat pump (GWHP) systems. Uncertainties are given as standard deviation, except for the heating demand for which no uncertainty is given.

If we only consider the thermal energy stored in the Quaternary aquifer (Zhu et al., 2010), a GWT reduction of 5 K would yield an amount of thermal energy that is 1.2 and 3.1 times larger than the respective heating demands.

In contrast, the technical geothermal potential of all GWHP systems operating for 1800 h/a is ten times smaller than the theoretical geothermal potential. Due to the large system spacing of 25 m to 176 m, the total number of GWHP is limited and consequently, only a small fraction of the stored energy can be harnessed by GWHPs each year. In total, solely 11% and 29% of the heating demand before and after refurbishment can be satisfied by GWHP systems.

The technical geothermal potential of BHE applications on the other hand show more promising results. A higher heat extraction rate (scenario BHE_h) even increases the potential by 7.6%. After refurbishment the geothermal potential exceeds the

heating demand by a factor of two. Thus, in the current state 68% of Vienna's heating demand could be supplied by BHE. BHEs are assumed to be installed with a much higher density of systems than GWHP and thus the vertical ground heat flux can be exploited more efficiently. However, in reality adjacent BHEs may interfere and thus compromise the efficiency of heat extraction (Rivera, Blum, and Bayer, 2017; Beck et al., 2013). Yet, the current approach does not consider the efficiency of the geothermal technologies due to lack of data. Also, BHEs utilize large volumes of the ground, as a depth of 150 m is assumed for the study case of Vienna. In comparison, GWHPs extract heat from typically layered aquifers of lower thickness and thus induce broader thermal anomalies (Pophillat et al., 2018; Tissen et al., 2019).

Hence, the difference between theoretical and technical geothermal potential is just a matter of optimising the system spacing and technical method of energy extraction from the ground, while taking care of a sustainable management of this resource. Sustainability could be achieved if the annual anthropogenic heat input was recycled by BHE and/or GWHP applications. In fact, for 1.8% of the hexagons the anthropogenic heat flow is larger than the technical geothermal potential, and for 14% of the hexagons even larger than the heating demand of unrefurbished buildings.

4.3.3 Heat Supply Rate

The comparison of the technical geothermal potential and the heating demand leads to the heat supply rate. The average BHE heat supply rate per district is 12% to 180% before and even 35% to 427% after refurbishment. So in 7 or rather 14 out of 23 districts the average BHE potential is higher than the average heating demand before or after refurbishment, respectively. The highest GWHP heat supply is located in the southern parts of district 10 and reaches 34% in case of unrefurbished and 83% in case of refurbished buildings (Figure 5).

The BHE heat supply rate per hexagon is above 100% in 64% and 82% of all hexagons before and after refurbishment, respectively. Looking at these rates for the hexagons on district level, reveals that the outer districts 14, 21 and 22 are more likely to yield a heat supply rate above 100% than the inner-city districts 4, 7 and 8 (Figure 4.5c). This spatial distribution of the BHE heat supply rates exhibits a radial pattern with increasing supply rates from the city centre towards the outer districts, illustrated by the heat supply map in Figure 4.5a. The lower heat supply rates in the inner districts (1-9) are attributed to a larger gross floor area, higher population and building density, leading to less available space for system installations. Moreover, old buildings from the "Gründerzeit" epoch (19th century) in the city centre have a high heating demand. In contrast, in the outer districts (11, 14, 19, 21, 22, 23) with discontinuous urban fabric, heating demand is lower and also more space is available for geothermal systems. Dochev and Peters (2019) also conclude in their study that the heat supply rate depends more on the heating demand, than on geological conditions. They also obtain similar values for the heat supply rate (below 75%) in central areas of the city of Hamburg, Germany. In their study on the theoretical geothermal potential of the city of Ludwigsburg, Germany, Schiel et al. (2016) also pointed out that it is more likely to meet the heating demand in residential areas.

For 9% (unrefurbishment) and 22% (refurbishment) of all hexagons (Figure 2), the GWHP supply is above 100%. In contrast to the pronounced radial distribution of the BHE heat supply rate, the GWHP supply rate shows no distinct spatial distribution (Figure 4.5b). The likelihood of achieving a heat supply rate above 100% is higher in district 2, 10 and 11 in the south than in the inner and eastern district

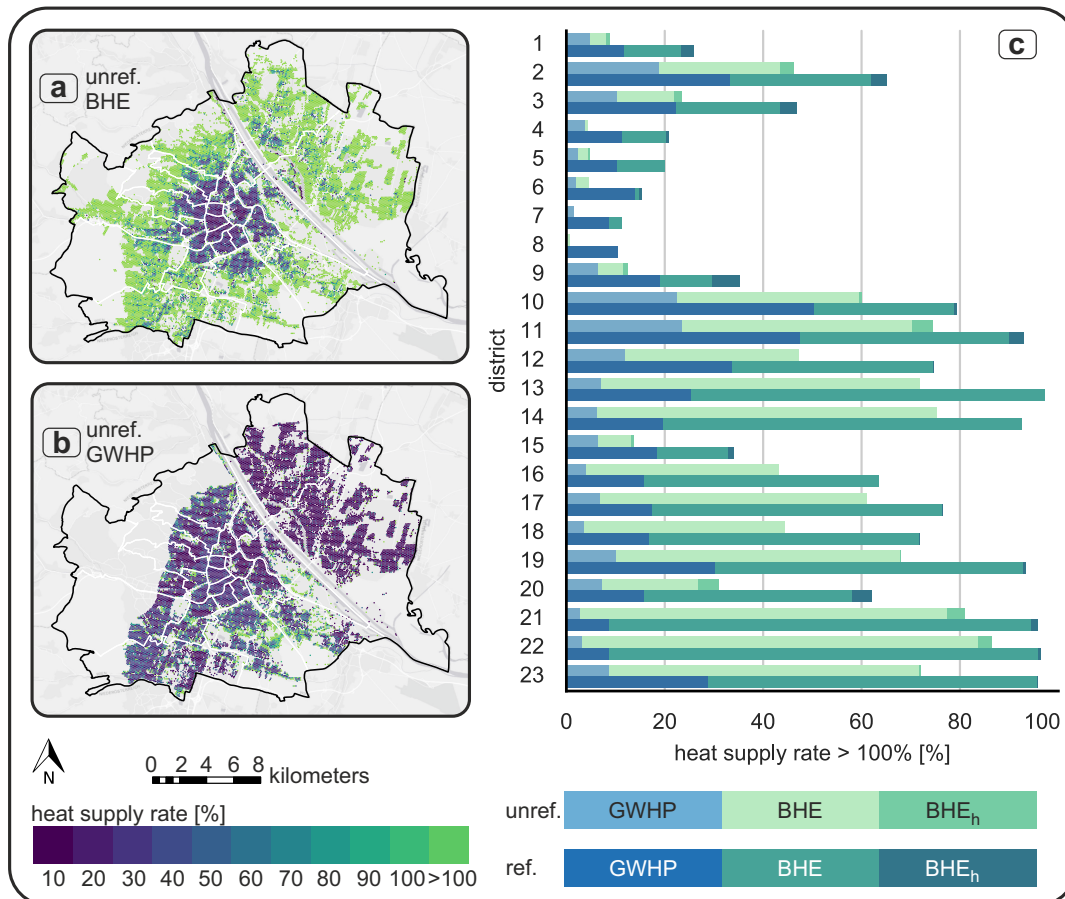


Figure 4.5: The maps display the spatial distribution of the heat supply rate referring to the heating demand of unrefurbished (unref.) buildings for borehole heat exchanger (BHE) (a) and groundwater heat pump (GWHP) systems (b). The bar graph shows the percentage of hexagons with a heat supply rate above 100% for all 23 districts (Figure 4.1) and a heating demand referring to un- (unref.) and refurbished (ref.) buildings (c). Scenario BHE_h considers partly higher heat extraction rates due to groundwater flow.

7, 21 and 22 (Figure 4.5c). As stated above, the GWHP potential, and so the heat supply rate (Figure 4.5c), are mainly influenced by the GWHP spacing and the number of potential GWHP systems, as well as the hydrogeological conditions (Figure A.20). The aquifer east of the Danube River (district 21 and 22) is the most productive aquifer with the highest yield. Given the large extension of the induced thermal plumes, the spacing between the systems is large here (176 m), and therefore, few installations are possible leading to the lowest total supply rate of Vienna. This finding appears to contradict the fact that this areas have the most productive aquifer, yet the extension of the thermal plume increases with groundwater flow velocity or pumping rate (Pophillat et al., 2018). In future studies, the definition of GWHP spacing based on temperature plumes has to be reconsidered, so that the technical geothermal potential can be increased and approach the theoretical geothermal potential of the aquifer. For this purpose more GWT, ground water level and flow velocity data are required, especially west of the Danube River, to improve spatial interpolation and the estimation of temperature plumes. In addition, a numerical heat transport

model could be developed to optimise the use of the groundwater.

4.3.4 Key Locations for Shallow Geothermal Use

Areas with a high heat supply rate as well as a high theoretical sustainable potential are the key locations for shallow geothermal use. Here, the heating demand could be met with BHE or GWHP systems. Additionally, the extracted energy is for a large part compensated by the anthropogenic heat input. To avoid competition with heat supply by district heating, we identify key locations only for city blocks without district heating (Figure 4.6). The DH network concentrates on the city centre, so that the DH-free areas are located in the outer districts, which conveniently also have the highest heat supply rates before refurbishment. Except for district 15, all districts show an average BHE heat supply rate above 100%. District 21 and 22 only have a GWHP supply rate of maximum 7%, however the southern parts of district 10 and 11 achieve a supply rate above 55%. The average sustainable potential per districts ranges between 8% and 58%. Epting et al. (2018) compared the waste heat, defined as higher GWT due to the heat input by buildings and reinjection of cooling water, to the heating demand of Basel, Switzerland. They concluded that for 30% of the area the waste heat is sufficient to satisfy the heat demand. In Vienna, a sustainable potential above 100% is obtained for 15% of the area without a district heating system. After refurbishment or for newly constructed low-energy buildings, the heat supply rate and sustainable potentials are even more propitious. For a heating demand reduced by 62%, a heat supply rate above 100% is achievable for 97% (BHE) and 26% (GWHP) of the hexagons. Additionally, over one third of the hexagons delineate a sustainable potential above 100%. These vast potentials are valuable assets for Vienna's urban energy development plans.

The circles on the maps in Figure 4.6 indicate the different potentials of settlement development described in Vienna's new urban development plan called STEP 2025 (MA 18, 2014). The plan comprises 480 to 9400 new housing units in areas all over Vienna (Kail, 2017). So far no (magenta circles) or only short branches (orange circles) of the DH system reach into these areas. Accordingly, shallow geothermal systems are revealed to be the ideal decentralised, renewable energy resource for these new housing units. The eastern and southern districts comprise the majority of the potential areas for settlement development. Moreover, here are also the areas with the highest BHE heat supply rate and sustainable potential. In regard to the smaller system spacing in the south-western city area, district 2, 10 and 11 are the most suitable areas for GWHP systems (Figure A.17). In the southern part of district 10, 5850 new housing units are planned in an area without a DH system and a high supply rates. The mere coincidence and winning combination of the three high potentials, namely geothermal, sustainable and settlement development potential, provide support for an easy assessment of feasibility and integration of geothermal system in local urban energy planning.

4.4 Conclusion

In this study, we develop the Python and ArcGIS based tool GeoEnPy and apply it to the city of Vienna to compute the anthropogenic heat flux and flow into the urban subsurface, the technical geothermal potential for closed and open-loop systems, the sustainable potential, as well as the heat supply rate. Parameter uncertainties and spatial variability are assessed by performing Monte Carlo simulations. We thus

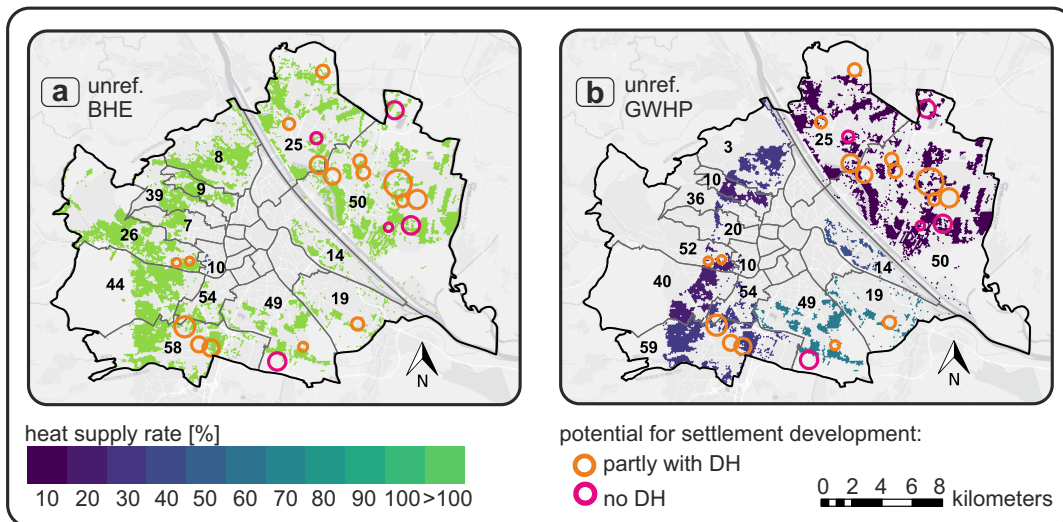


Figure 4.6: Spatial distribution of the average heat supply rate per district for borehole heat exchangers (BHE) (a) and groundwater heat pumps (GWHP) (b) assuming that all buildings are unrefurbished (unref.). The numbers within each district refer to the sustainable geothermal potential in percent. The circles indicate areas with potential for settlement development (Kail, 2017), where the district heating system (DH) is already partly expanded (orange) or no DH system (magenta) exists. Circle size represents the potential for settlement development (smallest circle: building design of 460 housing units, largest circle: building design of 9400 housing units).

identify the most attractive locations for BHE and GWHP systems in Vienna with respect to existing heating infrastructure. GeoEnPy relies on basic hydrogeological and city data, such as building stock and subsurface infrastructure information, and can therefore also be applied to other cities. To extend the geospatial analysis of GeoEnPy to a spatio-temporal analysis, seasonal and annual variations in heat and also cooling demands, as well as heat flow could be integrated in future studies. Furthermore, the theoretical sustainable and technical geothermal potential could be combined to investigate how much of the annual heat input could be technically extracted by BHE or GWHP.

The suburban districts 10, 12, 22 and 23 achieve high heat supply rates and the highest sustainable potential. Hence, these areas are the key locations for geothermal use in Vienna. In general, BHE systems achieve a higher supply rate than GWHP systems and are thus more attractive, due to the smaller spacing between the individual systems. The overall annual heat flow from anthropogenic heat sources in these four districts is 53% of the current heating demand. By extracting only this annually recharged thermal energy, a cooling of the ground and long-term reduction in system efficiency could be avoided. A further increase in efficiency and sustainability could be achieved by storing thermal energy in the subsurface, e.g. through borehole thermal energy storage (BTES) or aquifer thermal energy storage (ATES) systems and/or a combination with solar collectors. The illustration of the high geothermal and sustainable potentials, especially in case of closed-loop systems at the urban fringe, should encourage and support urban planners, energy agencies and public authorities to incorporate shallow geothermal energy in future urban development.

Acknowledgements

The authors are grateful for data exchange with Wiener Linien, Wien Energie, Technische Universität Wien and ZAMG (Zentralanstalt für Meteorologie und Geodynamik). The authors particularly thank Bernd Kowaschitz and Thilo Lehmann from Wien Kanal as well as Robert Lauter from Wien Energie for their informative conversations regarding sewage water temperature and heat loss rates of the local district heating network. We gratefully acknowledge the provision of tunnel data by Julia Della Porta from ASFINAG (Autobahnen- und Schnellstraßen-Finanzierungs-Aktiengesellschaft). The authors thank GRACE, the Graduate School for PhD students of the KIT-Center Climate and Environment at the Karlsruhe Institute of Technology (KIT) and Helmholtz Association of German Research Centres (HGF) portfolio project “Geoenergy” (grant number 35.14.01; POF III, LK 01) for funding this work.

5 Synthesis

5.1 Conclusion

Increased groundwater temperature (GWT) are observed in rural and urban areas worldwide. Increased GWT, in general, and GWT anomalies, in particular, are traceable to heat inputs from anthropogenic heat sources. These heat sources can occur locally, as a point source in the form of basements, underground car parks or swimming pools, but also on larger scale like contamination or mining. On account of the enormous number of anthropogenic heat sources, e.g. basements and sealed surfaces, all heat inputs into the subsurface add up and lead to the subsurface urban heat island (SUHI) effect. This additional, continuous, annual heat input by anthropogenic heat sources can be recovered and recycled by shallow geothermal systems to supply a quarter or an entire city with sustainable thermal energy.

Out of a huge GWT data set of 44,205 wells from ten European countries, bias-free annual mean GWTs and an anthropogenic heat intensity (AHI) for over 10,000 wells is determined. The anthropogenic heat intensity (AHI) relates the median rural background GWT to local, multi-annual mean GWT. Based on these 10,000 wells, the AHI is applied to localise and map positive temperature anomalies in central Europe. All wells are linked and categorised according to the three CORINE Land Cover (CLC) classes: 'natural', 'agricultural' and 'artificial' (CORINE, 2016). Wells on artificial surfaces have the highest mean temperature deviation from the natural background GWT (1.12 ± 1.50 K), while the mean AHI of wells beneath agricultural land is slightly increased (0.20 ± 1.00 K) and slightly negative for wells under natural surfaces (-0.06 ± 1.31 K). The upper 3% percentiles of each land cover classes define hot spots, or rather the most extreme positive GWT anomalies (AHI_{max}), numbering 318 wells in total. AHI > 3K under both natural and agricultural surfaces, can be traced back to hot springs or local anthropogenic sources, such as contamination caused by mining, landfills or wastewater treatment plants. Since wells located under artificial surfaces show highest AHIs, the locations, quantity and drivers of AHI_{max} for these wells are studied in more detail. Based on common land covers, the location of artificial AHI_{max} wells are categorised into with 20 detailed subclasses and six main land utilisation classes (LUC): industry park, waste, farming, automotive, city and factory. Wells close to 'factories' have on average the largest AHI (7 K) and wells in 'industry parks' have the smallest AHI (5 K) and impact on GWT. Most of the hot spots belong to the class 'city' (33%), followed by 'factory' and 'industry park' with 27% and 24%, respectively. The heat sources of 16 out of the 45 hot spots under artificial surfaces are identified and summarised in seven classes: hot spring, contamination, mining, basement, district heating (DH), swimming pool and underground car park (Figure 5.1). Highest GWT and AHI originate from natural hot springs. All remaining heat sources are attributed to anthropogenic activities. Contamination and mining have the largest extensions and mean AHIs with 7.04 ± 2.09 K and $8.36 \pm$ K, respectively. Basements, DH networks, swimming pools and underground car parks are more local, punctual heat sources. Underground

carparks can locally increase GWT by up to 6.80 K in comparison to rural, undisturbed GWTs.

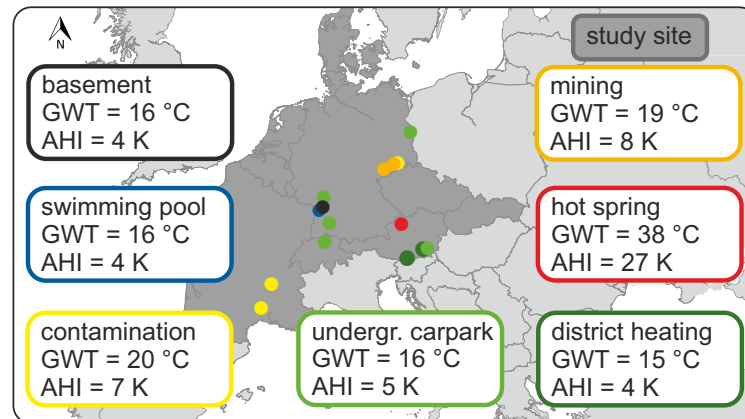


Figure 5.1: Overview of the survey area and location of the upper 3% percentiles of AHI for wells beneath artificial land cover (AHI_{max}). The seven heat sources of these hot spots are colour-coded according to their anthropogenic heat intensity (AHI). The local mean groundwater temperature (GWT) is also listed.

The first study (Chapter 2) quantifies the anthropogenic heat input in terms of AHI, whereas the third study (Chapter 4) expresses it terms of anthropogenic heat flux (AHF). The anthropogenic heat flux into Vienna's subsurface is calculated within 25 m x 25 m grid cells for seven heat sources: basements, elevated ground surface temperatures (GST), underground carparks, car tunnels, sewage, district heating (DH) and subway system. The mean heat flux per pixel of all heat sources is $5.22 \pm 0.82 \text{ W/m}^2$. The highest heat flux arises from underground carparks ($15.38 \pm 5.20 \text{ W/m}^2$) and DH systems ($13.67 \pm 1.91 \text{ W/m}^2$), the smallest AHF are by elevated GST ($0.11 \pm 0.01 \text{ W/m}^2$) and buildings ($2.58 \pm 2.15 \text{ W/m}^2$). The AHF is controlled by the depth to water table and temperature gradient. The shallower the GW the higher the AHF, and if the temperature of the heat source is larger than the GWT, the resulting heat flux is negative. In green urban areas and forest, where GST is cooler than GWT, a negative heat flux, so a flux directed towards the ground surface, can be observed. Summing up all AHF over the entire study area leads the total anthropogenic heat flow. Regarding the whole area of Vienna, basements and elevated GST have the highest heat flow, thus yield the biggest heat input into the subsurface, and represent the main drives for increased GWT. The results of Chapter 2 and 4 reveal that punctual heat input of subsurface structures, such as district heating pipes and underground carparks have a high heat flux and cause local temperature anomalies. However, basements and elevated GST are more frequent in urban areas and therefore, have in total a significant impact on city-wide GWT. Small-scale heat sources such as contamination and mining operations are less frequent, yet, due to their size and high AHI also important factors. In summary, the magnitude of the impact of the heat input into urban subsurface not only depends on the heat flux and its influencing factors (such as temperature as well as the space between the heat source and water table) but also on the spatial extent and frequency of the anthropogenic heat source.

In Chapter 3 and 4 the technical geothermal potential of open- and closed-loop

geothermal systems is calculated on quarter- and city-scale. The theoretical geothermal potential of GWHPs, representing the upper energy boundary of extractable energy, is also taken into consideration. The theoretical potential refers to the energy gained when cooling a given water volume of the aquifer. According to VDI 4640 part 4 (2004), a maximal cooling of the extracted groundwater (GW) of 6 K and minimum reinjection temperature of 5 K are appropriate. The technical geothermal potential is the part of the theoretical geothermal potential that can be actually extracted with a specific system. The ratio of the geothermal potentials to the annual heating demand, before and after the refurbishment of the building stock, is defined as heat supply rate. At first, the evaluation of the geothermal potential of the groundwater heat pump (GWHP), horizontal (hGSHP) and vertical (vGSHP) ground source heat pump systems, as well as the heat supply rate, are deduced for the case study in the quarter "Rintheimer Feld" (RF) in the eastern part of Karlsruhe, Germany (Chapter 3). After that, the evaluation of the geothermal potential of vGSHPs and GWHPs as well as the heat supply rate are expanded from quarter- to city-scale and applied to Vienna, the capital of Austria (Chapter 4).

The theoretical geothermal potential of GWHP systems is sufficient to meet the heat demand of the refurbished building stock in RF. To avoid thermal interference of adjacent GWHP systems, the spacing between reinjection wells is defined in terms of the maximum expansion of the $\Delta T = 1$ K isotherm the thermal plume from the reinjected water. The consideration of an appropriate spacing to avoid thermal interference results in a drastic decline in heat supply rate of 60% (Figure 5.2c). Results for the theoretical and technical potential in Vienna are similar. The energy stored in the upper aquifer is 1.2 and 3.1 times higher than the respective heating demand before and after refurbishment. Considering spacing and an annual operation time of 1800h/a the technical potential is ten times smaller than the theoretical one. On city-scale, GWHP can meet 11% and 29% of the heating demand before and after refurbishment. Although, the horizontally installed pipes of hGSHP take up much space, the available space in RF is sufficient to extract enough energy to meet the heat demand after refurbishment (Figure 5.2a). Standard heat extraction rates for borehole heat exchangers (BHE) are specified by VDI 4640 part 2 (2001) for specific geological units. Yet, higher heat extraction rates due to moderate to high GW flow are feasible. In Vienna, the average supply rate for BHEs per district is 12% to 180% before and even 35% to 427% after refurbishment. Higher heat extraction rates increase the technical geothermal potential on average by 7.6%. Vertical GSHP systems in RF yield a heat supply rate of 131% and 152% for standard and high heat extraction rates, respectively. After refurbishment, the heat supply rates are 277% and 322% (Figure 5.2b).

An inverse analysis allows an optimisation of BHE spacing to avoid an over-sizing as well as save material and drilling cost. It turns out, that for standard heat extraction rates a BHE spacing of 11 m and 16 m is sufficient to meet the heat demand before and after refurbishment, respectively. For high heat extraction rates, the spacing can be even raised to 12 m and 17.5 m.

The results of Chapter 3 and 4 reveal that geothermal potentials, in particular of vGSHP systems, are sufficient to meet the heat demand, before and after refurbishment, of the whole RF and specific districts in Vienna. Yet, there are circumstances which reduce the geothermal potential and in turn the heat supply rate. The heat supply is subject to hydro-, geological and thermal ground conditions as well as legal constraints and the local heat demand. For instance, due to a larger system spacing,

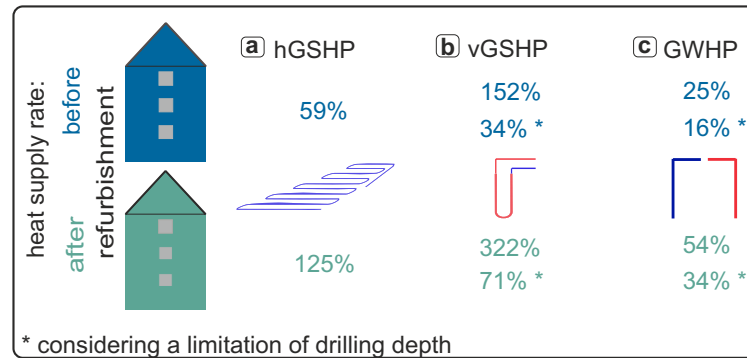


Figure 5.2: Results of the evaluation of the heat supply rate based on the technical geothermal potential of three different shallow geothermal systems: horizontal ground source heat pump (hGSHP), vertical ground source heat pump (vGSHP) considering an increased heat extraction rate and groundwater heat pump (GWHP). The heat supply rate refers to the heat demand before and after refurbishment.

the technical geothermal potential of GWHPs is lower than the one of BHEs for both case studies, Rintheimer Feld and Vienna. The expansion of the thermal plume, and thus the well spacing, increases with groundwater flow velocity and pumping rate. Consequently, the spacing varies with hydrogeological conditions over the study site. For BHEs a constant spacing of 10 m is employed in both case studies. Yet, the heat extraction rates vary in dependence of thermal conductivity and groundwater flow. With respect to the thermal conditions in the subsurface, higher GWT due to the SUHI effect raise the theoretical potential and technical geothermal potential of GWHPs and BHEs. Considering the local limitation of the drilling depth in the RF, boreholes can be only be drilled up to a depth of 17 m below ground. Consequently, the BHE length is cut down by 83 m, and the exploitable aquifer thickness drops from 31 m to 13 m. For a standard and high heat extraction rate, this legal constraint reduces the technical geothermal potential of BHE by 83% and 78%, respectively. In the case of GWHP, the theoretical potential decreases by 7% and the technical potential by 36%. The total heat demand of a quarter, district or entire city not only depends on the state of refurbishment but also on building age, population and building density. For example, the heat demand in Vienna's city centre, where old buildings from the "Gründerzeit" epoch (19th century) dominate, is comparably higher than in the outer districts with a discontinuous urban fabric.

As discussed above, in both case studies, BHEs achieve the highest heat supply rate, especially after refurbishment. In RF, for example, the supply rate after refurbishment is two times higher than before refurbishment. However, neither in RF nor in Vienna's suburbs a refurbishment is indispensable to meet the heating demand. Yet, in dense urban areas with a consequently higher heating demand and less space for system installation, a thermal refurbishment of the building and heating system would increase the likelihood to satisfy the heat demand by geothermal energy (Chapter 4).

The heat input by anthropogenic, local and small-scale heat sources (Chapter 2) and the wide-spread anthropogenic heat flow (Chapter 4) supplies a continuous thermal replenishment of the subsurface. This surplus of energy or waste heat can be recovered and recycled by geothermal systems to provide sustainable thermal

energy. The fraction of the heating demand that can be supplied by the annual, anthropogenic heat input into the subsurface is defined as theoretical sustainable potential. The theoretical sustainable potential does neither include the geothermal heat flux from below, nor the presently stored energy. However, the annual thermal recharge from the surface defines the lower boundary of the thermal energy in the subsurface that can be theoretically harnessed by geothermal systems. In Vienna, an annual heat input of 17.6 ± 6.99 PJ/a can be used by geothermal technologies to sustainably satisfy Vienna's heating demand. This heat input corresponds to 37.7% or 99.5% of Vienna's present heating demand or in case of thermally refurbished buildings. The outer suburbs of Vienna are discontinuous urban fabrics with a lower heating demand, where more space is available for geothermal systems than the inner districts. In addition, there is no DH installed which could act as a competitive heat supplier to geothermal use (Figure 5.3). To identify key locations for geothermal use in these city parts, both the anthropogenic heat flow and technical geothermal potential are spatially resolved and related to the annual heating demand.

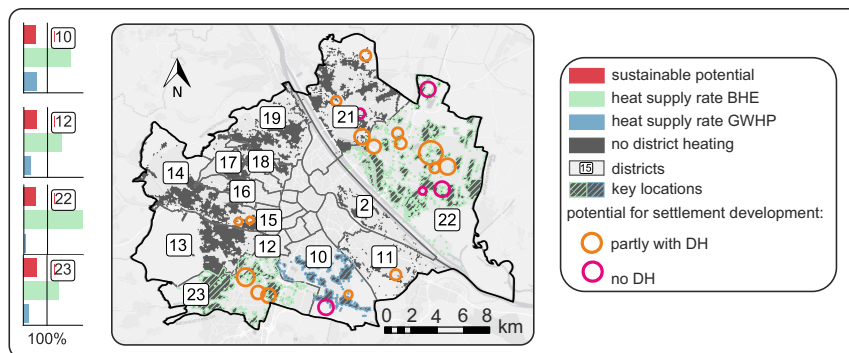


Figure 5.3: Spatial distribution of the key locations for shallow geothermal energy and bar graphs for the average theoretical sustainable potential and heat supply rate per district for borehole heat exchangers (BHE) as well as groundwater heat pumps (GWHP) for the present heating demand. The circles indicate areas with potential for settlement development (Kail, 2017), where the district heating system (DH) is already partly expanded (orange) or no DH system (magenta) exists. Circle size represents the potential for settlement development (smallest circle: building design of 460 housing units, largest circle: building design of 9400 housing units).

For 13 out of 14 districts with DH-free areas an average BHE heat supply rate above 100% can be obtained. In contrast, solely two districts reach a GWHP supply rate of 55%. A sustainable potential above 100% is achievable for 15% of the DH-free area. If Vienna's buildings stock is to be refurbished, the heating demand will be reduced by 62%, and a heat supply rate above 100% can be achieved for 97% (BHE) and 26% (GWHP) of the suburban area. In addition to this, over one third of the energy demand could be sustainably supplied. These vast potentials are convincing argument to promote the integration of geothermal systems in local urban energy planning. A powerful combination of a high technical geothermal and theoretical sustainable potential with urban development plans for new housing units can be achieved in four suburban districts (district 10, 12, 22 and 23 in Figure 5.3). If only the annual anthropogenic heat input in these four districts was extracted by geothermal systems, the current heating demand could be met to 53%. Thus, these areas are Vienna's key locations for geothermal use.

5.2 Perspective and Outlook

Groundwater (GW) serves multiple services and needs: It is a habitat for GW flora and fauna, the largest resource for drinking water in Europe and an energy reservoir for both heating and cooling purposes. Increased GWT have positive and negative side effects on GW ecology, geothermal systems and human health, and can enhance the competition between different interest groups.

On the one hand, the large- and small-scale anthropogenic heat input into the aquifer can be treated as pollution (WFD, 2000). Increased GWTs change the chemical and physical state of the GW which in turn impact GW quality negatively (Riedel, 2019; Sharma et al., 2012; Arning et al., 2006; Bonte et al., 2011a; Bonte, 2013; Bonte, Stuyfzand, and Breukelen, 2014; Griffioen and Appelo, 1993; Possemiers, Huysmans, and Batelaan, 2014). An increase in GWT detrimentally affects GW bacterial and fauna community composition, as well as biogeochemical processes and propagation of pathogen micro-organisms (Schweikert, 2014; Brielmann et al., 2009; Brielmann et al., 2011). Furthermore, high GWT stimulate the mobilisation and spreading of contaminations or pollutants such as arsenic (Bonte, 2013; Bonte, Breukelen, and Stuyfzand, 2013; Bonte, Stuyfzand, and Breukelen, 2014; Griebler et al., 2014). In the end, a deterioration of GW quality endangers the hygienic state of groundwater and the most important drinking water resource in the European Union (Commission, 2016).

Another negative aspect of increased GWT is the reduced efficiency and limited application of open geothermal systems. In Europe, various regulations define temperature limits for reinjected water from industrial cooling processes and/or open geothermal systems (Hähnlein, Bayer, and Blum, 2010). For instance, in Germany the allowed temperature difference between the extracted and reinjected water is $\Delta T = 6 \text{ K}$, while the maximum reinjection temperature is limited to $20 \text{ }^\circ\text{C}$. Especially in cities, where GWTs are already increased, this upper temperature boundary limits the possible temperature difference, which is required to efficiently run a cooling system (Epting, Händel, and Huggenberger, 2013; Ferguson and Woodbury, 2004). Beside GWHP and reinjection of cooling water, other anthropogenic heat sources exist, which may have a much larger and more widespread impact on GWTs (Epting, 2017; Epting and Huggenberger, 2013; Menberg et al., 2013b; Menberg et al., 2013a). The results in Chapter 2 show that local heat inputs by anthropogenic heat sources infringe the German, legally binding temperature thresholds. Out of 318 hot spots in total, in nine wells a absolute GWT above 20°C and in 34 wells an AHI above 6 K are detected. However, these heat sources are not subject to any legal framework. Consequently, regulations for the use of GWHP should be reviewed in order to be more flexible and adaptable to local GW quality, temperature conditions and the designated use. Furthermore, a holistic GW management is crucial to protect and preserve the natural state of GW ecosystems while ensuring a sustainable use of groundwater as energy resource (Datta, 2005; Flörke, Schneider, and McDonald, 2018; Epting, Händel, and Huggenberger, 2013).

On the other hand, the positive side effects of increased GWT are enhanced performance and economic benefits for the use of shallow geothermal energy systems. Increased GWT, due to anthropogenic heat inputs, can also be understood as an additional energy source for shallow geothermal use. The results of Chapter 4 show that the waste heat by anthropogenic heat sources can be recovered and recycled by shallow geothermal systems to ensure sustainable thermal energy. Previous studies

also noted the opportunity to use anthropogenic heat inputs to harness more energy from the subsurface and run shallow geothermal systems more sustainably (Arola and Korkka-Niemi, 2014; Bayer et al., 2019; Menberg et al., 2015; Rivera, Blum, and Bayer, 2017; Zhu et al., 2010). Furthermore, a cooling of the overheated aquifer by geothermal heat extraction can thermally remediate the aquifer, and so the natural thermal state can be restored.

The vast potentials of increased GWT and GWT anomalies for a sustainable thermal energy supply should encourage and support urban planners, municipalities, energy agencies and public authorities to incorporate shallow geothermal energy in urban energy development plans. To promote and demonstrate this potential to a broad community, GeoEnPy could be further developed and integrated into a web-based platform. An add on to estimate the installation costs of a specific geothermal system and its CO₂ mitigation would be also a valuable asset. Furthermore, coupling with other renewable energy resources, such as solar collectors, or integration of borehole thermal energy storage (BTES) or aquifer thermal energy storage (ATES) could be an option. That way, the online version of GeoEnPy would be easily accessible and applicable to other cities and enables an intelligent integration and linking of renewable energies for urban planning.

A Appendix

Appendix - Chapter 2

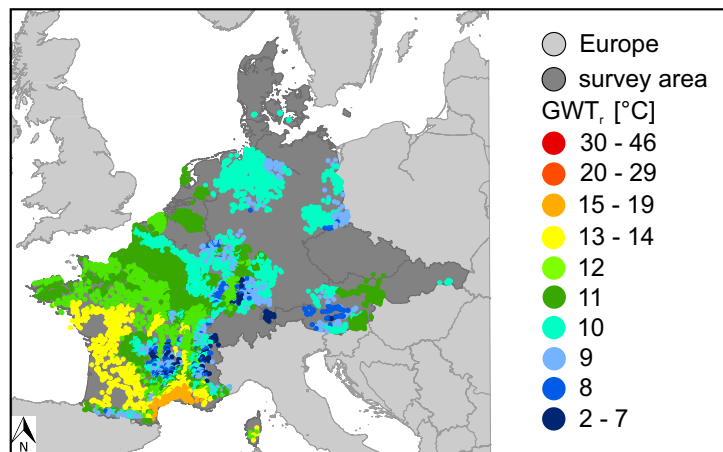


Figure A.1: Median rural background groundwater temperatures (GWT_r) for all AHI wells (10656 wells). The geographical distribution of the undisturbed GWT_r reflects the dependence on latitude and altitudes. In general, GWT_r increases from north to south (Denmark to the south of France). Higher altitudes such as the Alps, Massif Central and Pyrenees stand out with lower temperatures, whereas the Upper Rhine Graben (URG) has a higher GWT_r.

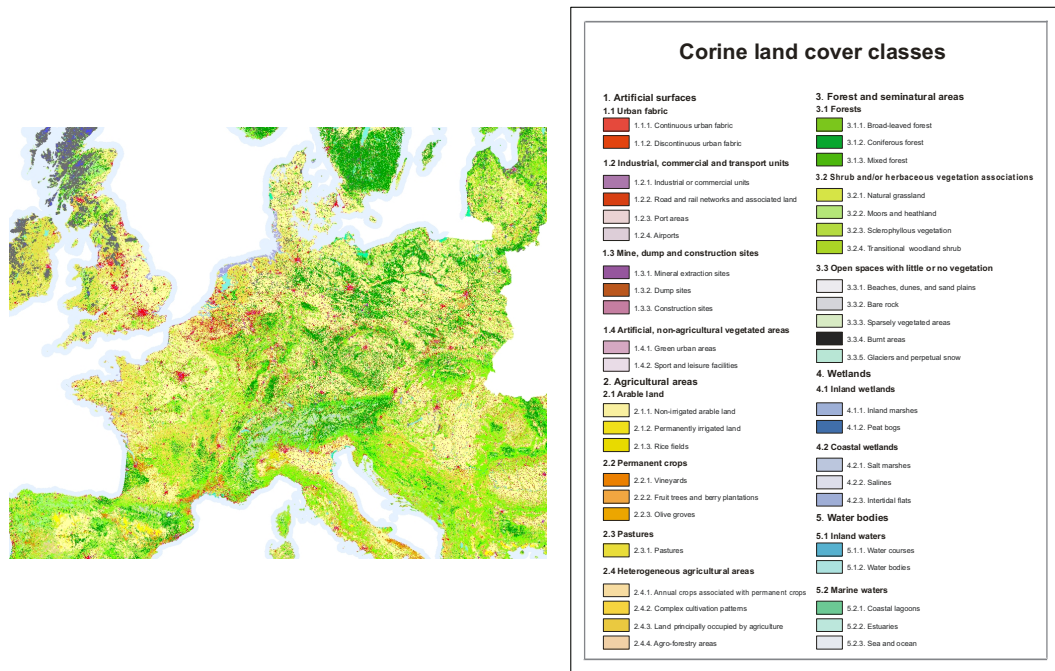


Figure A.2: Corine Land Cover (CLC) data of Europe (CORINE, 2016).

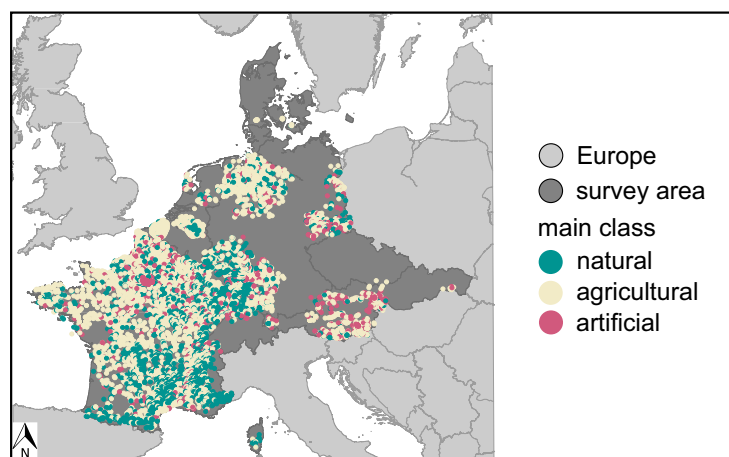


Figure A.3: AHI wells colour coded according to their main class. Classification scheme bases on CLC Level 1 (CORINE, 2016).

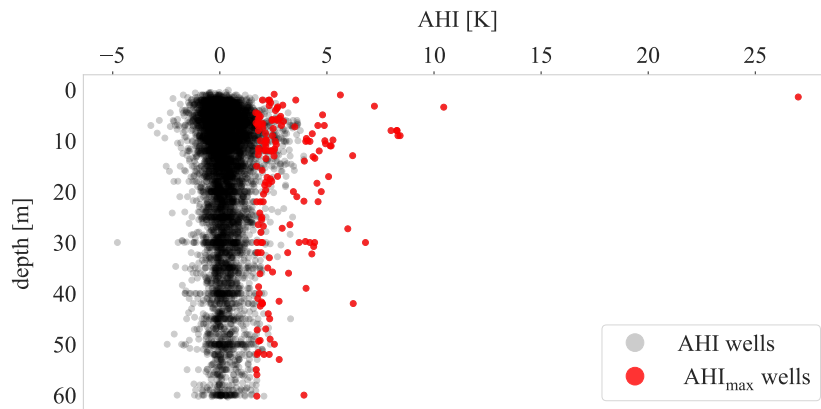


Figure A.4: Anthropogenic heat intensity (AHI) versus known measurement depth for AHI and AHI_{\max} wells. The correlation coefficient for depth and GWT is 0.03.

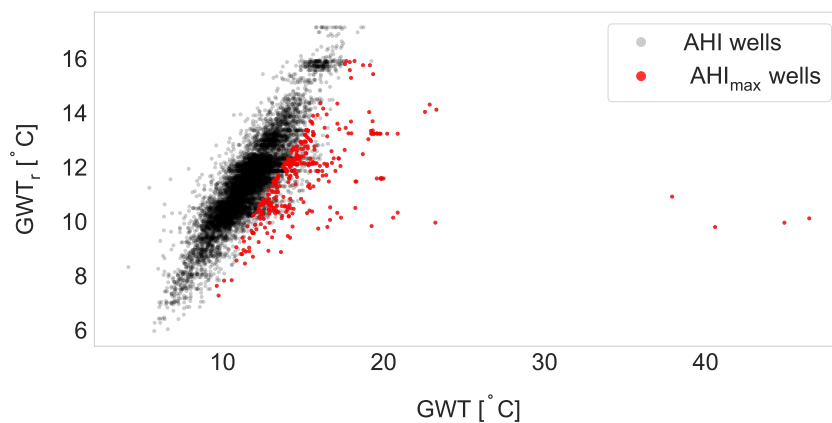


Figure A.5: Groundwater temperature (GWT) versus median rural background groundwater temperature (GWT_r) for the 10,656 wells with an anthropogenic heat intensity (AHI) and all 318 hot spots (AHI_{\max}).

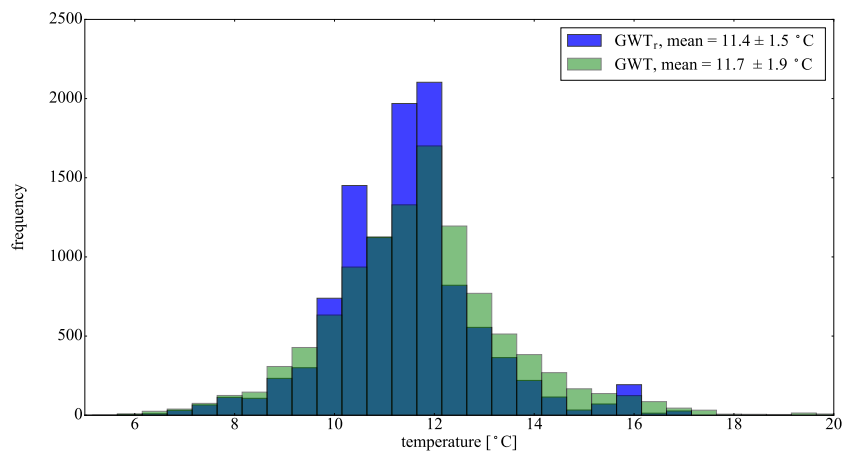


Figure A.6: Histograms of groundwater temperature (GWT) and median rural background groundwater temperature (GWT_r). Extreme GWTs above 20 °C are cut off from the plot.

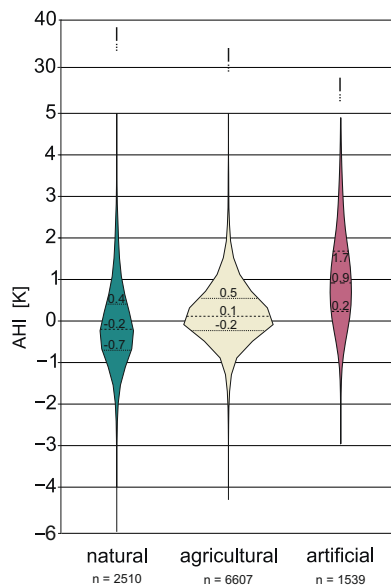


Figure A.7: The violin plot represents the distribution and probability densities of all wells with an anthropogenic heat intensity (AHI) for the three land cover classes natural, agricultural and artificial. Extremely high, positive AHIs are attributable to natural hot springs in Austria and southern Germany (Figure A.5). The AHI minima are due to springs along the French Alps, Massif Central and Pyrenees. Values for median, the 25th and the 75th quantiles are indicated by the dashed lines in the violins.

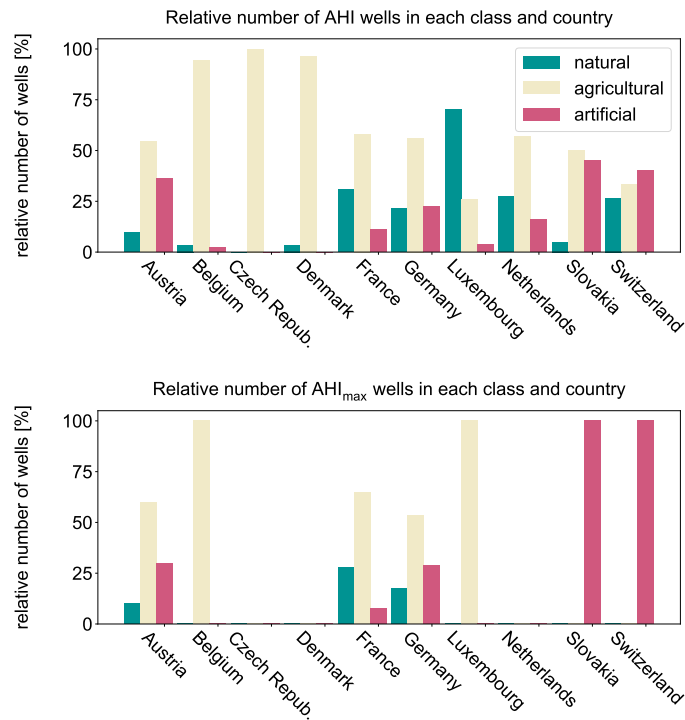


Figure A.8: Percentage of wells per main class and country for AHI (10,656 wells) and AHI_{max} wells (318 wells).

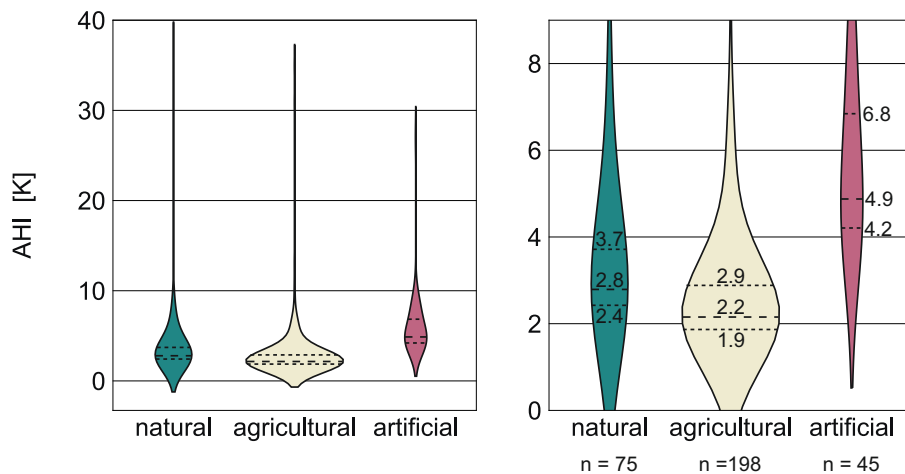


Figure A.9: Violin plot of all AHI_{max} wells for the main classes: natural, agricultural and artificial. Values for median, the 25th and the 75th quantiles are indicated by the dashed lines in the violins.



Figure A.10: Representative Google Earth shots of the six land utilisation classes (LUC): automotive, city, factory, farming, industry parks, and waste.

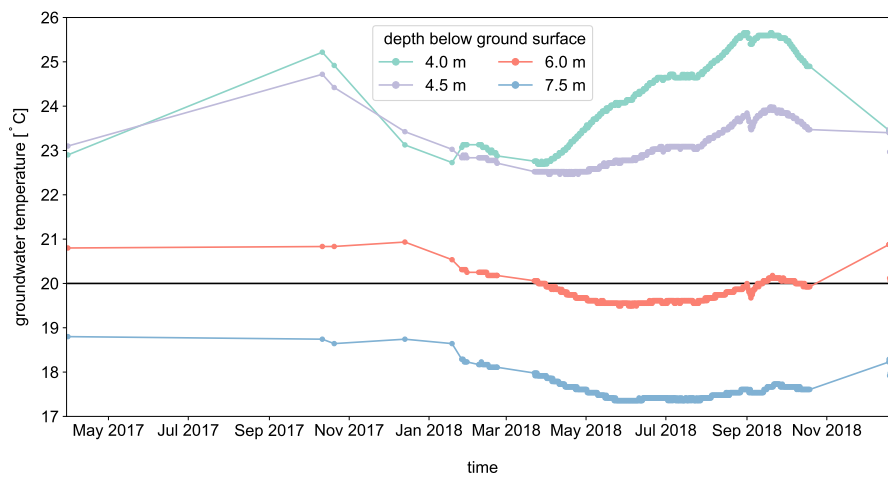


Figure A.11: Groundwater temperature time series at four different depth levels in a groundwater observation well in Vienna, 3.5 m away from a district heating pipe (data provided by GeoPLASMA-CE).

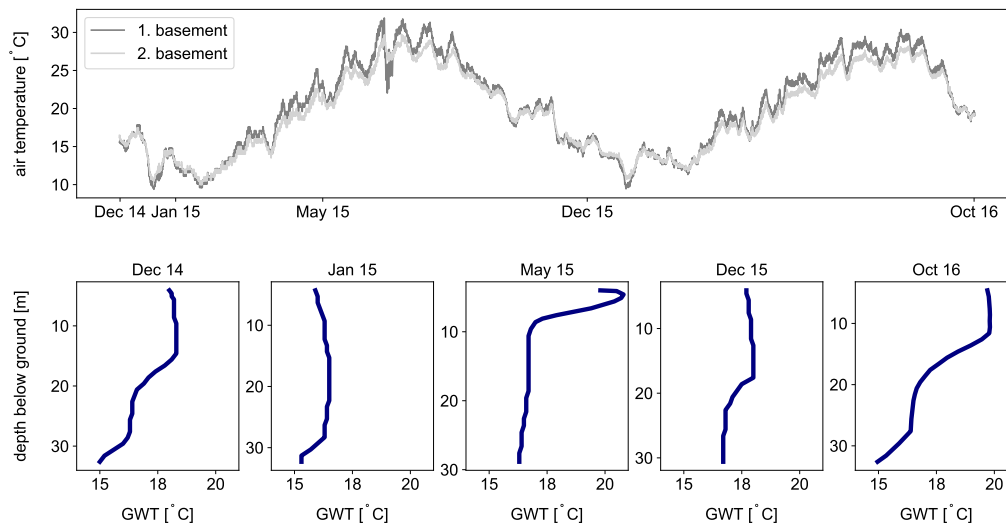


Figure A.12: Time series of air temperature (recorded with a temperature data logger) and groundwater temperature (GWT) (manually measured with an electric contact gauge) in an underground carpark in Switzerland.

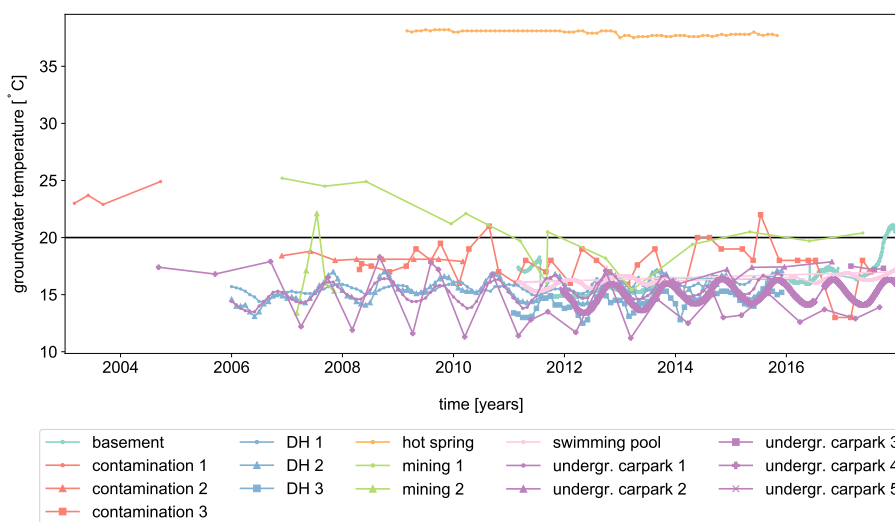


Figure A.13: Groundwater temperature time series within the analysed time frame (2003 – 2017) of the 19 identified heat sources. Colour coded according to their eight heat source classes. (DH = district heating).

Table A.1: Countries of the survey area, number of wells, depth and data source information

Country	Input	Number of wells			Well or measurement depth	Data source
		$r \leq 0.25$	AHI	AHI _{max}		
Austria	1117	1042	853	20	existing	BMLUFUW, 2018
Belgium	2786	2108	1446	6	inconsistent	VMM, 2018, Bruxelles, 2018
Czech Repub.	160	5	3	0	existing	CHMI, 2018
Denmark	73	40	29	0	existing	GEUS, 2018
France	31965	6059	5720	220	inconsistent	BRGM, 2018, ADES, 2018
Germany	6921	2549	2407	69	inconsistent	1
Luxembourg	174	104	104	1	inconsistent	AGE, 2018
Netherlands	876	115	44	0	existing	IHW, 2018
Slovakia	30	30	20	1	existing	SHMU, 2018
Switzerland	102	99	30	1	existing	BAFU, 2018
Sum	44205	12151	10656	318		

¹ LUBW, 2018, LfUB, 2018, LfUBB, 2018, SUBV, 2018, Zhu et al., 2010, Jung, 2013, HLNUG, 2018, TbKA, 2018, NLWKN, 2018, LANUV, 2018, LfURP, 2018, LUA, 2018, LfULG, 2018, LHW, 2018, TLUG, 2018

Appendix - Chapter 3

Table A.2: Input parameters for the estimation of the heat supply rate.
 UA = Upper Aquifer, LA = Lower Aquifer

Parameter	Symbol	Value
Hydro-/Geology		
Darcy velocity ^a	v_{fUA}	$3.5 \cdot 10^{-6}$ m/s
	v_{fLA}	$3.3 \cdot 10^{-7}$ m/s
	v_{fUA+LA}	$1.76 \cdot 10^{-6}$ m/s
Groundwater velocity ^a	v_{aUA}	$1.17 \cdot 10^{-5}$ m/s
	v_{aLA}	$1.65 \cdot 10^{-6}$ m/s
	v_{aUA+LA}	$8.78 \cdot 10^{-6}$ m/s
Porosity ^b	p_{UA}	0.2
	p_{LA}	0.1
	p_{UA+LA}	0.14
Hydraulic conductivity ^c	K_{UA}	$3.5 \cdot 10^{-3}$ m/s
	K_{LA}	$3.3 \cdot 10^{-4}$ m/s
	K_{UA+LA}	$1.66 \cdot 10^{-3}$ m/s
Hydraulic gradient ^d	i	0.001
	m_{UA}	13 m
Aquifer thickness ^e	m_{LA}	18 m
	m_{UA+LA}	31 m
	a_L	3.4 m
Longitudinal thermal dispersivity ^f	a_T	0.34 m
Transversal thermal dispersivity ^g	R	2
Retardation factor ^h	c_{pw}	$4.16 \cdot 10^6$ J/m ³ K
Volumetric heat capacity of water ⁱ		
Geothermal System		
Relative annual operation period (heating + DHW) ^j	t_h	1700 h
Heat extraction rate hGSHP ^k	q_{hGSHP}	33 W/m ²
BHE length	l_{vGSHP}^m	17 m
	l_{vGSHP}^l	100 m
Heat extraction rate vGSHP	q_{vGSHP}^j	60 W/m
	q_{vGSHP}^i	100 W/m
Hours per year	t_y	8760 h
Temperature difference ^g	ΔT	6 K
Time after reinjection ^g	t	1000 d
Coefficient of performance ^{g,n}	COP	4
Rintheimer Feld ^j		
Number of refurbished buildings		31
Area RF	A_{RF}	0.13 km ²
Average space heating demand: before refurbishment	h_b	136 kWh/m ²
Average space heating demand: after refurbishment	h_a	50 kWh/m ²
Total thermal energy demand: before refurbishment	H_b	10.12 GWh
Total thermal energy demand: after refurbishment	H_a	4.79 GWh
^a based on Hölting and Coldewey (2013)	^h Molina-Giraldo (2011)	
^b Busch, Luckner, and Tiemer (1974)	ⁱ VDI 4640 part 2 (2001)	
^c Wirsing and Luz (2007)	^j Jank and Kuklinski (2015)	
^d Tiefbauamt, City of Karlsruhe	^k Ramming (2007)	
^e Wirsing and Luz (2005)	^l BBergG (2017)	
^f Beims (1983)	^m LGRB (2017)	
^g Baden-Württemberg (2009a)	ⁿ Miglani, Orehounig, and Carmeliet (2018)	

Appendix - Chapter 4

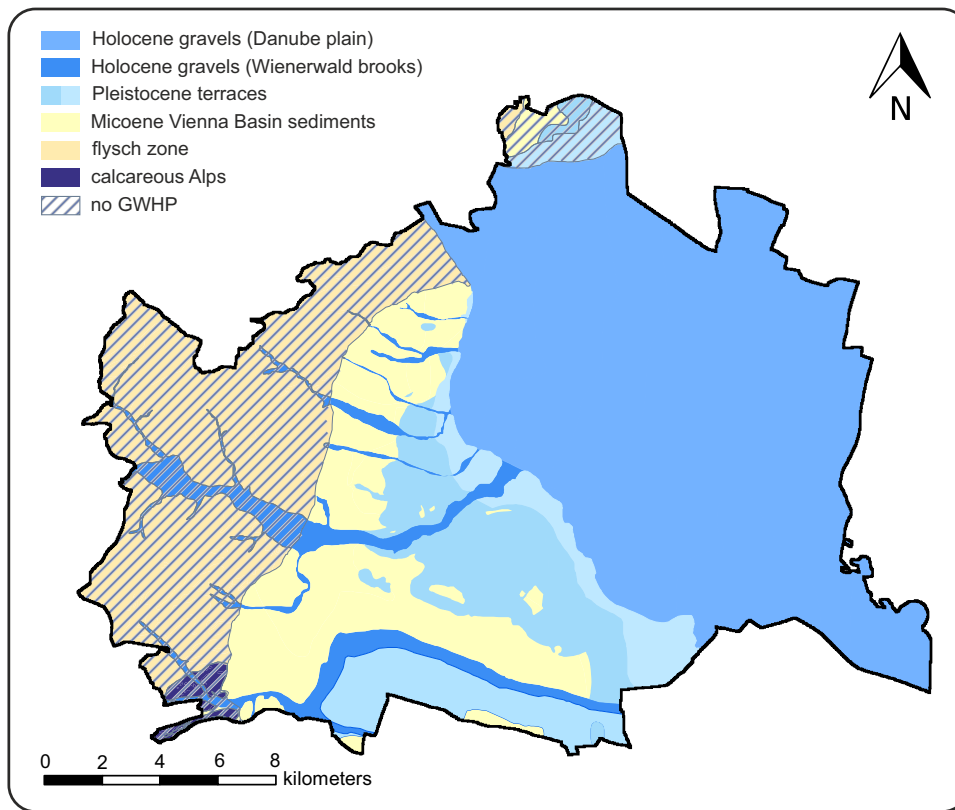


Figure A.14: Hydrogeological zones of Vienna (adapted from Götzl et al. (2014)). The striped zone indicates the area without groundwater heat pump (GWHP) installations in this study.

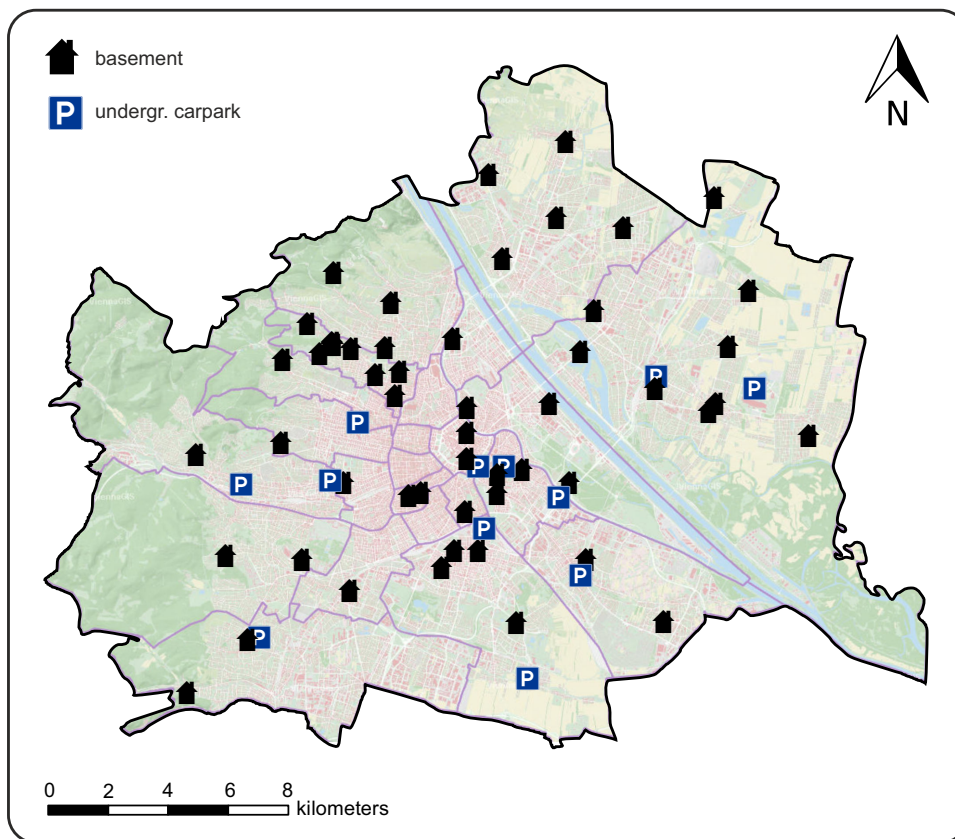


Figure A.15: Location of iButtons to measure the air temperature in basements and underground car parks.

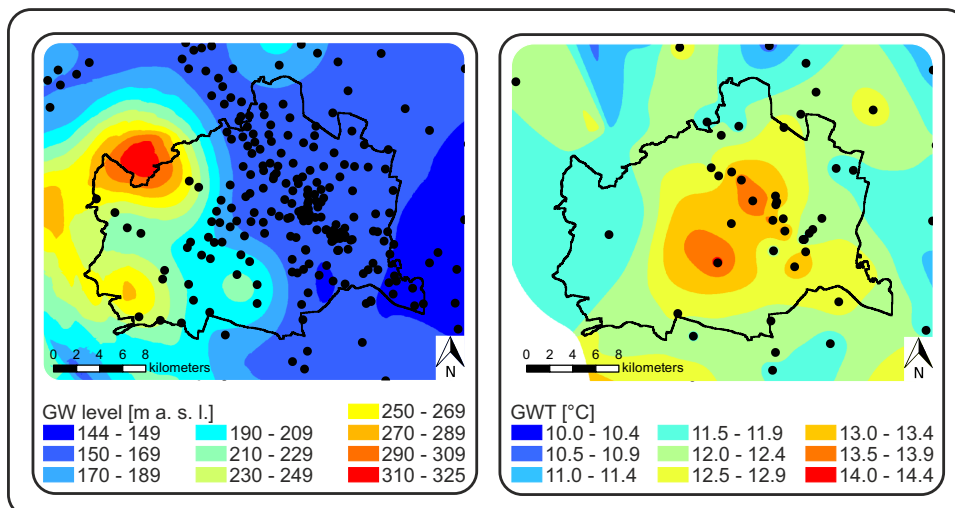


Figure A.16: Interpolation (ordinary kriging) of mean groundwater (GW) level and groundwater temperature (GWT) data from 2007 to 2016. Black points represent the measurement sites. Mean GW levels and GWT are 163.3 ± 19.1 m and 12.2 ± 1.0 °C. Maximum GW level (262.0 m) was measured in the north-western part of Vienna and the lowest (144.2 m) at the Danube River to the west of Vienna. The site with the highest GWT (14.5 °C) is south of the Central station, the site with the lowest GWT (10.2 °C) is in a forest north of Vienna.

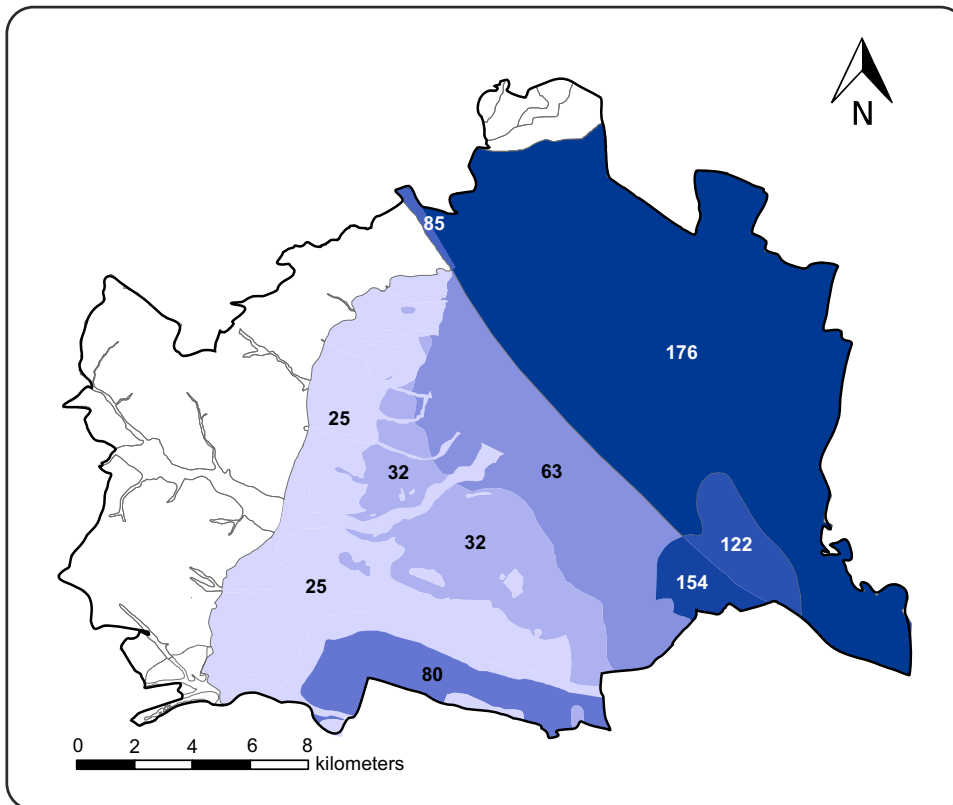


Figure A.17: The numbers indicate the maximum plume length of the $\Delta T = 1$ K isotherm which defines the distance between groundwater heat pump systems. The estimation of the temperature plume extension of the cooled, reinjected water bases on the analytical approach by Kinzelbach (1992).

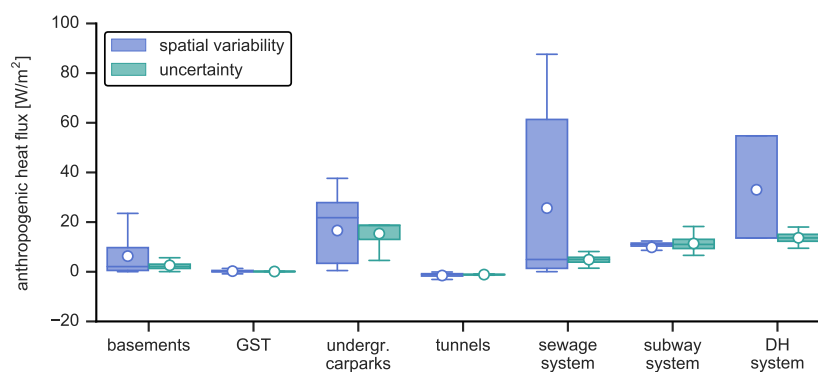


Figure A.18: Boxplots of the spatial variability and uncertainty of the individual anthropogenic heat fluxes. Mean values are indicated with a white dot. Abbreviations: ground surface temperature (GST), district heating system (DH).

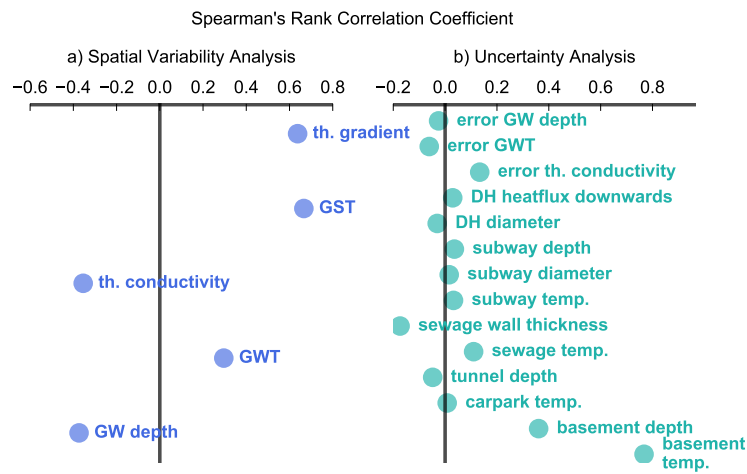


Figure A.19: Results of the spatial variability and uncertainty analysis. Spearman's rank correlation coefficients between the heat flux per pixel and the individual parameters (spatial variability) and between the heat flow and the individual parameters (parameter uncertainty). Abbreviations: groundwater (GW), groundwater temperature (GWT), ground surface temperature (GST), thermal (th.).

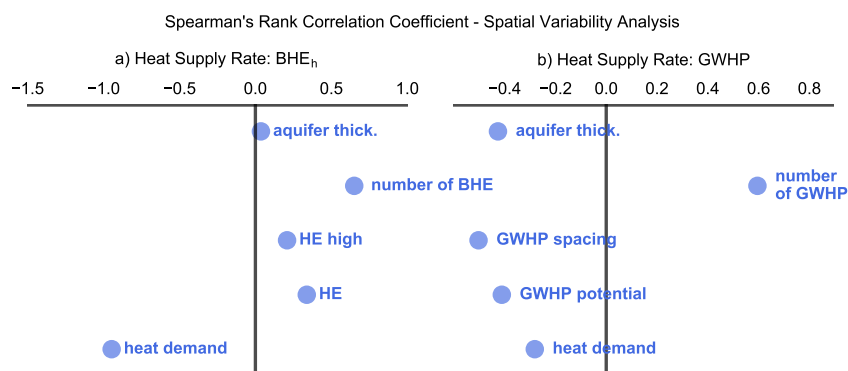


Figure A.20: Results of the spatial variability for borehole heat exchangers (BHE_h) with higher heat extraction (HE) rate and groundwater heat pump (GWHP) systems. Spearman's rank correlation coefficients between the heat supply rate per hexagon and the individual parameters.

Table A.3: Input files and parameters with their values, units and sources applied in the Monte Carlo simulation, heat flux and heat supply rate calculation. Abbreviation: borehole heat exchangers (BHE), district heating (DH), ground surface temperature (GST), groundwater (GW), groundwater heat pump (GWHP), groundwater temperature (GWT), heating demand (HD).

input files and parameters	value	unit	reference
flux evaluation: ground surface temperature (GST)			
area of Vienna	shapefile		Stadt Wien
thermal conductivity 0 - 30 m	raster	W/mK	GBA ¹
thermal conductivity error	-0.20, 0.00, 0.20	W/mK	Götzl et al. (2014)
digital elevation model	raster	m	Stadt Wien
air temperature	WFS	°C	ZAMG revised by GBA, GeoPLASMA-CE ¹
land use	shapefile		GMES
GWT	well data	°C	eHYD
error of GWT measurement	-0.10, 0.00, 0.10	°C	Benz et al. (2015)
mean groundwater level	well data	m	eHYD
error of GW level measurement	-0.01, 0.00, 0.01	m	Benz et al. (2015)
surface water	shapefile		Stadt Wien
bridges	shapefile		Stadt Wien

Continued on next page

Table A.3 – continued from previous page

input files and parameter	value	unit	reference
flux evaluation: building			
building footprints	shapefile		Stadt Wien
basement temperature	12.90, 15.70, 20.60	°C	iButton measurement
basement depth below ground	0.00, 2.50, 6.00	m	Benz et al. (2015)
building: thickness of the floor	0.30	m	Benz et al. (2015)
distance building - BHE	2.00	m	VDI 4640 part 2 (2015)
flux evaluation: underground carpark			
undergr. carpark footprint	shapefile		derived from building footprint file
undergr. carpark temperature	12.90, 17.50, 21.80	°C	iButton measurement
undergr. carpark depth	shapfile	m	iButton measurement
undergr. carpark wall thickness	0.30	m	Benz et al. (2015)
distance carpark - BHE	2.00	m	VDI 4640 part 2 (2015)
flux evaluation: tunnel			
tunnel footprint	shapefile		Stadt Wien
tunnel temperature	WFS	°C	see air temperature
tunnel tube depth below ground	1.00, 1.50, 2.00	m	asfinag
tunnel diameter	5.53	m	asfinag
tunnel wall thickness	0.80	m	asfinag
distance tunnel - BHE	2.00	m	VDI 4640 part 2 (2015)
flux evaluation: sewage system			
sewage network	shapefile		Wien Kanal
sewage water temperature	14.20, 18.50, 21.50	°C	Wien Kanal
sewage pipe depth below ground	shapefile	m	Wien Kanal
sewage pipe diameter	shapefile	m	Wien Kanal
pipe wall thickness	0.02, 0.10, 0.32	m	Benz et al. (2015), Wien Kanal

Continued on next page

Table A.3 – continued from previous page

input files and parameter	value	unit	reference
distance sewer - BHE	1.00	m	VDI 4640 part 2 (2015)
flux evaluation: subway system			
subway network	shapefile		Stadt Wien
subway temperature	17.30, 19.00, 24.30	°C	Wiener Linien revised by GBA ¹
subway tube depth below ground	10.00, 20.00, 30.00	m	Wiener Linien
subway tube diameter	6.90, 7.00, 7.30	m	Benz et al. (2015)
subway tube wall thickness	1.10	m	Benz et al. (2015)
distance subway - BHE	1.00	m	VDI 4640 part 2 (2015)
flux evaluation: district heating (DH) system			
DH network	WFS		Wien Energie revised by GBA 1
pipe diameter	0.17, 0.58, 1.00	m	Schmidt (2011)
heat loss primary network	84.51	W/m	Wien Energie ²
heat loss secondary network	21.04	W/m	Wien Energie ²
heat flux directed downwards	25.00, 37.50, 50.00	%	Benz et al. (2015)
pipe length	WFS	m	Wien Energie revised by GBA ¹
distance pipe - BHE	1.00	m	VDI 4640 part 2 (2015)
evaluation of the heat supply rate			
HD un-/refurbished buildings	WFS	MWh/a	TU Wien revised by GBA ¹
coefficient of performance	4.00		Tissen et al. (2019)
operation time	1800.00	h	VDI 4640 part 2 (2015)
heat extraction rate (HE)	shapefile	W/m	Stadt Wien, SIA 384/6 (2009)
HE high	shapefile	W/m	Stadt Wien, Erol (2011)
HE error	shapefile	W/m	Stadt Wien,
HE high error	-5.00, 0.00, 5.00	W/m	deduced from therm. conduc. error
BHE length	150.00	m	GBA ¹

Continued on next page

Table A.3 – continued from previous page

input files and parameter	value	unit	reference
BHE spacing	10.00	m	GBA ¹
GWHP potential	shapefile	kW	Stadt Wien
GWHP spacing	shapefile	m	based on: Baden-Württemberg (2009a) and Kinzelbach (1992)
evaluation of the GWHP spacing			
retardation	2.00		Tissen et al. (2019)
vol. heat capacity	2300000.00	J/m ³ /K	GBA ¹
temperature reduction	5.00	K	Götzl et al. (2014)
aquifer thickness	shapefile	m	GBA ¹
aquifer porosity	20.00	%	GBA ¹
hydraulic conductivity	shapefile	m/s	Umweltbundesamt GmbH (<i>H2O Fachdatenbank - Grundwasserkörperabfrage</i>)
Darcy velocity	raster	m/s	Darcy Velocity Tool ³
groundwater flow velocity	shapefile	m/s	based on: Baden-Württemberg (2009a)
pumping rate	shapefile	m ³ /s	based on: Baden-Württemberg (2009a)
longitudinal thermal dispersivity	shapefile	m	based on: Baden-Württemberg (2009a)
transversal thermal dispersivity	shapefile	m	based on: Baden-Württemberg (2009a)

¹personal correspondence with Geological Survey of Austria (GBA)

²personal correspondence with Wien Energie

³<http://desktop.arcgis.com/en/arcmap/latest/tools/spatial-analyst-toolbox/darcy-velocity.htm>

Table A.4: Land use categories according to the Urban Atlas (*Urban Atlas*), their coverage rate and add on air temperature defined by Dědeček, Šafanda, and Rajver (2012) for the ground surface temperature estimation.

land use type	surface type			add on air temp. [°C]			coverage rate [%]
	sand and bare soil	grass	asphalt	min.	mode	max.	
continuous urban fabric (S.L. > 80%)	5	10	85	3.50	3.96	4.43	6.77
discontinuous dense urban fabric (S.L. 50% - 80%)	10	25	65	2.80	3.23	3.65	9.07
discontinuous medium density (S.L. 30% - 50%)	10	50	40	1.85	2.23	2.60	8.38
discontinuous low density urban (S.L. 10% - 30%)	10	70	20	1.09	1.43	1.76	2.48
discontinuous very low density (S.L. < 10%)	10	85	5	0.52	0.83	1.13	0.10
isolated structures	0	0	100	4.00	4.50	5.00	0.10
industrial, commercial, public	5	0	95	3.88	4.36	4.85	12.54
fast transit roads and associated	0	0	100	4.00	4.50	5.00	0.51
other roads and associated land	0	0	100	4.00	4.50	5.00	6.20
railways and associated land	90	0	10	1.75	2.03	2.30	1.61
port areas	25	0	75	3.38	3.81	4.25	0.56
mineral extraction and dump sites	100	0	0	1.50	1.75	2.00	0.33
construction sites	100	0	0	1.50	1.75	2.00	0.55
land without current use	100	0	0	1.50	1.75	2.00	0.51
green urban areas	0	100	0	0.20	0.50	0.80	7.72
sports and leisure facilities	25	50	25	1.48	1.81	2.15	3.73
agricultural areas, semi-natural	50	50	0	0.85	1.13	1.40	17.01
forests	0	100	0	0.20	0.50	0.80	18.28
water	0	0	0		none		3.55

Table A.5: Spearman's rank correlation coefficient ρ and p-value for the spatial analysis and the uncertainty analysis of the heat flux. Abbreviation: district heating (DH), ground surface temperature (GST), groundwater (GW), groundwater temperature (GWT).

parameter	ρ	p-value
spatial variability		
GW depth	-0.37	0.00
GWT	0.29	0.00
th. conductivity	-0.35	0.00
GST	0.67	0.00
th. gradient	0.64	0.00
uncertainty		
basement temp.	0.77	0.00
basement depth	0.36	0.00
undergr. carpark temp.	0.01	0.80
tunnel depth	-0.05	0.13
sewage water temp.	0.11	0.00
sewer wall thickness	-0.17	0.00
subway air temp.	0.03	0.31
subway tube diameter	0.02	0.62
subway depth	0.04	0.26
DH diameter	-0.03	0.33
DH flux downwards	0.03	0.35
error GW level	-0.03	0.43
error GWT	-0.06	0.05
error th. conductivity	0.13	0.00

Table A.6: Spearman's rank correlation coefficient ρ and p-value for the spatial analysis of the heat supply rate.

parameter	ρ	p-value
borehole heat exchanger BHE		
heating demand	-0.95	0.00
gross floor area	0.94	0.00
heat extraction	0.34	0.00
heat extraction high	0.21	0.00
nr. of BHE	0.65	0.00
aquifer thicknes	0.04	0.00
groundwater heat pump GWHP		
heating demand	-0.28	0.00
GWHP potential	-0.41	0.00
GWHP spacing	-0.50	0.00
nr. of GWHP	0.60	0.00
aquifer thickness	-0.43	0.00

References

- Abu-Rumman, Mohammad, Mohammad Hamdan, and Osama Ayadi (2020). "Performance enhancement of a photovoltaic thermal (PVT) and ground-source heat pump system". In: *Geothermics* 85, p. 101809. DOI: [10.1016/j.geothermics.2020.101809](https://doi.org/10.1016/j.geothermics.2020.101809).
- ADES (2018). *Portail nationale d'Accès aux Données sur les Eaux Souterraines*. URL: <https://ades.eaufrance.fr/> (visited on 05/01/2019).
- AGE (2018). *Administration de la gestion de l'eau Luxembourg*. URL: <https://eau.public.lu/> (visited on 05/01/2019).
- Akankpo, O. and M. U. Igboekwe (2011). "Monitoring Groundwater Contamination Using Surface Electrical Resistivity and Geochemical Methods". In: *Journal of Water Resource and Protection* 03.5, pp. 318–324. DOI: [10.4236/jwarp.2011.35040](https://doi.org/10.4236/jwarp.2011.35040).
- Alcaraz, Mar, Alejandro García-Gil, Enric Vázquez-Suñé, and Violeta Velasco (2016). "Advection and dispersion heat transport mechanisms in the quantification of shallow geothermal resources and associated environmental impacts". In: *Science of The Total Environment* 543, pp. 536–546. DOI: [10.1016/j.scitotenv.2015.11.022](https://doi.org/10.1016/j.scitotenv.2015.11.022).
- Alcaraz, Mar, Luis Vives, and Enric Vázquez-Suñé (2017). "The T-I-G ER method: A graphical alternative to support the design and management of shallow geothermal energy exploitations at the metropolitan scale". In: *Renewable Energy* 109, pp. 213–221. DOI: [10.1016/j.renene.2017.03.022](https://doi.org/10.1016/j.renene.2017.03.022).
- Arning, E., M. Kölling, H.D. Schulz, B. Panteleit, and J. Reichling (2006). "Einfluss oberflächennaher Wärmegewinnung auf geochemische Prozesse im Grundwasserleiter". In: *Grundwasser* 11.1, pp. 27–39. DOI: [10.1007/s00767-006-0116-0](https://doi.org/10.1007/s00767-006-0116-0).
- Arola, Teppo, Lari Eskola, Jukka Hellen, and Kirsti Korkka-Niemi (2014). "Mapping the low enthalpy geothermal potential of shallow Quaternary aquifers in Finland". In: *Geothermal Energy* 2.1, p. 9. DOI: [10.1186/s40517-014-0009-x](https://doi.org/10.1186/s40517-014-0009-x).
- Arola, Teppo and Kirsti Korkka-Niemi (2014). "The effect of urban heat islands on geothermal potential: examples from Quaternary aquifers in Finland". In: *Hydrogeology Journal* 22.8, pp. 1953–1967. DOI: [10.1007/s10040-014-1174-5](https://doi.org/10.1007/s10040-014-1174-5).
- asfinag. *Autobahnen- und Schnellstraßen-Finanzierungs-Aktiengesellschaft*. URL: <https://www.asfinag.at/> (visited on 10/30/2019).
- Baden-Württemberg (2005). *Leitfaden zur Nutzung von Erdwärme mit Erdwärmesonden*. Stuttgart: Umweltministerium Baden-Württemberg.
- Baden-Württemberg (2008). *Leitfaden zur Nutzung von Erdwärme mit Erdwärmekollektoren*. Stuttgart: Umweltministerium Baden-Württemberg.
- Baden-Württemberg (2009a). *Arbeitshilfe zum Leitfaden zur Nutzung von Erdwärme mit Grundwasserwärmepumpen*. Stuttgart: Umweltministerium Baden-Württemberg.
- Baden-Württemberg (2009b). *Leitfaden zur Nutzung von Erdwärme mit Grundwasserwärmepumpen*. Stuttgart: Umweltministerium Baden-Württemberg.
- Baehr, Hans Dieter and Karl Stephan (2011). *Heat and mass transfer: with many worked examples and exercises*. 3., rev. ed. OCLC: 844847648. Berlin: Springer. 737 pp.
- BAFU (2018). *Bundesamt für Umwelt - Schweiz*. URL: <https://www.bafu.admin.ch/bafu/de/home.html> (visited on 05/01/2019).

- Balke, K (1977). "Das Grundwasser als Energieträger." In: *Brennstoff-Wärme-Kraft* 29, pp. 191–194.
- Bauer, Mathias Jürgen, Willi Freeden, Hans Jacobi, and Thomas Neu, eds. (2018). *Handbuch oberflächennahe Geothermie*. OCLC: 993703419. Berlin: Springer Spektrum. 817 pp.
- Bayer, Peter, Guillaume Attard, Philipp Blum, and Kathrin Menberg (2019). "The geothermal potential of cities". In: *Renewable and Sustainable Energy Reviews* 106, pp. 17–30. DOI: [10.1016/j.rser.2019.02.019](https://doi.org/10.1016/j.rser.2019.02.019).
- Bayer, Peter, Michael de Paly, and Markus Beck (2014). "Strategic optimization of borehole heat exchanger field for seasonal geothermal heating and cooling". In: *Applied Energy* 136, pp. 445–453. DOI: [10.1016/j.apenergy.2014.09.029](https://doi.org/10.1016/j.apenergy.2014.09.029).
- Bayer, Peter, Dominik Saner, Stephan Bolay, Ladislaus Rybach, and Philipp Blum (2012). "Greenhouse gas emission savings of ground source heat pump systems in Europe: A review". In: *Renewable and Sustainable Energy Reviews* 16.2, pp. 1256–1267. DOI: [10.1016/j.rser.2011.09.027](https://doi.org/10.1016/j.rser.2011.09.027).
- BBergG (2017). *Bundesberggesetz vom 13. August 1980 (BGBl. I S. 1310), das zuletzt durch Artikel 2 Absatz 4 des Gesetzes vom 20. Juli 2017 (BGBl. I S. 2808) geändert worden ist*.
- Beck, Markus, Peter Bayer, Michael de Paly, Jozsef Hecht-Méndez, and Andreas Zell (2013). "Geometric arrangement and operation mode adjustment in low-enthalpy geothermal borehole fields for heating". In: *Energy* 49, pp. 434–443. DOI: [10.1016/j.energy.2012.10.060](https://doi.org/10.1016/j.energy.2012.10.060).
- Beims, U. (1983). "Planung, Durchführung und Auswertung von Gütepumpversuchen". In: *Zeitschrift für Angewandte Geologie* 29.10, pp. 482–490.
- Beltrami, Hugo (2002). "Climate from borehole data: Energy fluxes and temperatures since 1500: GLOBAL SURFACE ENERGY BALANCE FOR THE LAST 500 YEARS". In: *Geophysical Research Letters* 29.23, pp. 26–1–26–4. DOI: [10.1029/2002GL015702](https://doi.org/10.1029/2002GL015702).
- Beltrami, Hugo, Evelise Bourlon, Lisa Kellman, and J. F. González-Rouco (2006). "Spatial patterns of ground heat gain in the Northern Hemisphere". In: *Geophysical Research Letters* 33.6. DOI: [10.1029/2006GL025676](https://doi.org/10.1029/2006GL025676).
- Beltrami, Hugo, Grant Ferguson, and Robert N. Harris (2005). "Long-term tracking of climate change by underground temperatures". In: *Geophysical Research Letters* 32.19. DOI: [10.1029/2005GL023714](https://doi.org/10.1029/2005GL023714).
- Beltrami, Hugo and Lisa Kellman (2003). "An examination of short- and long-term air–ground temperature coupling". In: *Global and Planetary Change* 38.3, pp. 291–303. DOI: [10.1016/S0921-8181\(03\)00112-7](https://doi.org/10.1016/S0921-8181(03)00112-7).
- Bense, Victor and Hugo Beltrami (2007). "Impact of horizontal groundwater flow and localized deforestation on the development of shallow temperature anomalies". In: *Journal of Geophysical Research* 112 (F4). DOI: [10.1029/2006JF000703](https://doi.org/10.1029/2006JF000703).
- Benz, Susanne A, Peter Bayer, and Philipp Blum (2017a). "Global patterns of shallow groundwater temperatures". In: *Environmental Research Letters* 12.3, p. 034005. DOI: [10.1088/1748-9326/aa5fb0](https://doi.org/10.1088/1748-9326/aa5fb0).
- Benz, Susanne A., Peter Bayer, and Philipp Blum (2017b). "Identifying anthropogenic anomalies in air, surface and groundwater temperatures in Germany". In: *Science of The Total Environment* 584–585, pp. 145–153. DOI: [10.1016/j.scitotenv.2017.01.139](https://doi.org/10.1016/j.scitotenv.2017.01.139).
- Benz, Susanne A., Peter Bayer, Philipp Blum, Hideki Hamamoto, Hirotaka Arimoto, and Makoto Taniguchi (2018a). "Comparing anthropogenic heat input and heat accumulation in the subsurface of Osaka, Japan". In: *Science of The Total Environment* 643, pp. 1127–1136. DOI: [10.1016/j.scitotenv.2018.06.253](https://doi.org/10.1016/j.scitotenv.2018.06.253).

- Benz, Susanne A., Peter Bayer, Frank M. Goettsche, Folke S. Olesen, and Philipp Blum (2016). "Linking Surface Urban Heat Islands with Groundwater Temperatures". In: *Environmental Science & Technology* 50.1, pp. 70–78. DOI: [10.1021/acs.est.5b03672](https://doi.org/10.1021/acs.est.5b03672).
- Benz, Susanne A., Peter Bayer, Kathrin Menberg, Stephan Jung, and Philipp Blum (2015). "Spatial resolution of anthropogenic heat fluxes into urban aquifers". In: *Science of The Total Environment* 524–525, pp. 427–439. DOI: [10.1016/j.scitotenv.2015.04.003](https://doi.org/10.1016/j.scitotenv.2015.04.003).
- Benz, Susanne A., Peter Bayer, Gerfried Winkler, and Philipp Blum (2018b). "Recent trends of groundwater temperatures in Austria". In: *Hydrology and Earth System Sciences* 22.6, pp. 3143–3154. DOI: [10.5194/hess-22-3143-2018](https://doi.org/10.5194/hess-22-3143-2018).
- Bertermann, D., H. Klug, and L. Morper-Busch (2015). "A pan-European planning basis for estimating the very shallow geothermal energy potentials". In: *Renewable Energy* 75, pp. 335–347. DOI: [10.1016/j.renene.2014.09.033](https://doi.org/10.1016/j.renene.2014.09.033).
- Bertermann, D., H. Klug, L. Morper-Busch, and C. Bialas (2014). "Modelling vSGPs (very shallow geothermal potentials) in selected CSAs (case study areas)". In: *Energy* 71, pp. 226–244. DOI: [10.1016/j.energy.2014.04.054](https://doi.org/10.1016/j.energy.2014.04.054).
- Bezelgues-Courtade, Sophie, Jean-Claude Martin, Suzanne Schomburgk, Pascal Monnot, Denis Nguyen, Morgane Le Brun, Alain Desplan, and others (2010). "Geothermal Potential of Shallow Aquifers: Decision-Aid Tool for Heat-Pump Installation". In: *World Geothermal Congress 2010*, 9–p.
- Bidarmaghz, Asal, Ruchi Choudhary, Kenichi Soga, Holger Kessler, Ricky L. Terriington, and Stephen Thorpe (2019). "Influence of geology and hydrogeology on heat rejection from residential basements in urban areas". In: *Tunnelling and Underground Space Technology* 92, p. 103068. DOI: [10.1016/j.tust.2019.103068](https://doi.org/10.1016/j.tust.2019.103068).
- Blum, Philip et al. (2018). *Geospeicher.bw*. Fellbach, p. 28.
- Blum, Philipp, Gisela Campillo, and Thomas Kölbel (2011). "Techno-economic and spatial analysis of vertical ground source heat pump systems in Germany". In: *Energy* 36.5, pp. 3002–3011. DOI: [10.1016/j.energy.2011.02.044](https://doi.org/10.1016/j.energy.2011.02.044).
- Blum, Philipp, Gisela Campillo, Wolfram Münch, and Thomas Kölbel (2010). "CO2 savings of ground source heat pump systems – A regional analysis". In: *Renewable Energy* 35.1, pp. 122–127. DOI: [10.1016/j.renene.2009.03.034](https://doi.org/10.1016/j.renene.2009.03.034).
- BMLUFUW (2018). *Abteilung Wasserhaushalt im Bundesministerium für Land- und Forstwirtschaft, Umwelt und Wasserwirtschaft*. URL: <https://ehyd.gv.at/> (visited on 04/30/2019).
- BMWi (2018). *Energiedaten: Gesamtausgabe—Stand: Oktober 2017*. Berlin: Bundesministerium für Wirtschaft und Energie.
- Bonsor, H C, P Dahlqvist, L Moosmann, N Classen, J Epting, P Huggenberger, A Garica-Gil, M Janža, G Laursen, R Stuurman, and C R Gogu (2017). *Groundwater, Geothermal modelling and monitoring at city-scales – identifying good practice, and effective knowledge exchange*. British Geological Survey Open Report, p. 75.
- Bonte, M., P. J. Stuyfzand, G. A. van den Berg, and W. A. M. Hijnen (2011a). "Effects of aquifer thermal energy storage on groundwater quality and the consequences for drinking water production: a case study from the Netherlands". In: *Water Science and Technology* 63.9, pp. 1922–1931. DOI: [10.2166/wst.2011.189](https://doi.org/10.2166/wst.2011.189).
- Bonte, Matthijs (2013). "Impacts of shallow geothermal energy on groundwater quality: A hydrochemical and geomicrobial study of the effects of ground source heat pumps and aquifer thermal energy storage". OCLC: 911399557. PhD thesis. Amsterdam: Vrije Universiteit.
- Bonte, Matthijs, Boris M. van Breukelen, and Pieter J. Stuyfzand (2013). "Temperature-induced impacts on groundwater quality and arsenic mobility in anoxic aquifer

- sediments used for both drinking water and shallow geothermal energy production". In: *Water Research* 47.14, pp. 5088–5100. DOI: [10.1016/j.watres.2013.05.049](https://doi.org/10.1016/j.watres.2013.05.049).
- Bonte, Matthijs, Wilfred F. M. Röling, Egija Zaura, Paul W. J. J. van der Wielen, Pieter J. Stuyfzand, and Boris M. van Breukelen (2013). "Impacts of Shallow Geothermal Energy Production on Redox Processes and Microbial Communities". In: *Environmental Science & Technology* 47.24, pp. 14476–14484. DOI: [10.1021/es4030244](https://doi.org/10.1021/es4030244).
- Bonte, Matthijs, Pieter J. Stuyfzand, and Boris M. van Breukelen (2014). "Reactive Transport Modeling of Thermal Column Experiments to Investigate the Impacts of Aquifer Thermal Energy Storage on Groundwater Quality". In: *Environmental Science & Technology* 48.20, pp. 12099–12107. DOI: [10.1021/es502477m](https://doi.org/10.1021/es502477m).
- Bonte, Matthijs, Pieter J. Stuyfzand, Adriana Hulsmann, and Patrick Van Beelen (2011b). "Underground Thermal Energy Storage: Environmental Risks and Policy Developments in the Netherlands and European Union". In: *Ecology and Society* 16.1, art22. DOI: [10.5751/ES-03762-160122](https://doi.org/10.5751/ES-03762-160122).
- BRGM (2018). *Bureau de Recherches Géologiques et Minières*. URL: <http://infoterre.brgm.fr/viewer/MainTileForward.do> (visited on 05/01/2019).
- Briellmann, Heike, Christian Griebler, Susanne I. Schmidt, Rainer Michel, and Tillmann Lueders (2009). "Effects of thermal energy discharge on shallow groundwater ecosystems: Ecosystem impacts of groundwater heat discharge". In: *FEMS Microbiology Ecology* 68.3, pp. 273–286. DOI: [10.1111/j.1574-6941.2009.00674.x](https://doi.org/10.1111/j.1574-6941.2009.00674.x).
- Briellmann, Heike, Tillmann Lueders, Kathrin Schreglmann, Francesco Ferraro, Maria Avramov, Verena Hammerl, Philipp Blum, Peter Bayer, and Christian Griebler (2011). "Oberflächennahe Geothermie und ihre potenziellen Auswirkungen auf Grundwasserökosysteme". In: *Grundwasser* 16.2, pp. 77–91. DOI: [10.1007/s00767-011-0166-9](https://doi.org/10.1007/s00767-011-0166-9).
- Brink, Cors van den, Giuseppe Frapporti, Jasper Griffioen, and Willem Jan Zaadnoordijk (2007). "Statistical analysis of anthropogenic versus geochemical-controlled differences in groundwater composition in The Netherlands". In: *Journal of Hydrology* 336.3, pp. 470–480. DOI: [10.1016/j.jhydrol.2007.01.024](https://doi.org/10.1016/j.jhydrol.2007.01.024).
- Brons, H. J., J. Griffioen, C. A. J. Appelo, and A. J. B. Zehnder (1991). "(Bio) geochemical reactions in aquifer material from a thermal energy storage site". In: *Water research* 25.6, pp. 729–736.
- Bruxelles (2018). *Bruxelles Environnement*. Bruxelles Environnement. URL: <https://environnement.brussels/> (visited on 05/01/2019).
- Böttcher, Fabian, Alessandro Casasso, Gregor Götzl, and Kai Zosseder (2019). "TAP - Thermal aquifer Potential: A quantitative method to assess the spatial potential for the thermal use of groundwater". In: *Renewable Energy* 142, pp. 85–95. DOI: [10.1016/j.renene.2019.04.086](https://doi.org/10.1016/j.renene.2019.04.086).
- Böttcher, Norbert, Norihiro Watanabe, Uwe-Jens Görke, and Olaf Kolditz (2016). *Geoenergy Modeling I*. SpringerBriefs in Energy. Cham: Springer International Publishing. DOI: [10.1007/978-3-319-31335-1](https://doi.org/10.1007/978-3-319-31335-1).
- Bucci, Arianna, Diego Barbero, Manuela Lasagna, M. Gabriella Forno, and Domenico Antonio De Luca (2017). "Shallow groundwater temperature in the Turin area (NW Italy): vertical distribution and anthropogenic effects". In: *Environmental Earth Sciences* 76.5. DOI: [10.1007/s12665-017-6546-4](https://doi.org/10.1007/s12665-017-6546-4).
- Busch, Karl-Franz, Ludwig Luckner, and Klaus Tiemer (1974). *Geohydraulik*. 2. Stuttgart: Enke. 442 pp.
- Carslaw, H. S. and J. C. Jaeger (1959). *Conduction of Heat in Solids*. 2. Edition. New York: Oxford University Press.

- Casasso, Alessandro and Rajandrea Sethi (2014). "Efficiency of closed loop geothermal heat pumps: A sensitivity analysis". In: *Renewable Energy* 62, pp. 737–746. DOI: [10.1016/j.renene.2013.08.019](https://doi.org/10.1016/j.renene.2013.08.019).
- Casasso, Alessandro and Rajandrea Sethi (2016). "G.POT: A quantitative method for the assessment and mapping of the shallow geothermal potential". In: *Energy* 106 (Supplement C), pp. 765–773. DOI: [10.1016/j.energy.2016.03.091](https://doi.org/10.1016/j.energy.2016.03.091).
- Casasso, Alessandro and Rajandrea Sethi (2017). "Assessment and mapping of the shallow geothermal potential in the province of Cuneo (Piedmont, NW Italy)". In: *Renewable Energy* 102, pp. 306–315. DOI: [10.1016/j.renene.2016.10.045](https://doi.org/10.1016/j.renene.2016.10.045).
- Chapuis, Robert P. (2010). "Using a leaky swimming pool for a huge falling-head permeability test". In: *Engineering Geology* 114.1, pp. 65–70. DOI: [10.1016/j.enggeo.2010.04.004](https://doi.org/10.1016/j.enggeo.2010.04.004).
- CHMI (2018). *Czech Hydrometeorological Institute*. Groundwater quality station search. URL: <http://hydro.chmi.cz/isarrow/mfilter.php?agenda=PZV&lng=eng> (visited on 05/01/2019).
- Colombani, Nicolò, Beatrice Maria Sole Giambastiani, and Micòl Mastrocicco (2016). "Use of shallow groundwater temperature profiles to infer climate and land use change: interpretation and measurement challenges: Effect of Land Use and Climate Changes on Groundwater Temperature". In: *Hydrological Processes* 30.14, pp. 2512–2524. DOI: [10.1002/hyp.10805](https://doi.org/10.1002/hyp.10805).
- Commission, European (2016). *Synthesis Report on the Quality of Drinking Water in the Union examining Member States' reports for the 2011-2013 period, foreseen under Article 13(5) of Directive 98/83/EC*. Brussels.
- CORINE (2016). *CORINE Land Cover — Copernicus Land Monitoring Service*. URL: <https://land.copernicus.eu/pan-european/corine-land-cover> (visited on 12/13/2018).
- Dahlem, Karl-Heinz (2000). "The effect of groundwater on the heat loss of building parts in contact with the ground". PhD thesis. Universität Kaiserslautern: Bauphysik/Technische Gebäudeausrüstung/ Baulicher Brandschutz. 180 pp.
- Danielopol, Dan L., Janine Gibert, Christian Griebler, Amara Gunatilaka, Hans Jürgen Hahn, Giuseppe Messina, Jos Notenboom, and Boris Sket (2004). "Incorporating ecological perspectives in European groundwater management policy". In: *Environmental Conservation* 31.3, pp. 185–189. DOI: [10.1017/S0376892904001444](https://doi.org/10.1017/S0376892904001444).
- Datta, P. S. (2005). "Groundwater ethics for its sustainability". In: *Current Science* 89.5, pp. 812–817.
- Dědeček, Petr, Jan Šafanda, and Dušan Rajver (2012). "Detection and quantification of local anthropogenic and regional climatic transient signals in temperature logs from Czechia and Slovenia". In: *Climatic Change* 113.3, pp. 787–801. DOI: [10.1007/s10584-011-0373-5](https://doi.org/10.1007/s10584-011-0373-5).
- De Carli, Michele, Antonio Galgaro, Michele Pasqualetto, and Angelo Zarrella (2014). "Energetic and economic aspects of a heating and cooling district in a mild climate based on closed loop ground source heat pump". In: *Applied Thermal Engineering* 71.2, pp. 895–904. DOI: [10.1016/j.applthermaleng.2014.01.064](https://doi.org/10.1016/j.applthermaleng.2014.01.064).
- Dochev, Ivan and Irene Peters (2019). "Potential for utilising near surface geothermal heat via heat pumps. A case study from Hamburg." In: *Simulation in den Umwelt- und Geowissenschaften - Workshop Kassel*. Kassel, p. 10.
- Dwyer, Tim and Yan Evans (2010). *Module 15: The increasing potential for ground source heat pumps*. CIBSE Journal. Library Catalog: www.cibsejournal.com. URL: <https://www.cibsejournal.com/cpd/modules/2010-04/> (visited on 04/24/2020).

- EEA, European Environment Agency (2006). *The thematic accuracy of Corine land cover 2000: Assessment using LUCAS (land use cover area frame statistical survey)*. Technical Report No 7. OCLC: 836343078. Copenhagen: EEA.
- eHYD. *eHYD – der Zugang zu hydrographischen Daten Österreichs*. Bundesministerium für Nachhaltigkeit und Tourismus. URL: <https://ehyd.gv.at/> (visited on 11/12/2019).
- eHYD (2015). *Hydrographisches Jahrbuch Von Österreich 2015 – Erläuterungen UWQ*. Wien: Bundesministerium für Nachhaltigkeit und Tourismus, pp. 1–270.
- Eicker, Ursula, Ruben Pesch, Felix Thumm, and Antoine Dalibard (2011). “Geothermal energy use for heating and cooling of a low energy building”. In: *Proceedings of IX International Scientific and Technical Conference on New Building Technologies and Design Problems, 20e21*. Vol. 10.
- Engine, Google Earth (2015). *Google earth engine: a planetary-scale geospatial analysis platform*. URL: <https://earthengine.google.com> (visited on 03/13/2019).
- Epting, J., F. Händel, and P. Huggenberger (2013). “Thermal management of an unconsolidated shallow urban groundwater body”. In: *Hydrology and Earth System Sciences* 17.5, pp. 1851–1869. DOI: [10.5194/hess-17-1851-2013](https://doi.org/10.5194/hess-17-1851-2013).
- Epting, Jannis (2017). “Thermal management of urban subsurface resources - Delineation of boundary conditions”. In: *Procedia Engineering* 209, pp. 83–91. DOI: [10.1016/j.proeng.2017.11.133](https://doi.org/10.1016/j.proeng.2017.11.133).
- Epting, Jannis, Matteo Baralis, Rouven Künze, Matthias H. Mueller, Alessandra Insana, Marco Barla, and Peter Huggenberger (2020a). “Geothermal potential of tunnel infrastructures – development of tools at the city-scale of Basel, Switzerland”. In: *Geothermics* 83, p. 101734. DOI: [10.1016/j.geothermics.2019.101734](https://doi.org/10.1016/j.geothermics.2019.101734).
- Epting, Jannis, Fabian Böttcher, Matthias H. Mueller, Alejandro García-Gil, Kai Zosseder, and Peter Huggenberger (2020b). “City-scale solutions for the energy use of shallow urban subsurface resources – Bridging the gap between theoretical and technical potentials”. In: *Renewable Energy* 147, pp. 751–763. DOI: [10.1016/j.renene.2019.09.021](https://doi.org/10.1016/j.renene.2019.09.021).
- Epting, Jannis, Alejandro García-Gil, Peter Huggenberger, Enric Vázquez-Suñe, and Matthias H. Mueller (2017a). “Development of concepts for the management of thermal resources in urban areas – Assessment of transferability from the Basel (Switzerland) and Zaragoza (Spain) case studies”. In: *Journal of Hydrology* 548, pp. 697–715. DOI: [10.1016/j.jhydro1.2017.03.057](https://doi.org/10.1016/j.jhydro1.2017.03.057).
- Epting, Jannis and Peter Huggenberger (2013). “Unraveling the heat island effect observed in urban groundwater bodies – Definition of a potential natural state”. In: *Journal of Hydrology* 501, pp. 193–204. DOI: [10.1016/j.jhydro1.2013.08.002](https://doi.org/10.1016/j.jhydro1.2013.08.002).
- Epting, Jannis, Matthias H. Müller, Dieter Genske, and Peter Huggenberger (2018). “Relating groundwater heat-potential to city-scale heat-demand: A theoretical consideration for urban groundwater resource management”. In: *Applied Energy* 228, pp. 1499–1505. DOI: [10.1016/j.apenergy.2018.06.154](https://doi.org/10.1016/j.apenergy.2018.06.154).
- Epting, Jannis, Stefan Scheidler, Annette Affolter, Paul Borer, Matthias H. Mueller, Lukas Egli, Alejandro García-Gil, and Peter Huggenberger (2017b). “The thermal impact of subsurface building structures on urban groundwater resources – A paradigmatic example”. In: *Science of The Total Environment* 596-597, pp. 87–96. DOI: [10.1016/j.scitotenv.2017.03.296](https://doi.org/10.1016/j.scitotenv.2017.03.296).
- Erneuerbare Energie Österreich (2019). *Positionspapier Wärmewende - Ein Konzept des Dachverbandes Erneuerbare Energie Österreich*. Wien, p. 51.
- Erol, Selçuk (2011). “Estimation of heat extraction rates of GSHP systems under different hydrogeological conditions”. Masterarbeit. Tübingen: Universität Tübingen. 85 pp.

- European Union (EU) (2018). *Directive (EU) 2018/ 2001 of the European Parliament and of the Council - of 11 December 2018 - On the Promotion of the Use of Energy from Renewable Sources*.
- eurostat (2019). *Agri-environmental indicator - Irrigation*. Statistics Explained. URL: https://ec.europa.eu/eurostat/statistics-explained/index.php/Agri-environmental_indicator_-_irrigation (visited on 03/14/2019).
- Felix, M., A. Sohr, P. Riedel, and L. Assmann (2009). *Gefährdungspotenzial Steinkohlengruben Zwickau/Oelsnitz - Kurzbericht zu den Forschungsberichten 2005 bis 2007 zur Thematik*. Freiberg: LfULG, p. 95.
- Ferguson, G and H Beltrami (2006). "Transient lateral heat flow due to land-use changes". In: *Earth and Planetary Science Letters* 242.1, pp. 217–222. DOI: [10.1016/j.epsl.2005.12.001](https://doi.org/10.1016/j.epsl.2005.12.001).
- Ferguson, Grant and Allan D. Woodbury (2004). "Subsurface heat flow in an urban environment". In: *Journal of Geophysical Research: Solid Earth* 109 (B2), B02402. DOI: [10.1029/2003JB002715](https://doi.org/10.1029/2003JB002715).
- Ferguson, Grant and Allan D Woodbury (2005). "Thermal sustainability of groundwater-source cooling in Winnipeg, Manitoba". In: *Canadian Geotechnical Journal* 42.5, pp. 1290–1301. DOI: [10.1139/t05-057](https://doi.org/10.1139/t05-057).
- Ferguson, Grant and Allan D. Woodbury (2006). "Observed thermal pollution and post-development simulations of low-temperature geothermal systems in Winnipeg, Canada". In: *Hydrogeology Journal* 14.7, pp. 1206–1215. DOI: [10.1007/s10040-006-0047-y](https://doi.org/10.1007/s10040-006-0047-y).
- Ferguson, Grant and Allan D. Woodbury (2007). "Urban heat island in the subsurface". In: *Geophysical Research Letters* 34.23, p. L23713. DOI: [10.1029/2007GL032324](https://doi.org/10.1029/2007GL032324).
- Flörke, Martina, Christof Schneider, and Robert I. McDonald (2018). "Water competition between cities and agriculture driven by climate change and urban growth". In: *Nature Sustainability* 1.1, pp. 51–58. DOI: [10.1038/s41893-017-0006-8](https://doi.org/10.1038/s41893-017-0006-8).
- Foley, J. A. (2005). "Global Consequences of Land Use". In: *Science* 309.5734, pp. 570–574. DOI: [10.1126/science.1111772](https://doi.org/10.1126/science.1111772).
- Fujii, Hikari, Tadasuke Inatomi, Ryuichi Itoi, and Youhei Uchida (2007). "Development of suitability maps for ground-coupled heat pump systems using groundwater and heat transport models". In: *Geothermics* 36.5, pp. 459–472. DOI: [10.1016/j.geothermics.2007.06.002](https://doi.org/10.1016/j.geothermics.2007.06.002).
- Galgaro, Antonio, Eloisa Di Sipio, Giordano Teza, Elisa Destro, Michele De Carli, Sergio Chiesa, Angelo Zarrella, Giuseppe Emmi, and Adele Manzella (2015). "Empirical modeling of maps of geo-exchange potential for shallow geothermal energy at regional scale". In: *Geothermics* 57, pp. 173–184. DOI: [10.1016/j.geothermics.2015.06.017](https://doi.org/10.1016/j.geothermics.2015.06.017).
- García-Gil, Alejandro, Enric Vázquez-Suñe, Maria M. Alcaraz, Alejandro Serrano Juan, José Ángel Sánchez-Navarro, Marc Montlleó, Gustavo Rodríguez, and José Lao (2015). "GIS-supported mapping of low-temperature geothermal potential taking groundwater flow into account". In: *Renewable Energy* 77 (Supplement C), pp. 268–278. DOI: [10.1016/j.renene.2014.11.096](https://doi.org/10.1016/j.renene.2014.11.096).
- GBA. GBA: *Geologische Bundesanstalt*. URL: <https://www.geologie.ac.at/ueber-uns/unser-haus/standort/> (visited on 04/14/2020).
- Gemelli, Alberto, Adriano Mancini, and Sauro Longhi (2011). "GIS-based energy-economic model of low temperature geothermal resources: A case study in the Italian Marche region". In: *Renewable Energy* 36.9, pp. 2474–2483. DOI: [10.1016/j.renene.2011.02.014](https://doi.org/10.1016/j.renene.2011.02.014).
- GeoPLASMA-CE (2018). *Interreg CENTRAL EUROPE - GeoPLASMA-CE: Shallow Geothermal Energy Planning, Assessment and Mapping Strategies in Central Europe*. URL:

- <http://www.interreg-central.eu/Content.Node/GeoPLASMA-CE.html> (visited on 04/11/2019).
- Georgiev, Aleksandar, Rumen Popov, and Emil Toshkov (2020). "Investigation of a hybrid system with ground source heat pump and solar collectors: Charging of thermal storages and space heating". In: *Renewable Energy* 147, pp. 2774–2790. DOI: [10.1016/j.renene.2018.12.087](https://doi.org/10.1016/j.renene.2018.12.087).
- GEUS (2018). *Geological Survey of Denmark and Greenland*. URL: <https://www.geus.dk/> (visited on 05/01/2019).
- GMES. *Urban Atlas*. Global Monitoring for environment and security - European Environment Agency. URL: <https://www.eea.europa.eu/data-and-maps/data/urban-atlas> (visited on 10/30/2019).
- Green, Timothy R., Makoto Taniguchi, Henk Kooi, Jason J. Gurdak, Diana M. Allen, Kevin M. Hiscock, Holger Treidel, and Alice Aureli (2011). "Beneath the surface of global change: Impacts of climate change on groundwater". In: *Journal of Hydrology* 405.3, pp. 532–560. DOI: [10.1016/j.jhydrol.2011.05.002](https://doi.org/10.1016/j.jhydrol.2011.05.002).
- Griebler, Christian, Kellermann, Claudia, Kuntz, David, Walker-Hertkorn, Simone, Stumpp, Christine, and Hegler, Florian (2014). *Auswirkungen thermischer Veränderungen infolge der Nutzung oberflächennaher Geothermie auf die Beschaffenheit des Grundwassers und seiner Lebensgemeinschaften – Empfehlungen für eine umweltverträgliche Nutzung* –. Umweltbundesamt, pp. 1–153.
- Griffioen, Jasper and C. Anthony J. Appelo (1993). "Nature and extent of carbonate precipitation during aquifer thermal energy storage". In: *Applied Geochemistry* 8.2, pp. 161–176. DOI: [10.1016/0883-2927\(93\)90032-C](https://doi.org/10.1016/0883-2927(93)90032-C).
- Götzl, Gregor, M. Fuchsluger, F. A. Rodler, P. Lipiarski, and S. Pfeleiderer (2014). *Projekt WC-31 Erdwärmepotenzialerhebung Stadtgebiet Wien, Modul 1 Endbericht*. Wien: Magistrat der Stadt Wien Magistratsabteilung 20 – Energieplanung, p. 70.
- Götzl, Gregor, V. Ostermann, R. Kalasek, R. Heimrath, P. Steckler, A. Zottl, A. Novak, G. Haindlmaier, R. Hackl, S. Shadlau, and H. Reitner (2010). "GEO-Pot: Seichtes Geothermie Potenzial Österreichs. Überregionale, interdisziplinäre Potenzialstudie zur Erhebung und Darstellung des oberflächennahen geothermischen Anwendungspotenzials auf Grundlage eines regelmäßigen Bearbeitungsrasters". In: *Osterr Wasser- Abfallw* 5-6.
- Gunawardhana, Luminda Niroshana and So Kazama (2012). "Statistical and numerical analyses of the influence of climate variability on aquifer water levels and groundwater temperatures: The impacts of climate change on aquifer thermal regimes". In: *Global and Planetary Change* 86-87, pp. 66–78. DOI: [10.1016/j.gloplacha.2012.02.006](https://doi.org/10.1016/j.gloplacha.2012.02.006).
- Hahn, Hans Jürgen, Christian Schweer, and Christian Griebler (2018). "Are groundwater ecosystems rights being preserved?" In: *Grundwasser* 23.3.
- Hall, Edward K, Claudia Neuhauser, and James B Cotner (2008). "Toward a mechanistic understanding of how natural bacterial communities respond to changes in temperature in aquatic ecosystems". In: *The ISME Journal* 2.5, pp. 471–481. DOI: [10.1038/ismej.2008.9](https://doi.org/10.1038/ismej.2008.9).
- Hartmann, Stephan (2016). *Transform+ Transformationsplan Wien*. Wien: Magistratsabteilung MA 18 - Stadtentwicklung und Stadtplanung.
- Hemmerle, Hannes, Sina Hale, Ingo Dressel, Susanne A. Benz, Guillaume Attard, Philipp Blum, and Peter Bayer (2019). "Estimation of Groundwater Temperatures in Paris, France". In: *Geofluids* 2019, pp. 1–11. DOI: [10.1155/2019/5246307](https://doi.org/10.1155/2019/5246307).
- Herb, William R., Ben Janke, Omid Mohseni, and Heinz G. Stefan (2008). "Ground surface temperature simulation for different land covers". In: *Journal of Hydrology* 356.3, pp. 327–343. DOI: [10.1016/j.jhydrol.2008.04.020](https://doi.org/10.1016/j.jhydrol.2008.04.020).

- Hähnlein, Stefanie, Peter Bayer, and Philipp Blum (2010). "International legal status of the use of shallow geothermal energy". In: *Renewable and Sustainable Energy Reviews* 14.9, pp. 2611–2625. DOI: [10.1016/j.rser.2010.07.069](https://doi.org/10.1016/j.rser.2010.07.069).
- Hähnlein, Stefanie, Peter Bayer, Grant Ferguson, and Philipp Blum (2013). "Sustainability and policy for the thermal use of shallow geothermal energy". In: *Energy Policy* 59, pp. 914–925. DOI: [10.1016/j.enpol.2013.04.040](https://doi.org/10.1016/j.enpol.2013.04.040).
- Hähnlein, Stefanie, Philipp Blum, and Peter Bayer (2011). "Oberflächennahe Geothermie – aktuelle rechtliche Situation in Deutschland". In: *Grundwasser* 16.2, pp. 69–75. DOI: [10.1007/s00767-011-0162-0](https://doi.org/10.1007/s00767-011-0162-0).
- Hähnlein, Stefanie, Nelson Molina-Giraldo, Philipp Blum, Peter Bayer, and Peter Grathwohl (2010). "Ausbreitung von Kältefahnen im Grundwasser bei Erdwärmesonden". In: *Grundwasser* 15.2, pp. 123–133. DOI: [10.1007/s00767-009-0125-x](https://doi.org/10.1007/s00767-009-0125-x).
- HLNUG (2018). *Hessisches Landesamt für Naturschutz, Umwelt und Geologie*. URL: <https://www.hlnug.de/start.html> (visited on 05/01/2019).
- Hölting, Bernward and Wilhelm Georg Coldewey (2013). *Hydrogeologie: Einführung in die Allgemeine und Angewandte Hydrogeologie*. Heidelberg: Spektrum Akademischer Verlag. DOI: [10.1007/978-3-8274-2354-2](https://doi.org/10.1007/978-3-8274-2354-2).
- Huang, Shaopeng, Makoto Taniguchi, Makoto Yamano, and Chung-ho Wang (2009). "Detecting urbanization effects on surface and subsurface thermal environment — A case study of Osaka". In: *Science of The Total Environment* 407.9, pp. 3142–3152. DOI: [10.1016/j.scitotenv.2008.04.019](https://doi.org/10.1016/j.scitotenv.2008.04.019).
- IHW (2018). *Informatiehuis Water*. URL: <https://www.ihw.nl/index.html> (visited on 05/01/2019).
- Iskander, Magued, Walid Aboumoussa, and Pierre Gouvin (2001). "Instrumentation and Monitoring of a Distressed Multistory Underground Parking Garage". In: *Journal of Performance of Constructed Facilities* 15.3, pp. 115–123. DOI: [10.1061/\(ASCE\)0887-3828\(2001\)15:3\(115\)](https://doi.org/10.1061/(ASCE)0887-3828(2001)15:3(115)).
- Jakob, Martin, Karin Flury, Nadja Gross, Gregor Martius, and Benjamin Sunarjo (2014). *Kurzbericht Konzept Energieversorgung 2050: Szenarien für eine 2000-Watt-kompatible Wärme-versorgung für die Stadt Zürich*. Zürich: Departement der Industriellen Betriebe.
- Jank, Reinhard (2013). *Integrales Quartiers-Energiekonzept Karlsruhe-Rintheim: Optimierungsmethoden, Praxiserfahrungen mit technischen Innovationen, Umsetzungsergebnisse*. Volkswohnung Karlsruhe GmbH. DOI: [10.2314/GBV:790783096](https://doi.org/10.2314/GBV:790783096).
- Jank, Reinhard and Reiner Kuklinski (2015). *Integrales Quartiers-Energiekonzept Karlsruhe-Rintheim: Optimierungsmethoden ; Praxiserfahrungen ; Ergebnisse*. OCLC: 908616795. Stuttgart: Fraunhofer-IRB-Verl. 133 pp.
- Jaudin, Florence et al. (2013). *D2.2: General Report of the current situation of the regulatøve framework for the SGE systems -Overview of Shallow Geothermal Legislation in Europe*.
- Jung, Stephan (2013). "Wärmefluss in der urbanen Wärmeinsel Köln". Masterarbeit. Karlsruhe: Karlsruher Institut für Technologie. 112 pp.
- Kail, Eva (2017). "Smart City Wien – Stadtentwicklungsplan 2025". Wien.
- Kübert, Markus, Simone Walker-Hertkorn, Dierk Schreyer, and Erich Eyth (2010). "Geothermie. Oberflächennahe. Geothermie SONDERHEFT Aufschlussbohrungen. Grundwassermessstellen. Brunnenbau. Brunnensanierung.pdf". In: *bbr Fachmagazin für Brunnen- und Leitungsbau Sonderheft Oberflächennahe Geothermie 2010*, pp. 84–90.
- Keim, B. and U. Lang (2008). *Thermische Nutzung von Grundwasser durch Wärmepumpen*. Stuttgart: Umweltministerium Baden-Württemberg.
- Kerl, Marco, Nicolas Runge, Horst Tauchmann, and Nico Goldscheider (2012). "Hydrogeologisches Konzeptmodell von München: Grundlage für die thermische

- Grundwassernutzung". In: *Grundwasser* 17.3, pp. 127–135. DOI: [10.1007/s00767-012-0199-8](https://doi.org/10.1007/s00767-012-0199-8).
- Kinzelbach, Wolfgang (1992). *Numerische Methoden zur Modellierung des Transports von Schadstoffen im Grundwasser*. München: Oldenbourg Verlag.
- Krcmar, David, Renata Flakova, Ivana Ondrejko, Kamila Hodasova, Daniela Rusnakova, Zlatica Zenisova, and Martin Zatlakovic (2020). "Assessing the Impact of a Heated Basement on Groundwater Temperatures in Bratislava, Slovakia". In: *Groundwater*, gwat.12986. DOI: [10.1111/gwat.12986](https://doi.org/10.1111/gwat.12986).
- Krämer, E. (2010). "Bohrungen für Erdwärmesonden mit Hohlbohrschnecken". In: *bbr- Leitungsbau Brunnenbau Geothermie H5*, pp. 24–27.
- Krümpelbeck, Inge (2000). "Untersuchungen zum langfristigen Verhalten von Siedlungsabfalldeponien". PhD thesis. Wuppertal: Bergischen Universität - Gesamthochschule Wuppertal. 216 pp.
- Kupfersberger, Hans, Gerhard Rock, and Johannes C. Draxler (2017). "Inferring near surface soil temperature time series from different land uses to quantify the variation of heat fluxes into a shallow aquifer in Austria". In: *Journal of Hydrology* 552, pp. 564–577. DOI: [10.1016/j.jhydro.2017.07.030](https://doi.org/10.1016/j.jhydro.2017.07.030).
- Kurevija, Tomislav, Domagoj Vulin, and Vedrana Krapec (2012). "Effect of borehole array geometry and thermal interferences on geothermal heat pump system". In: *Energy Conversion and Management*. Special issue of Energy Conversion and Management dedicated to ECOS 2011 - the 24th International Conference on Efficiency, Costs, Optimization, Simulation and Environmental Impact of Energy Systems 60, pp. 134–142. DOI: [10.1016/j.enconman.2012.02.012](https://doi.org/10.1016/j.enconman.2012.02.012).
- Kurylyk, B. L., C. P.-A. Bourque, and K. T. B. MacQuarrie (2013). "Potential surface temperature and shallow groundwater temperature response to climate change: an example from a small forested catchment in east-central New Brunswick (Canada)". In: *Hydrology and Earth System Sciences* 17.7, pp. 2701–2716. DOI: [10.5194/hess-17-2701-2013](https://doi.org/10.5194/hess-17-2701-2013).
- LANUV (2018). *Landesamt für Natur, Umwelt und Verbraucherschutz Nordrhein-Westfalen*. URL: <https://www.lanuv.nrw.de/> (visited on 05/01/2019).
- Lewis, Trevor J. and Kelin Wang (1998). "Geothermal evidence for deforestation induced warming: Implications for the Climatic impact of land development". In: *Geophysical Research Letters* 25.4, pp. 535–538. DOI: [10.1029/98GL00181](https://doi.org/10.1029/98GL00181).
- LfUB (2018). *Bayerisches Landesamt für Umwelt*. URL: <https://www.lfu.bayern.de/index.htm> (visited on 05/01/2019).
- LfUBB (2018). *Landesamt für Umwelt - Brandenburg*. URL: <https://lfu.brandenburg.de/sixcms/detail.php/bb1.c.285413.de> (visited on 05/01/2019).
- LfULG (2010). *Geologie und Bergbaufolgen im Steinkohlerevier Lugau/Oelsnitz - Geoprofil 13*. Dresden.
- LfULG (2018). *Landesamt für Umwelt, Landwirtschaft und Geologie Sachsen*. URL: [/index.html](http://index.html) (visited on 05/01/2019).
- LfURP (2018). *Landesamt für Umwelt Rheinland-Pfalz*. lfu.rlp.de. URL: <https://lfu.rlp.de/de/startseite/> (visited on 05/01/2019).
- LGRB (2017). *Informationssystem oberflächennahe Geothermie Baden-Württemberg (ISONG)*. URL: <http://isong.lgrb-bw.de/> (visited on 04/19/2018).
- LHW (2018). *Landesbetrieb für Hochwasserschutz und Wasserwirtschaft Sachsen-Anhalt*. Landesportal Sachsen-Anhalt. URL: <https://lhw.sachsen-anhalt.de/> (visited on 05/01/2019).
- Li, Deren, Xia Zhao, and Xi Li (2016). "Remote sensing of human beings – a perspective from nighttime light". In: *Geo-spatial Information Science* 19.1, pp. 69–79. DOI: [10.1080/10095020.2016.1159389](https://doi.org/10.1080/10095020.2016.1159389).

- LUA (2018). *Landesamt für Umwelt- und Arbeitsschutz Saarland*. URL: https://www.saarland.de/landesamt_umwelt_arbeitsschutz.htm (visited on 05/01/2019).
- LUBW (2018). *Landesamt für Umwelt, Messungen und Naturschutz Baden-Württemberg*. URL: <http://jdkgw.lubw.baden-wuerttemberg.de/servlet/is/200/> (visited on 05/01/2019).
- Lund, H., B. Möller, B.V. Mathiesen, and A. Dyrelund (2010). "The role of district heating in future renewable energy systems". In: *Energy* 35.3, pp. 1381–1390. DOI: [10.1016/j.energy.2009.11.023](https://doi.org/10.1016/j.energy.2009.11.023).
- Lund, John W. and Tonya L. Boyd (2016). "Direct utilization of geothermal energy 2015 worldwide review". In: *Geothermics* 60, pp. 66–93. DOI: [10.1016/j.geothermics.2015.11.004](https://doi.org/10.1016/j.geothermics.2015.11.004).
- Luo, Jin, Zequan Luo, Jihai Xie, Dongsheng Xia, Wei Huang, Haibin Shao, Wei Xiang, and Joachim Rohn (2018). "Investigation of shallow geothermal potentials for different types of ground source heat pump systems (GSHP) of Wuhan city in China". In: *Renewable Energy* 118, pp. 230–244. DOI: [10.1016/j.renene.2017.11.017](https://doi.org/10.1016/j.renene.2017.11.017).
- MA 18 (2014). *Step 2025 - Stadtentwicklungsplan Wien*. Wien: Magistratsabteilung MA 18 - Stadtentwicklung und Stadtplanung, p. 143.
- MA 20 (2019). "Energie! voraus - Energiebericht der Stadt Wien". In: p. 76.
- Manteuffel, Bernhard von, Carsten Petersdorff, Kjell Bettgenhäuser, and Thomas Boermans (2016). "EU pathways to a decarbonised building sector" *How replacing inefficient heating systems can help reach the EU climate ambitions*. Ecofys.
- McMahon, Richard, Hugo Santos, and Zenaida Sobral Mourão (2018). "Practical considerations in the deployment of ground source heat pumps in older properties—A case study". In: *Energy and Buildings* 159, pp. 54–65. DOI: [10.1016/j.enbuild.2017.08.067](https://doi.org/10.1016/j.enbuild.2017.08.067).
- Menberg, K., P. Blum, B. L. Kurylyk, and P. Bayer (2014). "Observed groundwater temperature response to recent climate change". In: *Hydrology and Earth System Sciences* 18.11, pp. 4453–4466. DOI: [10.5194/hess-18-4453-2014](https://doi.org/10.5194/hess-18-4453-2014).
- Menberg, Kathrin, Peter Bayer, Kai Zosseder, Sven Rumohr, and Philipp Blum (2013a). "Subsurface urban heat islands in German cities". In: *Science of The Total Environment* 442, pp. 123–133. DOI: [10.1016/j.scitotenv.2012.10.043](https://doi.org/10.1016/j.scitotenv.2012.10.043).
- Menberg, Kathrin, Philipp Blum, Jaime Rivera, Susanne Benz, and Peter Bayer (2015). "Exploring the Geothermal Potential of Waste Heat Beneath Cities". In: *Proceedings World Geothermal Congress*. Melbourne, Australia, p. 5.
- Menberg, Kathrin, Philipp Blum, Axel Schaffitel, and Peter Bayer (2013b). "Long-Term Evolution of Anthropogenic Heat Fluxes into a Subsurface Urban Heat Island". In: *Environmental Science & Technology* 47.17, pp. 9747–9755. DOI: [10.1021/es401546u](https://doi.org/10.1021/es401546u).
- Meng, Boyan, Thomas Vienken, Olaf Kolditz, and Haibing Shao (2019). "Evaluating the thermal impacts and sustainability of intensive shallow geothermal utilization on a neighborhood scale: Lessons learned from a case study". In: *Energy Conversion and Management* 199, p. 111913. DOI: [10.1016/j.enconman.2019.111913](https://doi.org/10.1016/j.enconman.2019.111913).
- Miglani, Somil, Kristina Orehounig, and Jan Carmeliet (2018). "A methodology to calculate long-term shallow geothermal energy potential for an urban neighbourhood". In: *Energy and Buildings* 159, pp. 462–473. DOI: [10.1016/j.enbuild.2017.10.100](https://doi.org/10.1016/j.enbuild.2017.10.100).
- Molina-Giraldo, Nelson (2011). "Heat transport modeling in shallow aquifers - The role of thermal dispersion in aquifers and heat conduction into confining layers". Dissertation. Tübingen: Eberhard Karls Universität Tübingen. 89 pp.

- Mueller, Matthias H., Peter Huggenberger, and Jannis Epting (2018). "Combining monitoring and modelling tools as a basis for city-scale concepts for a sustainable thermal management of urban groundwater resources". In: *Science of The Total Environment* 627, pp. 1121–1136. DOI: [10.1016/j.scitotenv.2018.01.250](https://doi.org/10.1016/j.scitotenv.2018.01.250).
- Nam, Yujin and Ryoza Ooka (2011). "Development of potential map for ground and groundwater heat pump systems and the application to Tokyo". In: *Energy and Buildings* 43.2, pp. 677–685. DOI: [10.1016/j.enbuild.2010.11.011](https://doi.org/10.1016/j.enbuild.2010.11.011).
- Nawalany and Sokołowski (2019). "Building–Soil Thermal Interaction: A Case Study". In: *Energies* 12.15, p. 2922. DOI: [10.3390/en12152922](https://doi.org/10.3390/en12152922).
- NLWKN (2018). *Nds. Landesbetrieb für Wasserwirtschaft, Küsten- und Naturschutz*. URL: <http://www.nlwkn.niedersachsen.de/startseite/> (visited on 05/01/2019).
- Noorollahi, Younes, Hamidreza Gholami Arjenaki, and Roghayeh Ghasempour (2017). "Thermo-economic modeling and GIS-based spatial data analysis of ground source heat pump systems for regional shallow geothermal mapping". In: *Renewable and Sustainable Energy Reviews* 72, pp. 648–660. DOI: [10.1016/j.rser.2017.01.099](https://doi.org/10.1016/j.rser.2017.01.099).
- Oke, Tim R. (1973). "City size and the urban heat island". In: *Atmospheric Environment (1967)* 7.8, pp. 769–779.
- Ondreka, Joris, Maike Inga Rüsgen, Ingrid Stober, and Kurt Czurda (2007). "GIS-supported mapping of shallow geothermal potential of representative areas in south-western Germany—Possibilities and limitations". In: *Renewable Energy* 32.13, pp. 2186–2200. DOI: [10.1016/j.renene.2006.11.009](https://doi.org/10.1016/j.renene.2006.11.009).
- Pahud, Daniel (2015). *Simulationen gemessener Erdwärmesondenfelder*. Schlussbericht. EnergieSchweiz, p. 22.
- Patton, A. M., G. Farr, D. P. Boon, D. R. James, B. Williams, L. James, R. Kendall, S. Thorpe, G. Harcombe, D. I. Schofield, A. Holden, and D. White (2020). "Establishing an urban geo-observatory to support sustainable development of shallow subsurface heat recovery and storage". In: *Quarterly Journal of Engineering Geology and Hydrogeology* 53.1, pp. 49–61. DOI: [10.1144/qjegh2019-020](https://doi.org/10.1144/qjegh2019-020).
- Perego, Rodolfo, Sebastian Pera, and Antonio Galgaro (2019). "Techno-Economic Mapping for the Improvement of Shallow Geothermal Management in Southern Switzerland". In: *Energies* 12.2, p. 279. DOI: [10.3390/en12020279](https://doi.org/10.3390/en12020279).
- Pfleiderer, Sebastian (2019). "Hydrochemistry of Groundwater in the City of Vienna, Austria". *Groundwater Quality* 2019. Liège.
- Pfleiderer, Sebastian and Thomas Hofmann (2004). *Digitaler angewandter Geo-Atlas der Stadt Wien - Projekt WC 21 HYDRO-Modul*. Wien: Geological Survey of Austria.
- Pfleiderer, Sebastian and Thomas Hofmann (2007). "Digitaler Angewandter Geo-Atlas – Stadtgeologie am Beispiel von Wien". In: *Jb. Geol. B.-A.* 147 (Heft 1+2), pp. 263–273.
- Pollack, H. N. (1998). "Climate Change Record in Subsurface Temperatures: A Global Perspective". In: *Science* 282.5387, pp. 279–281. DOI: [10.1126/science.282.5387.279](https://doi.org/10.1126/science.282.5387.279).
- Pophillat, William, Guillaume Attard, Peter Bayer, Jozsef Hecht-Méndez, and Philipp Blum (2018). "Analytical solutions for predicting thermal plumes of groundwater heat pump systems". In: *Renewable Energy*. DOI: [10.1016/j.renene.2018.07.148](https://doi.org/10.1016/j.renene.2018.07.148).
- Possemiers, Mathias, Marijke Huysmans, and Okke Batelaan (2014). "Influence of Aquifer Thermal Energy Storage on groundwater quality: A review illustrated by seven case studies from Belgium". In: *Journal of Hydrology: Regional Studies* 2, pp. 20–34. DOI: [10.1016/j.ejrh.2014.08.001](https://doi.org/10.1016/j.ejrh.2014.08.001).

- Pu, Liang, Lingling Xu, Di Qi, and Yanzhong Li (2018). "Structure optimization for horizontal ground heat exchanger". In: *Applied Thermal Engineering* 136, pp. 131–140. DOI: [10.1016/j.applthermaleng.2018.02.101](https://doi.org/10.1016/j.applthermaleng.2018.02.101).
- Ramming, Klaus (2007). "Bewertung und Optimierung oberflächennaher Erdwärmekollektoren für verschiedene Lastfälle". Dissertation. Dresden: Technischen Universität Dresden. 149 pp.
- Recknagel, Hermann, Eberhard Sprenger, and Ernst-Rudolf Schramek (2007). *Taschenbuch für Heizung+ Klimatechnik 07/08*. 73rd ed. München: Oldenbourg Industrieriv-erlag.
- Riedel, Thomas (2019). "Temperature-associated changes in groundwater quality". In: *Journal of Hydrology* 572, pp. 206–212. DOI: [10.1016/j.jhydrol.2019.02.059](https://doi.org/10.1016/j.jhydrol.2019.02.059).
- Rivera, Jaime A., Philipp Blum, and Peter Bayer (2015a). "Analytical simulation of groundwater flow and land surface effects on thermal plumes of borehole heat exchangers". In: *Applied Energy* 146, pp. 421–433. DOI: [10.1016/j.apenergy.2015.02.035](https://doi.org/10.1016/j.apenergy.2015.02.035).
- Rivera, Jaime A., Philipp Blum, and Peter Bayer (2015b). "Ground energy balance for borehole heat exchangers: Vertical fluxes, groundwater and storage". In: *Renewable Energy* 83, pp. 1341–1351. DOI: [10.1016/j.renene.2015.05.051](https://doi.org/10.1016/j.renene.2015.05.051).
- Rivera, Jaime A., Philipp Blum, and Peter Bayer (2017). "Increased ground temperatures in urban areas: Estimation of the technical geothermal potential". In: *Renewable Energy* 103, pp. 388–400. DOI: [10.1016/j.renene.2016.11.005](https://doi.org/10.1016/j.renene.2016.11.005).
- Rudakov, Dmytro and Oleksandr Inkin (2019). "An assessment of technical and economic feasibility to install geothermal well systems across Ukraine". In: *Geothermal Energy* 7.1, p. 17. DOI: [10.1186/s40517-019-0134-7](https://doi.org/10.1186/s40517-019-0134-7).
- Sbrana, Alessandro, Paola Marianelli, Giuseppe Pasquini, Paolo Costantini, Francesco Palmieri, Valentina Ciani, and Michele Sbrana (2018). "The Integration of 3D Modeling and Simulation to Determine the Energy Potential of Low-Temperature Geothermal Systems in the Pisa (Italy) Sedimentary Plain". In: *Energies* 11.6, p. 1591. DOI: [10.3390/en11061591](https://doi.org/10.3390/en11061591).
- Schiel, Kerry, Olivier Baume, Geoffrey Caruso, and Ulrich Leopold (2016). "GIS-based modelling of shallow geothermal energy potential for CO 2 emission mitigation in urban areas". In: *Renewable Energy* 86, pp. 1023–1036. DOI: [10.1016/j.renene.2015.09.017](https://doi.org/10.1016/j.renene.2015.09.017).
- Schmidt, Ralf-Roman (2011). "Thermische Netzwerke/ Fernwärme".
- Schweikert, Svenja (2014). "Untersuchung der Grundwasserökologie von Karlsruhe". Masterarbeit. Karlsruhe: Karlsruher Institut für Technologie.
- Self, Stuart J., Bale V. Reddy, and Marc A. Rosen (2013). "Geothermal heat pump systems: Status review and comparison with other heating options". In: *Applied Energy* 101, pp. 341–348. DOI: [10.1016/j.apenergy.2012.01.048](https://doi.org/10.1016/j.apenergy.2012.01.048).
- Sharma, Laxman, Janek Greskowiak, Chittaranjan Ray, Paul Eckert, and Henning Prommer (2012). "Elucidating temperature effects on seasonal variations of biogeochemical turnover rates during riverbank filtration". In: *Journal of Hydrology* 428–429, pp. 104–115. DOI: [10.1016/j.jhydrol.2012.01.028](https://doi.org/10.1016/j.jhydrol.2012.01.028).
- Sharp, John M. (2010). "The impacts of urbanization on groundwater systems and recharge". In: *AQUAmundi - Journal of water sciences* 1, pp. 051–056. DOI: [10.4409/Am-004-10-0008](https://doi.org/10.4409/Am-004-10-0008).
- SHMU (2018). *Slovak Hydrometeorological Institute*. URL: http://www.shmu.sk/sk/?page=1&id=ran_sprav (visited on 05/01/2019).
- SIA 384/6 (2009). *Erdwärmesonden*.

- Singh, R D and C P Kumar (2010). "Impact of Climate Change on Groundwater Resources". In: *International Journal of Climate Change Strategies and Management*. Proceedings of 2nd National Ground Water Congress, p. 15.
- Smerdon, Jason E., Henry N. Pollack, John W. Enz, and Matthew J. Lewis (2003). "Conduction-dominated heat transport of the annual temperature signal in soil". In: *Journal of Geophysical Research: Solid Earth* 108 (B9). DOI: [10.1029/2002JB002351](https://doi.org/10.1029/2002JB002351).
- Solomon, Adina (2017). *Welcome to the Steam-Powered Suburbs*. CityLab. URL: <https://www.citylab.com/environment/2017/11/geothermal-suburbs/545354/> (visited on 03/06/2018).
- Somogyi, Viola, Viktor Sebestyén, and Georgina Nagy (2017). "Scientific achievements and regulation of shallow geothermal systems in six European countries – A review". In: *Renewable and Sustainable Energy Reviews* 68, pp. 934–952. DOI: [10.1016/j.rser.2016.02.014](https://doi.org/10.1016/j.rser.2016.02.014).
- Stadt Wien. *data.gv.at - offene Daten Österreichs – lesbar für Mensch und Maschine*. Open Government Wien - Bundesministerium für Digitalisierung und Wirtschaftsstandort. URL: <https://www.data.gv.at/> (visited on 10/30/2019).
- Stadt Wien (2016). *Smart City Wien, Rahmenstrategie*. Wien: Magistrat der Stadt Wien, p. 111.
- Stadt Wien (2017). *Energy Framework Strategy 2030 for Vienna*. Vienna, p. 30.
- Stadt Wien (2019). *Smart City Wien Rahmenstrategie 2019-2050 - Die Wiener Strategie für eine nachhaltige Entwicklung*. Wien, p. 172.
- Stauffer, Fritz, Peter Bayer, Philipp Blum, Nelson Molina-Giraldo, and Wolfgang Kinezlbach (2014). *Thermal Use of Shallow Groundwater*. OCLC: 1020635550. S.I.: CRC Press.
- Österreichisches Institut für Bautechnik (2015). *OIB Richtlinie 6 Energieeinsparung und Wärmeschutz*.
- Stober, Ingrid and Kurt Bucher (2012). *Geothermie*. Berlin, Heidelberg: Springer Berlin Heidelberg. DOI: [10.1007/978-3-642-24331-8](https://doi.org/10.1007/978-3-642-24331-8).
- SUBV (2018). *Der Senator für Umwelt, Bau und Verkehr*. URL: <https://www.bauumwelt.bremen.de/> (visited on 05/01/2019).
- Taniguchi, Makato, Jun Shimada, Tadashi Tanaka, Isamu Kayane, Yasuo Sakura, Yasuo Shimano, S. Dapaah-Siakwan, and Shinichi Kawashima (1999). "Disturbances of temperature-depth profiles due to surface climate change and subsurface water flow: 1. An effect of linear increase in surface temperature caused by global warming and urbanization in the Tokyo Metropolitan Area, Japan". In: *Water Resources Research* 35.5, pp. 1507–1517. DOI: [10.1029/1999WR900009](https://doi.org/10.1029/1999WR900009).
- Taniguchi, Makoto, Jun Shimada, Yoichi Fukuda, Makoto Yamano, Shin-ichi Onodera, Shinji Kaneko, and Akihisa Yoshikoshi (2009). "Anthropogenic effects on the subsurface thermal and groundwater environments in Osaka, Japan and Bangkok, Thailand". In: *Science of The Total Environment* 407.9, pp. 3153–3164. DOI: [10.1016/j.scitotenv.2008.06.064](https://doi.org/10.1016/j.scitotenv.2008.06.064).
- Taniguchi, Makoto, Takeshi Uemura, and Karen Jago-on (2007). "Combined Effects of Urbanization and Global Warming on Subsurface Temperature in Four Asian Cities". In: *Vadose Zone Journal* 6.3, p. 591. DOI: [10.2136/vzj2006.0094](https://doi.org/10.2136/vzj2006.0094).
- Taylor, Craig A. and Heinz G. Stefan (2009). "Shallow groundwater temperature response to climate change and urbanization". In: *Journal of Hydrology* 375.3, pp. 601–612. DOI: [10.1016/j.jhydro.2009.07.009](https://doi.org/10.1016/j.jhydro.2009.07.009).
- TbKA (2018). *Tiefbauamt Karlsruhe*. URL: <https://www.karlsruhe.de/b3/bauen/tiefbau.de> (visited on 05/01/2019).

- Tissen, Carolin, Kathrin Menberg, Peter Bayer, and Philipp Blum (2019). "Meeting the demand: geothermal heat supply rates for an urban quarter in Germany". In: *Geothermal Energy* 7.1. DOI: [10.1186/s40517-019-0125-8](https://doi.org/10.1186/s40517-019-0125-8).
- TLUG (2018). *Thüringer Landesanstalt für Umwelt und Geologie*. URL: <https://www.thueringen.de/th8/tlug/> (visited on 05/01/2019).
- Tsagarakis, Konstantinos P. et al. (2018). "A review of the legal framework in shallow geothermal energy in selected European countries: Need for guidelines". In: *Renewable Energy*. DOI: [10.1016/j.renene.2018.10.007](https://doi.org/10.1016/j.renene.2018.10.007).
- Umweltbundesamt GmbH. *H2O Fachdatenbank - Grundwasserkörperabfrage*. URL: <https://wasser.umweltbundesamt.at/h2odb/stammdaten/igwk.xhtml> (visited on 08/27/2019).
- VDI 4640 part 1 (2010). *Thermische Nutzung des Untergrunds - Grundlagen, Genehmigungen, Umweltaspekte*. Berlin: Beuth Verlag.
- VDI 4640 part 2 (2001). *Thermische Nutzung des Untergrundes - Erdgekoppelte Wärmepumpenanlagen*. Berlin: Beuth Verlag.
- VDI 4640 part 2 (2015). *Thermische Nutzung des Untergrunds - Erdgekoppelte Wärmepumpenanlagen*. Berlin: Beuth Verlag.
- VDI 4640 part 4 (2004). *Thermische Nutzung des Untergrundes - Direkte Nutzungen*. Berlin: Beuth Verlag.
- Vienken, T., S. Schelenz, K. Rink, and P. Dietrich (2015). "Sustainable Intensive Thermal Use of the Shallow Subsurface-A Critical View on the Status Quo". In: *Groundwater* 53.3, pp. 356–361. DOI: [10.1111/gwat.12206](https://doi.org/10.1111/gwat.12206).
- Viesi, Diego, Antonio Galgaro, Paola Visintainer, and Luigi Crema (2018). "GIS-supported evaluation and mapping of the geo-exchange potential for vertical closed-loop systems in an Alpine valley, the case study of Adige Valley (Italy)". In: *Geothermics* 71, pp. 70–87. DOI: [10.1016/j.geothermics.2017.08.008](https://doi.org/10.1016/j.geothermics.2017.08.008).
- VMM (2018). *Vlaamse Milieumaatschappij*. URL: <https://www.vmm.be> (visited on 05/01/2019).
- Wang, Huajun, Chengying Qi, Hongpu Du, and Jihao Gu (2009). "Thermal performance of borehole heat exchanger under groundwater flow: A case study from Baoding". In: *Energy and Buildings* 41.12, pp. 1368–1373. DOI: [10.1016/j.enbuild.2009.08.001](https://doi.org/10.1016/j.enbuild.2009.08.001).
- Water, Sydney (2011). *Best practice guidelines for water management in aquatic leisure centres*.
- WFD (2000). "Directive 2000/60/EC of the European Parliament and of the Council of 23 October 2000 – establishing framework for community action in the field of water policy resource.pdf". In: *Official Journal of the European Communities* L 327/1, p. 72.
- Wien Energie (2013). *Technische Richtlinien - Technische Auslegungsbedingungen*.
- Wien Kanal. *KANIS - Kanalinformationssystem*. URL: <http://www.kanis.at/> (visited on 10/30/2019).
- Wiener Linien. *So tief fährt die U-Bahn*. URL: https://www.wienerlinien.at/media/files/2016/u2u5_tiefe_neubaugasse_179582.pdf (visited on 10/30/2019).
- Wiener Linien. *Unternehmen | Wiener Linien*. www.wienerlinien.at. URL: <http://www.wienerlinien.at/portal3/ep/tab.do?pageTypeId%3D66528> (visited on 01/20/2020).
- Wiener Stadtwerke (2015). *Wie die Wiener Stadtwerke wirken*. Wien: Wiener Stadtwerke.
- Wiener Stadtwerke (2018). *Nachhaltigkeitsbericht 2017. Unsere Verantwortung für Generationen*. Wien.

- Willscher, S., T. Hertwig, M. Frenzel, M. Felix, and S. Starke (2010). "Results of remediation of hard coal overburden and tailing dumps after a few decades: Insights and conclusions". In: *Hydrometallurgy* 104.3, pp. 506–517. DOI: [10.1016/j.hydromet.2010.03.031](https://doi.org/10.1016/j.hydromet.2010.03.031).
- Wirsing, G. and A. Luz (2007). *Hydrogeologischer Bau und Aquifereigenschaften der Lockergesteine im Oberrheingraben (Baden-Württemberg)*. Freiburg i. Br.: Regierungspräsidium Freiburg, Landesamt für Geologie, Rohstoffe und Bergbau.
- Wirsing, Gunther and Alexander Luz (2005). *Hydrogeologischer Bau und Aquifereigenschaften der Lockergesteine im Oberrheingraben (Baden-Württemberg)*.
- Yousefi, Hossein, Atefeh Abbaspour, and HamidReza Seraj (2019). "The Role of Geothermal Energy Development on CO2 Emission by 2030". In: 44th Workshop on Geothermal Reservoir Engineering. Stanford, California, p. 6.
- ZAMG. SPARTACUS. Zentralanstalt für Meteorologie und Geodynamik (ZAMG). URL: <https://www.zamg.ac.at/cms/de/forschung/klima/klimatografien/spartacus><http://link.springer.com/10.1007/s00704-015-1411-4> (visited on 11/14/2019).
- Zhang, Changxing, Yusheng Wang, Yufeng Liu, Xiangqiang Kong, and Qing Wang (2018). "Computational methods for ground thermal response of multiple borehole heat exchangers: A review". In: *Renewable Energy* 127, pp. 461–473. DOI: [10.1016/j.renene.2018.04.083](https://doi.org/10.1016/j.renene.2018.04.083).
- Zhang, Y., K. Soga, and R. Choudhary (2014). "Shallow geothermal energy application with GSHPs at city scale: study on the City of Westminster". In: *Géotechnique Letters* 4.2, pp. 125–131. DOI: [10.1680/geolett.13.00061](https://doi.org/10.1680/geolett.13.00061).
- Zhu, Ke, Peter Bayer, Peter Grathwohl, and Philipp Blum (2015). "Groundwater temperature evolution in the subsurface urban heat island of Cologne, Germany". In: *Hydrological Processes* 29.6, pp. 965–978. DOI: [10.1002/hyp.10209](https://doi.org/10.1002/hyp.10209).
- Zhu, Ke, Philipp Blum, Grant Ferguson, Klaus-Dieter Balke, and Peter Bayer (2010). "The geothermal potential of urban heat islands". In: *Environmental Research Letters* 5. DOI: [10.1088/1748-9326/6/1/019501](https://doi.org/10.1088/1748-9326/6/1/019501).

Acknowledgements

This thesis would not be possible without the help and support of many people. I would like to thank...

- ... Prof. Dr. Philipp Blum and Prof. Dr. Stefan Hinz for the opportunity to do a PhD and accepting me into their PhD program, for their guidance, continuous encouragement and steadily support. I like to express my particular thank to Philipp who opened my eyes for the "bigger picture" and always fetch me back when I got lost in details. I am also grateful for the freedom you gave me to develop my own ideas and concepts, to broaden my horizon and to acquire competent and valuable knowledge for my future.
- ... for the financial support by the Graduate School for PhD students of the KIT-Center Climate and Environment at the Karlsruhe Institute of Technology (GRACE), GeoCool project (project no. B2850/3-1) and the Helmholtz Association of German Research Centres (HGF) portfolio project "Geoenergy" (35.14.01; POF III, LK 01).
- ... all co-authors of my three studies for their valuable and profound comments and thorough reviews. Special thank to Prof. Dr. Peter Bayer for constructive and critical comments and an objective view on the studies.
- ... Dr. Kathrin Menberg and Dr. Susanne A. Benz for scientific exchange, inspiring discussions as well as motivation and advice whenever I needed it.
- ... my friends and colleagues at the Department of Engineering Geology and Hydrogeology, especially Sina Hale, Linda Schindler, Rebecca Ilehag, Simon Schüppler, Paul Fleuchaus, Simon Breuer, Markus Merk and Hagen Steger for a great working atmosphere, enjoyable and relaxing times in the cafeteria and "Kaffeerunde", and activities off-campus.
- ...Cornelia Steiner for the joint field work and collection of temperature data in basements and underground carparks in Vienna, Austria.
- ... and above all I thank my parents for their generous, heart-warming, moral and emotional support, especially during the last steps of the completion of this thesis.

Declaration of Authorship

Chapter 2

Tissen, C., Benz, S. A., Menberg, K., Bayer, P. and Blum, P.: Groundwater temperature anomalies in central Europe, Environ. Res. Lett., 14(10), 104012, doi:10.1088/1748-9326/ab4240, 2019.

CT acquired and analysed the data as well as wrote the manuscript. SB provided the Matlab code to calculate the anthropogenic heat intensity. SB, KM, PBl and PBa provided scientific supervision, guidance for the research and revised the draft. All authors read and approved the final manuscript.

Chapter 3

Tissen, C., Menberg, K., Bayer, P. and Blum, P.: Meeting the demand: geothermal heat supply rates for an urban quarter in Germany, Geothermal Energy, 7(1), doi:10.1186/s40517-019-0125-8, 2019.

CT acquired and analysed the data as well as wrote the manuscript. KM, PBl and PBa provided scientific supervision and guidance for the research. All authors read and approved the final manuscript.

Chapter 4

Tissen, C., Menberg, K., Benz, S. A., Bayer, P., Steiner, C., Götzl, G. and Blum, P.: Identifying key locations for shallow geothermal use in Vienna, Renewable Energy, (submitted manuscript).

CT acquired and analysed the data as well as wrote the manuscript. SB, KM, PBl and PBa provided scientific supervision and guidance for the research. Valuable revisions of the manuscript were made by SB, KM, PBl, PBa and GG. CS also acquired data and established contact to local authorities for data interchange. All authors read and approved the final manuscript.

Eidesstattliche Versicherung gemäß §6 Abs. 1 Ziff. 4 der Promotionsordnung des Karlsruher Instituts für Technologie, Fakultät für Bauingenieur-, Geo- und Umweltwissenschaften.

1. Bei der eingereichten Dissertation zu dem Thema "Increased Groundwater Temperatures and Their Potential for Shallow Geothermal Use in Urban Areas" handelt es sich um meine eigenständig erbrachte Leistung.
2. Ich habe nur die angegebenen Quellen und Hilfsmittel benutzt und mich keiner unzulässigen Hilfe Dritter bedient. Insbesondere habe ich wörtlich oder sinngemäß aus anderen Werken übernommene Inhalte als solche kenntlich gemacht.
3. Die Arbeit oder Teile davon habe ich bislang nicht an einer Hochschule des In- oder Auslands als Bestandteil einer Prüfungs- oder Qualifikationsleistung vorgelegt.
4. Die Richtigkeit der vorstehenden Erklärungen bestätige ich.
5. Die Bedeutung der eidesstattlichen Versicherung und die strafrechtlichen Folgen einer unrichtigen oder unvollständigen eidesstattlichen Versicherung sind mir bekannt.

Ich versichere an Eides statt, dass ich nach bestem Wissen die reine Wahrheit erklärt und nichts verschwiegen habe.

Karlsruhe, 27.04.2020